CANADIAN THESES

THÈSES CANADIENNES

NOTICE

The quality of this microfiche is heavily dependent upon the quality of the original thesis submitted for microfilming. Every effort has been made to ensure the highest quality of reproduction possible.

If pages are missing, contact the university which granted the degree.

Some pages may have indistinct print especially if the original pages were typed with a poor typewriter ribbon or if the university sent us an inferior photocopy.

Previously copyrighted materials (journal articles, published tests, etc.) are not filmed.

Reproduction in full or in part of this film is governed by the Canadian Copyright Act, R.S.C. 1970, c. C-30.

AVIS

La qualité de cette microfiche dépend grandement de la qualité de la thèse soumise au microfilmage. Nous avons tout fait pour assurer une qualité supérieure de reproduction.

S'il manque des pages, veuillez communiquer avec l'université qui a conféré le grade.

La qualité d'impression de certaines pages peut laisser à désirer, surtout si les pages originales ont été dactylographiées à l'aide d'un ruban usé ou si l'université nous a fait parvenir une photocopie de qualité inférieure.

Les documents qui font déjà l'objet d'un droit d'auteur (articles de revue, examens publiés, etc.) ne sont pas microfilmés.

La reproduction, même partielle, de ce microfilm est soumise à la Loi canadienne sur le droit d'auteur, SRC 1970, c. C-30.

THIS DISSERTATION
HAS BEEN MICROFILMED
EXACTLY AS RECEIVED

LA THÈSE A ÉTÉ
MICROFILMÉE TELLE QUE
NOUS L'AVONS REÇUE

NL-339 (r. 86/06)

Canada

Meson and Dibaryon Masses in a QCD based Consistent Quark Model

Sherif Barbari

A Thesis

in

The Department

of

Physics

Presented in Partial Fulfillment of the Requirements
for the Degree of Doctor of Philosophy at
Concordia University
Montréal, Québec, Canada

March '1986

ISBN 0-315-30688-2

ABSTRACT

Meson and Dibaryon Masses
in a QCD based Consistent Quark Model

Sherif Barbari, Ph.D.
Concordia University, 1986

A QCD based consistent quark model is applied to test for the identity of forces in baryons and mesons, by calculating meson masses using parameters obtained from a fit to baryons. The results confirm that the same forces occur in both mesons and baryons. The same baryon parameters are then used to calculate dibaryon masses in the (u,d) sector

Dedication

This thesis is dedicated to my father and to Dr. C.S. Kalman, who never gave up on me.

Acknowledgment

I wish to express my gratitude to Dr. C.S. Kalman without whose guidance, encouragment and patience, this work would not have been possible. I wish to thank Dr. S.K. Misra for his support and guidance during my many years at Concordia.

Last but not least I wish to thank all those in the Physics Department who through the years helped make this day possible.

TABLE OF CONTENTS

LIST OF ILLUSTRATIONS

LIST OF TABLES

LIST OF APPENDICES

INTRODUCTION

Subatomic particles can be classified in families based on the type of interactions they participate in. The four fundamental forces believed to account for all observed interactions are, the gravitational force, electromagnetism, the strong force and the weak force.

The gravitational force influences all matter and has an infinite range. In the subatomic realm however, its effects are vanishingly small due to the infinitesimal masses involved and can be ignored. The electromagnetic force acts only on matter that carries an electric charge or current. The electromagnetic interaction also has an infinite range and may be considered as mediated by the exchange of photons between charged particles. The photon is the carrier or quantum of the electromagnetic force; it has no mass and no charge. The strong interaction has a short range extending only to about 10^{-13}cm. When two strongly interacting particles approach each other to within this distance the probability that they will interact is at least a hundred times higher than that of electromagnetic interaction. The range of the weak force is at most a hundredth that of the strong force. Two particles must approach to within 10^{-15}cm to interact and even at that range the probability of interaction is less than 10^{-10} that of the strong force.

All particles except the photon can be classified according to their response to the strong and weak forces. Particles which interact through the strong force are called hadrons and can be further subdivided into classes called mesons and baryons. The baryons include the proton and the neutron and it is the strong force which binds these particles in an atomic nucleus. The mesons include the pion and the kaon, they are generally less massive than the baryons. Particles that do not "feel" the strong force but respond to the weak force are called leptons. Electrons, neutrinos and muons are examples of leptons.

While the leptons seem to be truly elementary, having no internal structure, the hadrons have a finite size (about 10^{-13}cm). Evidence of an internal structure to the hadrons appears in experiments in which protons or neutrons collide at high energy with other particles. Debris emerging from the collisions with large momenta transverse to the collision axis and with a larger probability than one might expect if the proton or neutron were a diffuse distribution of matter suggests the existence of discrete scattering centres within the nucleon.

It was the great multiplicity of hadrons which led to the formulation of the quark model. This model replaced the great variety of hadrons with a limited number of fundamental building blocks called quarks.

The great success of the theory of quantum electrodynamics (QED) in describing the electromagnetic interaction prompted the development of analogous models based on a picture in which the interaction between particles is mediated by the exchange of field quanta. QED is an Abelian gauge theory, a characteristic of such theories is that a particle carrying a quantum number or charge, generates a long range quantized field whose strength is proportional to the quantum number. In QED the quantum number in question is the electric charge and the field quanta are the photons. Non-Abelian gauge theories are distinguished from QED by the fact that the field quanta themselves carry quantum numbers. Field quanta are themselves sources of the field and interact with one another. The theory describing the strong interaction is quantum chromodynamics (QCD) which is a non-Abelian gauge theory. The quantum number which generates the strong force field is the colour charge, of which there are three types (colours). The field quanta are the gluons, there are eight of them and they carry colour.

In this research we use a non-relativistic quark model within a QCD framework to test for the identity of forces in baryons and mesons. Next we apply this model to the calculation of the splitting of energy levels in the ground state of six quark composite systems (dibaryons).

In Chapter 1 of this thesis we introduce the ingredients of our model: The notion of quarks as the fundamental constituents of hadrons and the QCD based ideas which govern their interactions. The specific model we use and the background leading to it are developed in Chapter 2. In Chapter 3 we present the first phase of this research; a calculation of the energy levels of mesons using baryon parameters in the consistent quark model. The results confirm the validity of using this model to relate parameters in structures of different quark composition. We then proceed to calculate dibaryon spectra using baryon parameters in Chapter 4. Our conclusions are presented in Chapter 5.

We have included some examples of calculations as well as a copy of the publication describing the first part of this research in the appendices.

CHAPTER 1

QUARKS AND QCD

1.1 Quarks as Fundamental Particles

Quarks were first proposed in 1964 by Gell-Mann and Zweig[1,2] to simplify book keeping in the elementary particle zoo. At that time few people took the idea seriously as it meant accepting many peculiarities, including the notion of fractional electric charges. Since then the quark idea has developed from a bold hypothesis to a viable and generally accepted theory.

Quarks are spin $^1/_2$ fermions which are thought to be the fundamental building blocks of all strongly interacting particles, the hadrons.

The quark model emerged from symmetry considerations to explain the apparent multiplet structure in meson and baryon spectroscopy. The Hamiltonian of the strong interactions has an SU(2) isospin symmetry which is broken by the electric charge defining a direction in isospin-space and thus lifting the degeneracy. The neutron and proton are the two states of the nucleon occupying the two-dimensional or fundamental representation of the isospin group. The three and four dimensional representations are occupied by the

charge states of the π meson and Δ baryon respectively. The strange particles were also observed to form isospin multiplets having the same spin and parity but with different magnitudes of strangeness, the masses of these multiplets increasing by about 150 Mev for each unit increase in strangeness. This led to the incorporation of strangeness in the symmetry scheme and the use of SU(3) representations to accommodate the observed particle multiplets. These multiplets are apparent (fig. 1.1 and 1.2) even though the symmetry is clearly broken.

Mesons were observed in singlets and octets, while baryons were found in singlets, octets and decuplets. Other SU(3) representations did not appear to be realized in nature, specifically the fundamental three dimensional representation. Gell-Mann[1] and Zweig[2] proposed that the fundamental representation is occupied by three quarks and that these three types or flavours of quark combine in SU(3) to form $q\bar{q}$ meson states and qqq baryon states.

$$q\bar{q} \equiv 3 \otimes \bar{3} = 1 \oplus 8$$

$$qqq \equiv 3 \otimes 3 \otimes 3 = 1 \oplus 8 \oplus 8 \oplus 10$$

The observed hadron states emerged naturally from this scheme but the quark quantum numbers required to balance the books seemed very peculiar e.g. fractional charge and baryon number. Today the quark model is well established with quarks being considered as physical entities dynamically confined within hadrons, exhibiting a multiplet structure

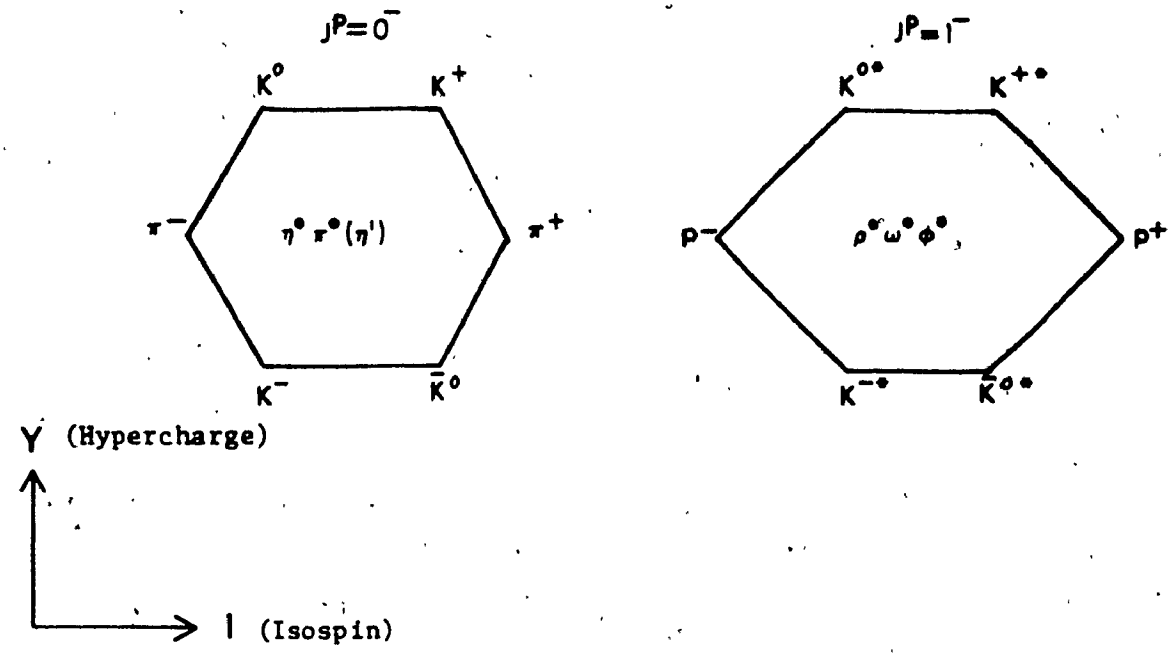

Fig.1.1 Pseudoscalar and vector meson.

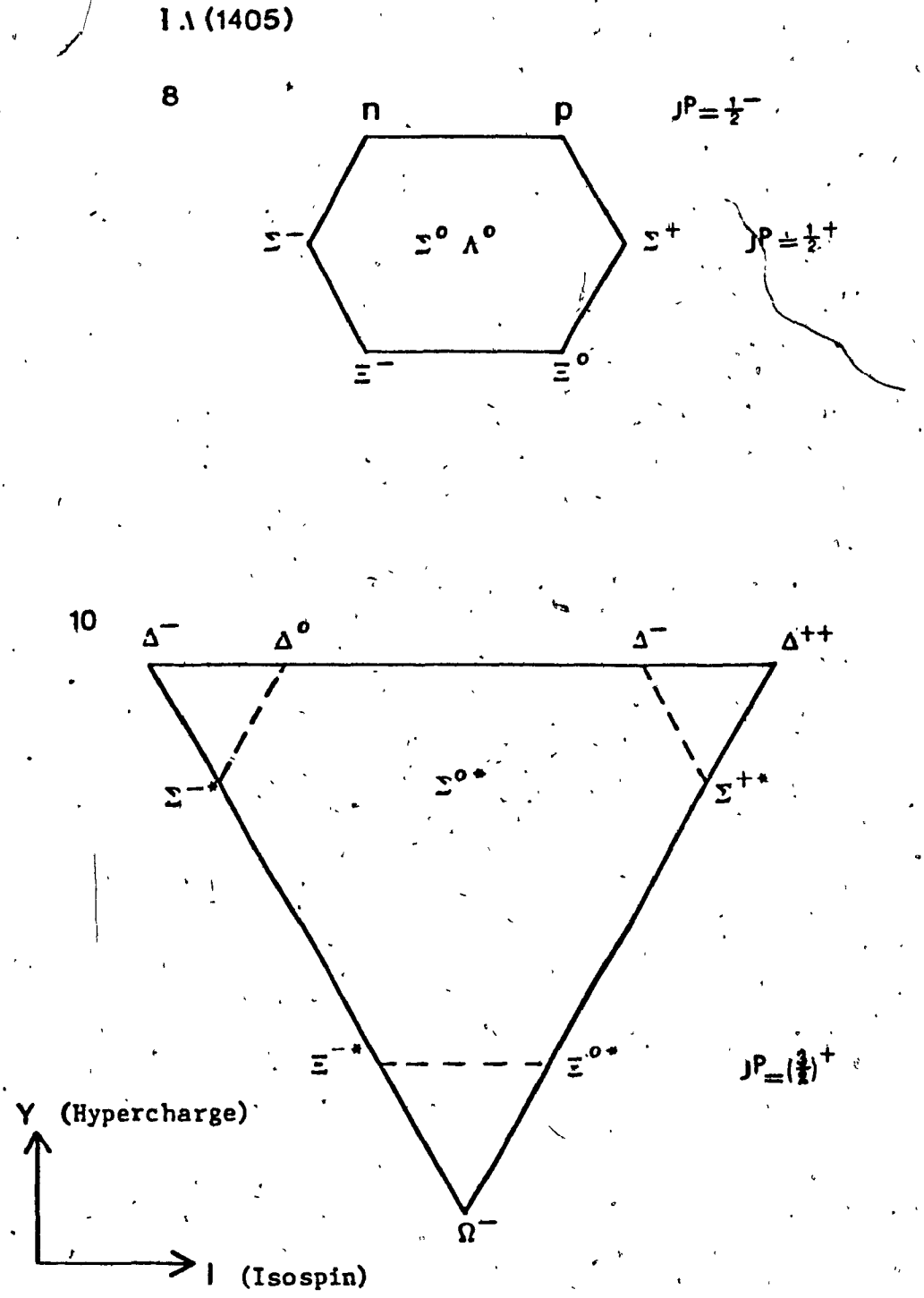

Fig. 1.2 Octet $\frac{1}{2}^+$ and decuplet $\frac{3}{4}^+$ baryons.

rooted in N flavours of quark contained in the fundamental representation of an approximate SU(N) symmetry.

With the inclusion of the charm, top and bottom flavours in the symmetry scheme, one arrives at $SU(6)_F$ symmetry (the F subscript denotes flavour) representations (Table 1.1). While the isospin $SU(2)_F$ symmetry breaking is of the order of the electromagnetic coupling constant $\alpha = 1/137$ and can be explained by electromagnetic interactions, the higher internal symmetry groups exhibit much stronger symmetry breaking, 20 % in the case of $SU(3)_F$, up to 200 % for $SU(4)_F$ and increasing with the number of flavours. However we are still able to discern the underlying symmetry structure.

The search for free quarks has been unsuccessful to date though La Rue et al.[3] have claimed evidence for the existence of fractionally charged matter on superconducting niobium balls in an experiment similar to the Millikan oil drop experiment, the result is not conclusive and is attributed to the possibility of systematic error. Reviews by Goldhaber[4], Jones[5] and others deal with the subject of quark searches.

The success of quantum chromodynamics (QCD) as a field theory of the strong interactions and the proposals for quark confinement mechanisms[6,7], sometimes called infrared slavery, within the framework of QCD have lent support to the hypothesis that quarks are permanently confined within

TABLE 1.1

Quarks and their quantum numbers

Flavour	u	d	s	c	t	b
Charge	$\frac{2}{3}$	$-\frac{1}{3}$	$-\frac{1}{3}$	$\frac{2}{3}$	$\frac{2}{3}$	$-\frac{1}{3}$
Isospin	$\frac{1}{2}$	$\frac{1}{2}$	0	0	0	0
I_3	$+\frac{1}{2}$	$-\frac{1}{2}$	0	0	0	0
Strangeness	0	0	-1	0	0	0
Charm	0	0	0	1	0	0
Top	0	0	0	0	1	0
Bottom	0	0	0	0	0	1
Baryon numbers	$\frac{1}{3}$	$\frac{1}{3}$	$\frac{1}{3}$	$\frac{1}{3}$	$\frac{1}{3}$	$\frac{1}{3}$
SU(N) group	SU(2)					
	SU(3)					
	SU(4)					
	SU(5)					
	SU(6)					

hadrons. Independently of whether free quarks exist, the quark model has been very successful in explaining the properties of hadrons in terms of the properties of bound quarks.

1.2 Hadrons as Bound States of Quarks

Hadron spectroscopy gives further evidence for composite quark structures. Meson spectroscopy in particular exhibits a striking regularity of internal quantum numbers which can be immediately attributed to their quark-antiquark bound state structure. Here an analogy is drawn with positronium which is an electron-positron bound state. In positronium the e^- and e^+ couple their intrinsic spins to either a triplet state (Spin = 1) or a singlet state (Spin = 0). When the total spin $\vec{S}$ is coupled with the orbital angular momentum $\vec{L}$ we get the total angular momentum of the system $\vec{J} = \vec{L} + \vec{S}$. We can then label the resulting states by their angular momentum quantum numbers using the notation $^{2s+1}L_J$. Here the same designation used in atomic physics S,P,D.... etc. corresponds to L = 0,1,2....etc. states. Also 2S + 1 is the multiplicity of spin states. The L = 0 states are $^1S_0$ and $^3S_1$, the L = 1 states are $^1P_1$, $^3P_0$, $^3P_1$, $^3P_2$ and so on. The pattern of the low lying energy levels of positronium is shown in fig. 1.3. In a quarkonium (quark-antiquark) system the same levelling structure should be apparent if we had only one flavour of quark. Meson

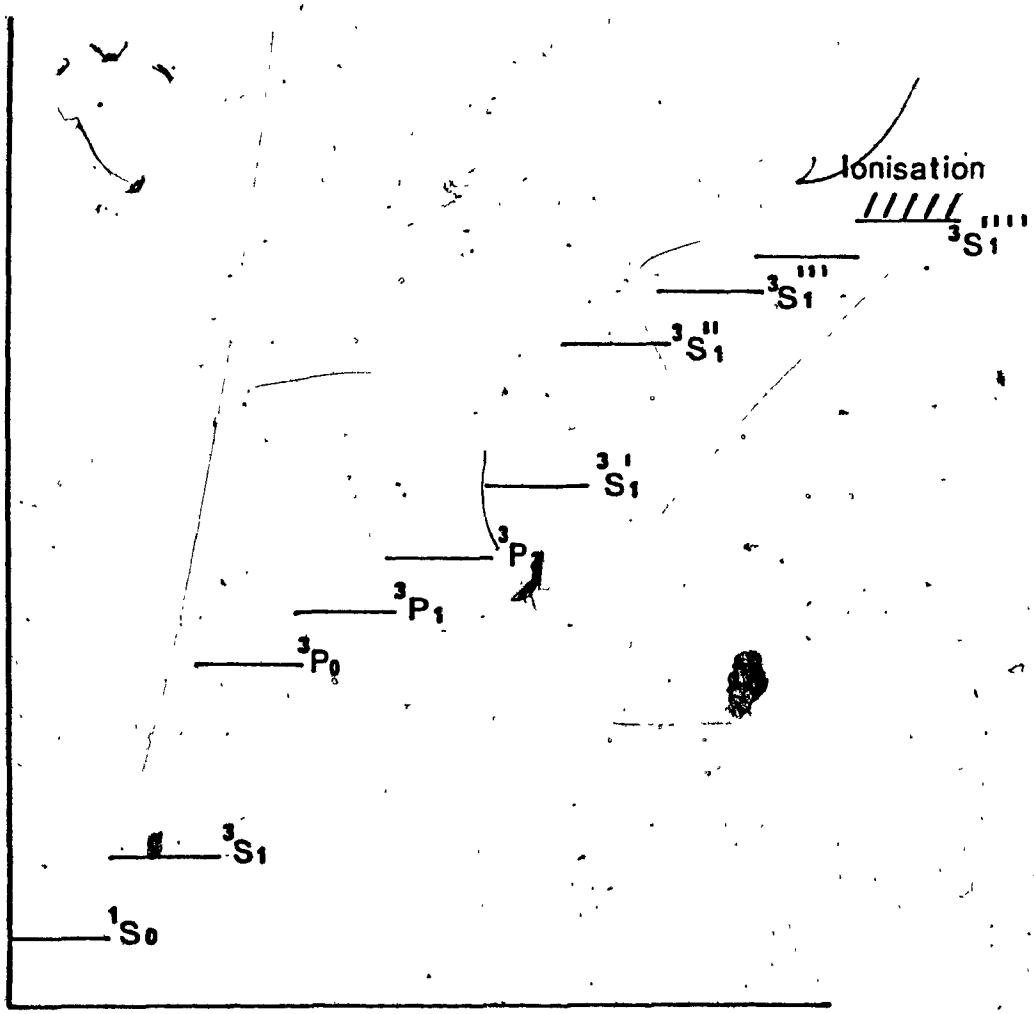

Fig. 1.3 Positronium energy levels

spectroscopy indicates that while the levelling scheme is generally followed, certain differences exist. First, instead of observing one meson at each level, we observe multiplets of mesons which would emerge naturally from N flavours of quark combining in a quark-antiquark system where all possible flavour combinations are allowed. Secondly, while the positronium energy levels exhibit the familiar Coulomb structure with an ionization level, the meson energy levels are roughly equally spaced and do not seem to possess an ionization limit. The level spacing of mesons hints at a different kind of potential such as linear or harmonic oscillator or even at a more complex form of the binding potential. The non-existence of an ionization limit means that feeding in more energy to the system merely excites it to higher states which then decay producing more mesons but never free quarks. This again brings to mind the idea of quark confinement which we will deal with later. The low lying energy levels of the J/ψ meson are shown in fig. 1.4 and the comparative levelling of Coulomb , linear and harmonic oscillator potentials is shown in fig. 1.5.

A further analogy can be drawn between baryons and nuclei composed of three nucleons such as H^3(pnn) and He^3(npp). In a baryon three quarks combine in S-wave to give J = 3/2 or 1/2 and as we excite a quark into P, D, F... states the parity of the system alternates S(+), P(-), D(+), F(-) and so on. Again, while nucleons can escape from

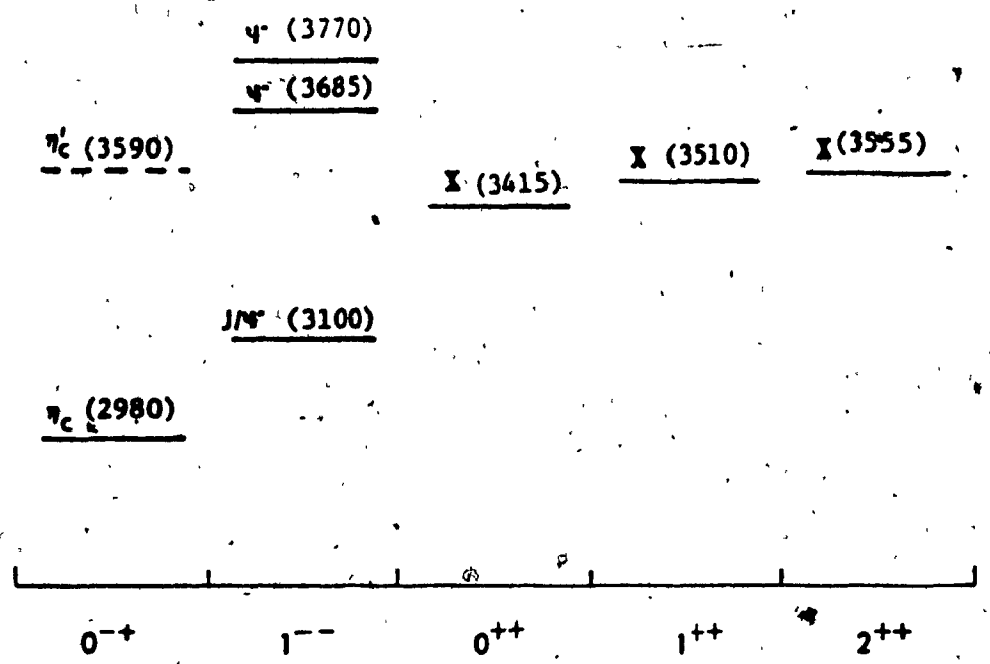

Fig. 1.4 Low lying energy states of charmonium

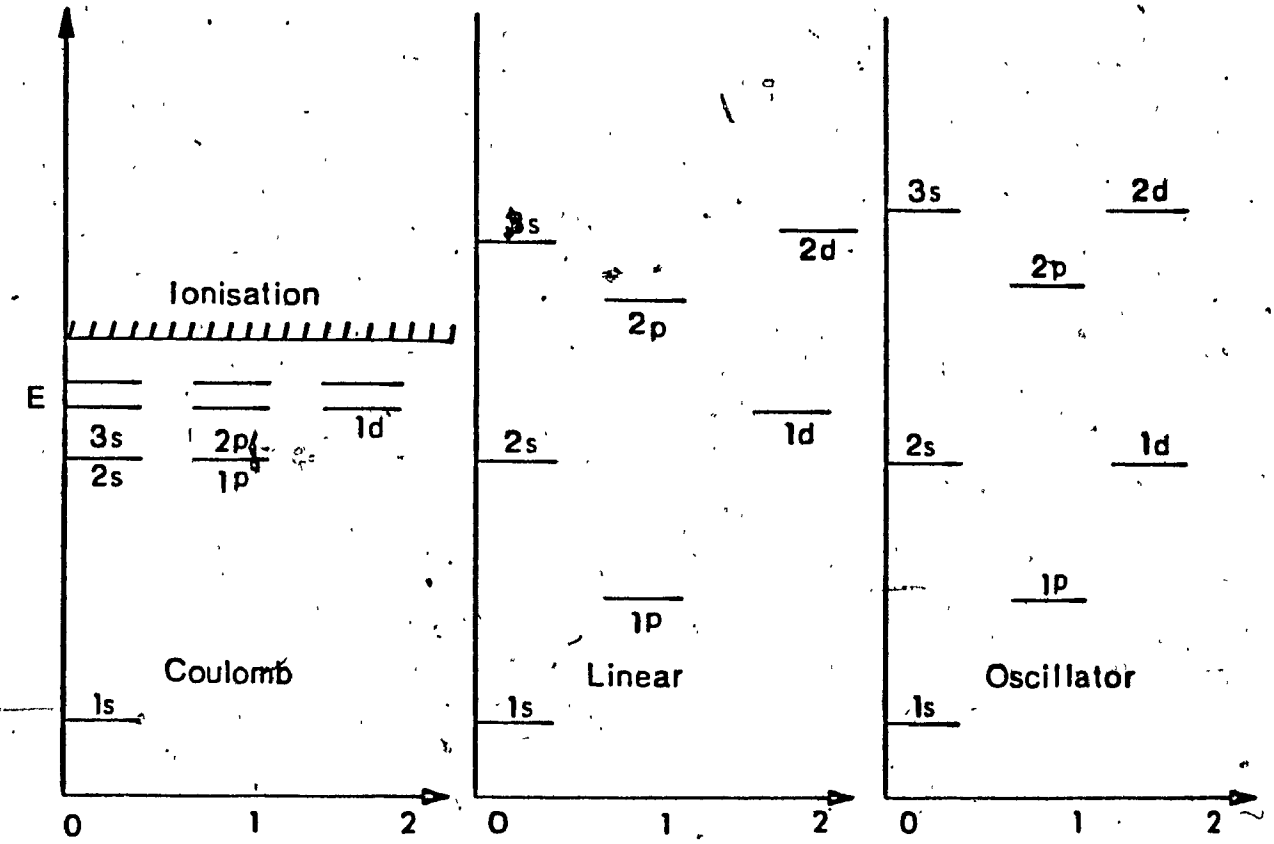

Fig. 1.5 Comparative spectroscopies of Coulomb, linear and oscillator potentials.

nuclei, quarks do not seem to be liberated from baryons. Two other observations can be made here. First, while there exist no selection rules regarding the number of nucleons in a nucleus hence H, H^2, H^3 and H^4, no quark systems are observed containing q,qq or qqqq. Secondly, while the nucleons in a nuclear system obey the Pauli principle which excludes the co-existence of fermions with identical quantum numbers, this does not seem to be the case with quarks in the $\Delta^{++}(uuu)$ and $\Omega^-(sss)$ systems all of which can co-exist in S-wave. These observations lead to the colour postulate, to a hypothesis on quark confinement and to a selection rule which determines allowed quark combinations.

1.3 The Colour Degree of Freedom

If we consider the $J_3 = {}^3/_2$ state of the Δ^{++} resonance and the Ω^- particle we find that in S-wave the combined spin, space and flavour wavefunctions

$$|\Delta^{++}, J_3 = {}^3/_2\rangle = |u\uparrow u\uparrow u\uparrow\rangle$$

and

$$|\Omega^-, J_3 = {}^3/_2\rangle = |s\uparrow s\uparrow s\uparrow\rangle$$

are symmetric with respect to interchange of quarks. If quarks are spin-½ particles then they must obey Fermi-Dirac statistics and their total wavefunction must be antisymmetric. A way out of the impasse was the suggestion by Greenberg[8] that quarks obey parastatistics of rank three, i.e. behave like bosons individually but take on fermion

characteristics when in groups of three. An alternative but equivalent postulate was the introduction by Han and Nambu[9] of three kinds of quark multiplets. The hidden quantum numbers which distinguish the quark multiplets are called the colours: red, blue and green. The antisymmetric colour wave function for baryons is written as

$$|B\rangle = \frac{1}{\sqrt{6}} \varepsilon_{abc} |q_A^a q_B^b q_C^c\rangle$$

where a, b, c, denote the quark colours and A, B, C the quark flavours. We can consider this wavefunction to be the singlet representation of an internal symmetry group called $SU(3)_c$, where the subscript c stands for colour. The three colours belong to the fundamental triplet representation of this group. Combining three colour triplets in $SU(3)_c$ we get

$$3 \otimes 3 \otimes 3 = 1 \oplus 8 \oplus 8 \oplus 10$$

There exist arguments from QCD why colour nonsinglet states should acquire infinite mass or at least why colour singlet states should lie low in mass. This would explain why the observed baryons are in colour singlet (white) states. Similarily a quark-antiquark combination gives

$$3 \otimes \bar{3} = 1 \oplus 8$$

which contains a colour singlet state, whereas diquarks and four-quark states cannot form a colour singlet.

The colour confinement postulate states that all hadrons and all physical observables are colour singlets. This

rules out the existence of unobserved states such as quarks, diquarks, four quark states and so on, while allowing baryons and mesons to exist. The confinement postulate however does not limit the allowed states to mesons and baryons but in addition allows the existence of higher mass colour singlet states which can be constructed from mesons and baryons, for example

$(qq\bar{q}\bar{q})$	baryonium
$(qqq\bar{q}q)$	mesobaryons
$(qqqqqq)$	dibaryons
etc.	etc.

Having accepted colour confinement we now seek evidence for colour, this is indirectly demonstrated in a number of ways.

1. The large magnitude of the cross-section for hadron production in e^-e^+ annihilation suggests that quarks are coloured. Below the charm production threshold

$$R = \frac{\sigma e^+e^- \rightarrow \text{hadrons}}{\sigma e^+e^- \rightarrow \mu^+\mu^-} = \sum_{i=u,d,s} Q_i^2 = \begin{cases} 2/3 & \text{uncoloured quarks} \\ 2 & \text{three colours} \end{cases}$$

experiment gives $R \simeq 2$

Above the charm and heavy lepton production threshold we have

$$R = \begin{cases} 10/9 & \text{uncoloured quarks} \\ 4\ 1/3 & \text{three colours} \end{cases}$$

Experiment gives $R \simeq 5$ which is in reasonable agreement with scheme based on coloured quarks.

2. The rate for the decay $\pi^0 \rightarrow 2\gamma$ as calculated by

Adler[10] when colour is included is in remarkably good agreement with experiment but differs by a factor of 9 if colour is not included.

3. In baryon spectroscopy the nucleons are fermions and therefore require antisymmetric wavefunctions yet in an uncoloured quark model their wavefunctions are symmetric. This was discussed earlier and examples of the Δ^{++} and Ω^{-} wavefunctions were given.

4. Colour provides a way of explaining why $q\bar{q}$ and qqq are low lying states while qq and $qqqq$ etc. states are not observed.

5. The observed ratio of the decay of the τ^{-} lepton to leptons and to hadrons corresponds to the predictions of a coloured quark model.

1.4 Quantum Chromodynamics

Once we introduce a colour quantum number and accept the postulate of colour confinement, the strong force between quarks must be able to distinguish between colour singlets and nonsinglets. This eliminates any theory of the strong interactions in which coloured quarks are coupled to colour singlet mediating bosons (gluons). In other words the gluon must be able to carry the colour quantum number.

We introduce a colour dependent potential between

quarks of the form $\left[\sum_{i=1}^{8} \frac{\lambda_i^a}{2} \cdot \frac{\lambda_i^b}{2}\right] \cdot V(r)$ where V(r) is a function of the relative distance between quarks, $\frac{\lambda_i^a}{2}$ is the $SU(3)_C$ matrix acting on quark a and $\frac{\lambda_i^b}{2}$ is the matrix acting on quark b.

In analogy to the F-spin operator of $SU(3)_F$ we introduce a colour spin-operator $\vec{\Lambda}$ whose square is a Casimir operator of $SU(3)_C$. The eigenvalues of $\vec{\Lambda}^2$ for the lowest lying $SU(3)_C$ representations are given in Table 1.2.

TABLE 1.2

Eigenvalues of the quadratic Casimir operator C for the lowest-dimensional representations of SU(3) (m = mixed, s = symmetric).

Dimension of representation	1	3	$\bar{3}$	6	$\bar{6}$	8	$\overline{10}$	10	$\overline{15}_m$	15_m	$\overline{15}_s$	15_s	$\overline{24}$	24	27
Quark indices p	0	1	1	2	2	2	3	3	3	3	4	4	4	4	4
q	0	0	1	0	2	1	0	3	1	2	0	4	1	3	2
Λ^2	0	$\frac{4}{3}$		$\frac{10}{3}$		3	6		$\frac{16}{3}$		$\frac{28}{3}$		$\frac{25}{3}$		8

Next we write a non-relativistic interaction Hamiltonian for a two quark system.

$$H = m_a + m_b + \frac{P_a^2}{2m_a} + \frac{P_b^2}{2m_b} + \left[\sum_{i=1}^{8} \frac{\lambda_i^a}{2} \cdot \frac{\lambda_i^b}{2}\right] V(r) \qquad (1.4.1)$$

Therefore,

$$H = m_a + m_b + \frac{P_a^2}{2m_a} + \frac{P_b^2}{2m_b} + \left[\vec{\Lambda}(a) \cdot \vec{\Lambda}(b)\right] V(r) \qquad (1.4.2)$$

Since the colour spin of a composite system is equal to the vector sum of the colour spin of the constituents, we have

$$[\vec{\Lambda}(a)+\vec{\Lambda}(b)]^2 = \vec{\Lambda}^2(a)+\vec{\Lambda}^2(b)+2\vec{\Lambda}(a)\cdot\vec{\Lambda}(b) \qquad (1.4.3)$$

and $\vec{\Lambda}^2(a) = \vec{\Lambda}^2(b) = 4/3$ a quark being a colour triplet. Then we can write the Hamiltonian as

$$H = m_a+m_b+\frac{P_a^2}{2m_a}+\frac{P_b^2}{2m_b}+\frac{1}{2}(\vec{\Lambda}^2_{Total}-\frac{8}{3})V(r) \qquad (1.4.4)$$

and the eigenvalues are given by

$$M = m_a+m_b+k_0+k_1\vec{\Lambda}^2_{Total} \qquad (1.4.5)$$

where k_0 and k_1 are constants, K_1 being positive if V(r) is attractive.

Similarly for multiquark systems where the colour interaction is due solely to two-body forces the eigenvalues can be written as

$$M = \sum_{i=1}^{N} m_i+k_0+k_1\cdot\vec{\Lambda}^2_{Total} \qquad (1.4.6)$$

where N in the number of quarks.

The last term disappears for colour singlet states and therefore the difference in mass between coloured states and observed hadrons is contained in this term. In potential models where the potential increases sufficiently as $r \to \infty$ such as is the case with linear and harmonic oscillator potentials we find that $K_1 \to \infty$, hence, total confinement. We also note that when K_1 acquires a finite value we have partial confinement up to some colour threshold. A finite

K_1 therefore introduces a new scale parameter $E_C = K_1 \Lambda^2_{Total}$ into the theory. It would be simpler if we can avoid this additional parameter, but, the general form of the theory is not altered significantly by this possibility.

Quantum chromodynamics is an SU(3) non-Abelian, gauge invariant, quantum theory for the interaction in colour space of an octet of massless vector gluons with a triplet of spin-$^1/_2$ quarks.

The Lagrangian of QCD[9,11] is given by

$$L_{QCD} = -\frac{1}{4} G^{\mu\nu}_k G_{\mu\nu k} + \Psi[i\gamma_\mu D^\mu - M]\Psi \qquad (1.4.7)$$

with

$$D^\mu = \partial^\mu + i g_s \frac{\lambda^k}{2} A^\mu_k \qquad (1.4.8)$$

the generalized gluon field strength is

$$G^{\mu\nu}_k = \partial^\mu A^\nu_k - \partial^\nu A^\mu_k + g_s f_{klm} A^\mu_l A^\nu_m \qquad (1.4.9)$$

Ψ is the quark spinor and can be written

$$\Psi(x) = \begin{Bmatrix} \psi_r(x) \\ \psi_b(x) \\ \psi_g(x) \end{Bmatrix}$$

where we have suppressed the flavour index for simplicity. A^μ_k is the massless gluon field, $\frac{\lambda_k}{2}$ are the normal Gell-Mann matrices for $SU(3)_C$ and obey the relations

$$\left[\frac{\lambda_i}{2} , \frac{\lambda_j}{2} \right] = i f^{ijk} \frac{\lambda_k}{2} \qquad (1.4.10)$$

$$\left\{ \frac{\lambda_i}{2} \quad \frac{\lambda_j}{2} \right\} = \frac{1}{6} \delta^{ij} + d^{ijk} \frac{\lambda_k}{2} \qquad (1.4.11)$$

where i, j, k, = 1,....8, the f^{ijk} structure constants being

antisymmetric under interchange of any pair of indices, while the d^{ijk} are symmetric under interchange of indices. g_s is a coupling constant which determines the strenght of the fermion-boson interactions; it is the analog of the bare charge in QED. M is the quark mass matrix and in colour space is a unit matrix. This implies that the masses of the coloured quarks for each flavour are the same and $SU(3)_c$ is an exact symmetry.

The difference between QED and QCD is the gauge group. QED has the gauge group U(1) and is an Abelian gauge theory whereas QCD has $SU(3)_c$ as the gauge group and is a non-Abelian gauge theory. Everything follows from the gauge group difference. The behaviour of the renormalized coupling constant illustrates this.

In QED an electron is surrounded by a sea of virtual electron - positron pairs. The electron charge attracts the positrons contained in the vaccuum polarization cloud. As a result the net charge seen from a certain distance (Thomson limit) is less than the bare charge. We can define an effective charge $e(Q^2)$, where $q^2 = -Q^2$ is the space-like momentum transfer of the photon. The larger Q, the smaller the distance probed.

For two electrons the product of their charges is

$$\alpha(Q^2) = \frac{e^2(Q^2)}{4\pi} \qquad (1.4.12)$$

The Feynman diagrams for the true (dressed) photon propagator as well as the diagram illustrating the effective charge interaction are shown in fig 1.6.

We replace the product of $\alpha_0 = e_0^2/4\pi$ (which contains the bare charge e_0) and the true photon propagator $D(q^2)$ by the product of $\alpha(Q^2)$ (the effective coupling constant) with the free propagator to get

$$\alpha_0 D(q^2) = \frac{\alpha(Q^2)}{q^2+i\epsilon} \qquad (1.4.13)$$

We then calculate $\alpha(Q^2)$ using perturbation theory in the limit $Q^2 > m_e^2$, where m_e is the electron mass.

This gives

$$\alpha(Q^2) = \alpha_0\left(1 - \frac{\alpha_0}{3\pi}\ln\frac{L^2}{Q^2} + \ldots\right) \qquad (1.4.14)$$

where L is the ultra violet cut-off. The second term is negative which indicates that the effective coupling constant decreases as Q^2 increases. In other words, charge screening is increasing at high momentum transfers or smaller distance probing.

In QCD due to the non-Abelian nature of the gauge group the gluons also carry a colour charge. As a result, a virtual gluon emitted from a quark does not only see the charge of another quark and the charge of virtual quark-antiquark pairs, but it also see the charge of other

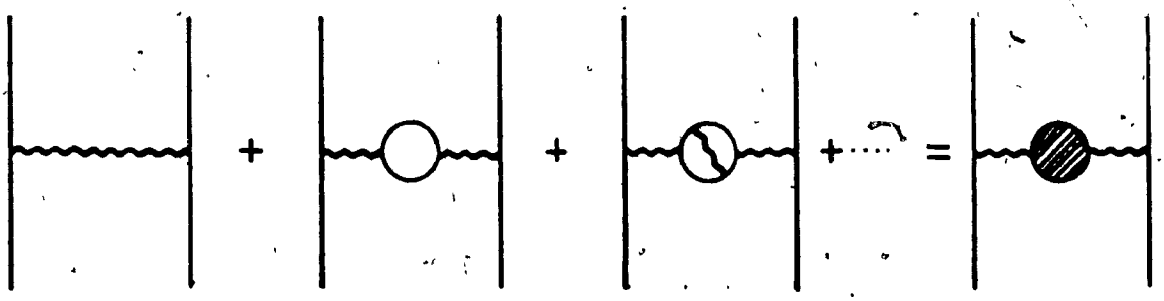

(a)

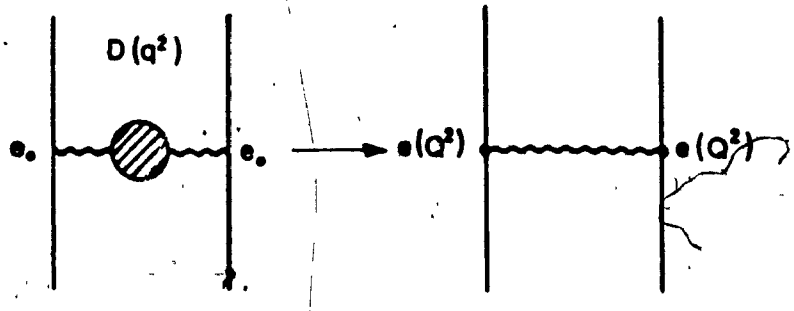

(b)

Fig. 1.6 The effective coupling constant $e(Q^2)$ in (b) contains the whole sum of diagrams of (a).

virtual gluons. This is shown in fig. 1.7.

The effective quark-quark coupling constant is then given by

$$\alpha_s(Q^2) = \frac{g_s^2(Q^2)}{4\pi} = \alpha_s^{(0)}\left[1-\frac{2}{3}f\frac{\alpha_s^{(0)}}{4\pi}\ln\frac{L^2}{Q^2} + 11\frac{\alpha_s^{(0)}}{4\pi}\ln\frac{L^2}{Q_2}\right] \qquad (1.4.15)$$

where $\alpha_s^{(0)} = g_s^{(0)2}/4\pi$, $g_s^{(0)}$ is the bare quark gloun coupling constant;

f is the number of quark flavours which contribute at the corresponding energy;

Q^2 is the space like momentum transfer;

and L is a cutoff parameter.

Again, the second term is negative and has a screening effect, the third term, which comes from the virtual gluon loop, is positive and gives antiscreening.

The massless gluon propagators in diagram C of fig. 1.7 can be decomposed in a Coulomb gauge[12,13] as shown in fig. 1.8. Diagram (a) in fig. 1.7 shows the transverse gluon loop component which leads to charge screening and can be written as

$$-\frac{\alpha_s^{(0)}}{4\pi}\ln\frac{L^2}{Q^2}$$

while diagram (b) consists of a transverse gluon and a "Coulomb" gluon and leads to antiscreening. This term is

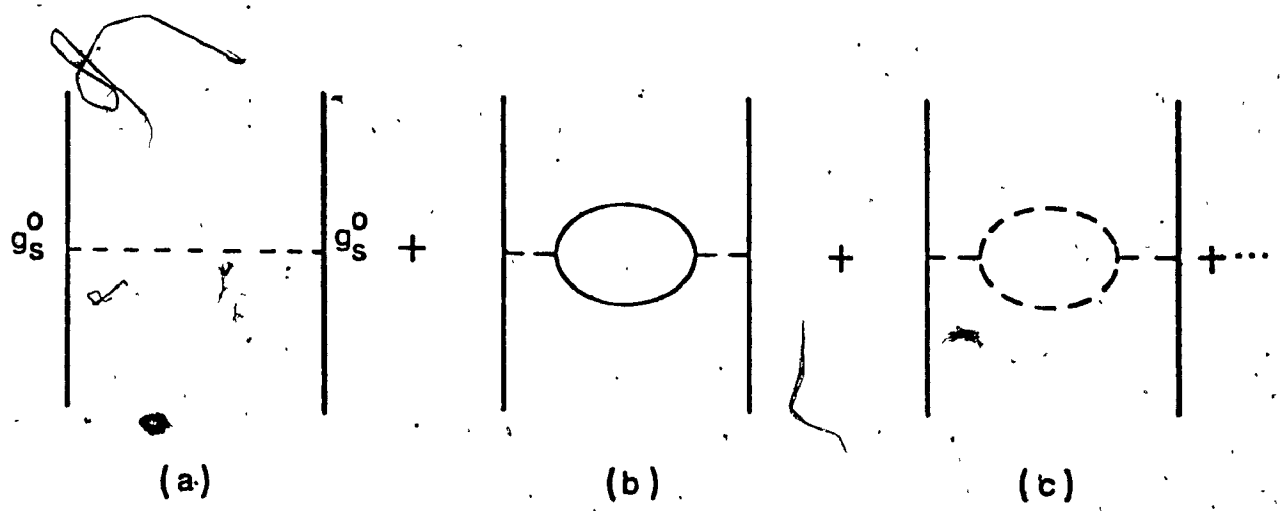

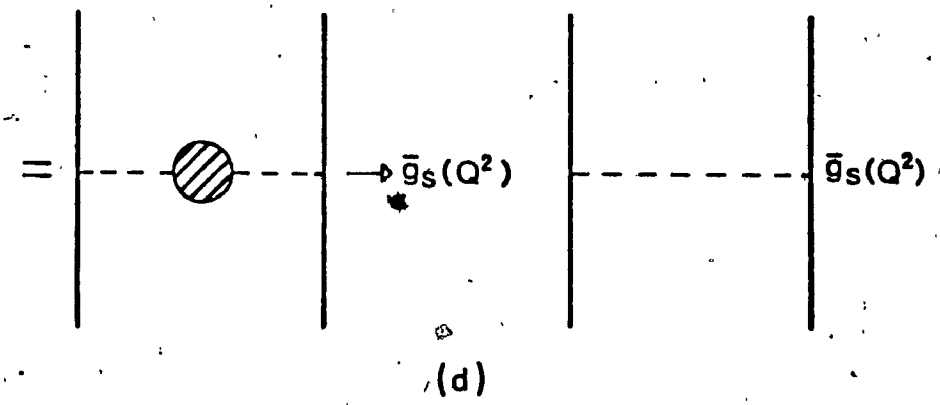

Fig. 1.7 Diagrams which contribute to second order in g_s^o to the running coupling constant.

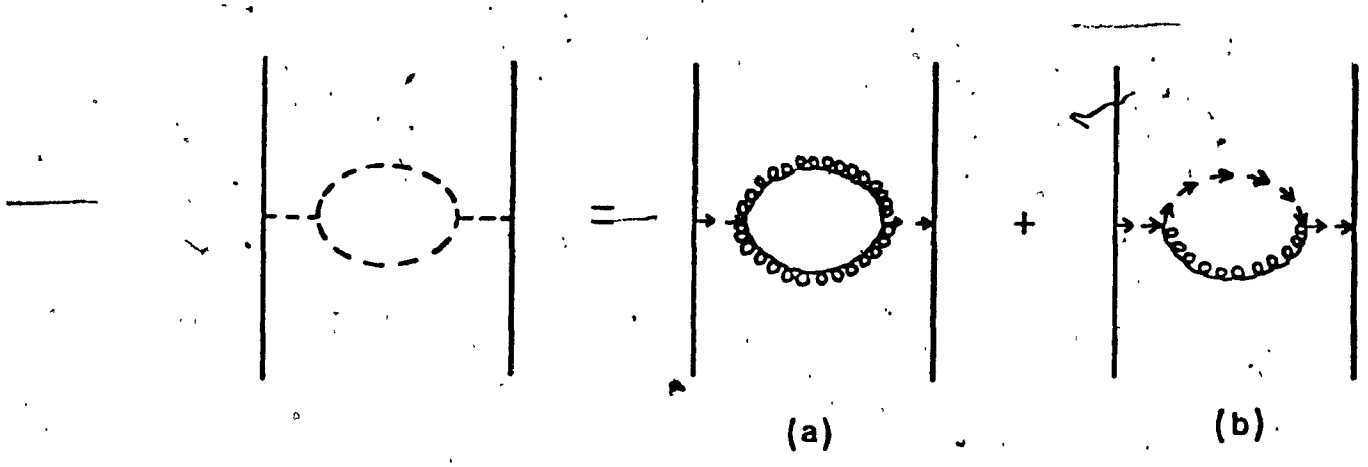

Fig. 1.8 Decomposition of the two gluon loop in Coulomb gauge into transverse components (wiggly lines) and "Coulomb" components (arrow lines). Only the self energy diagram (b) gives antiscreening.

written as

$$\frac{12\alpha_s^{(0)}}{4\pi} \ln \frac{L^2}{Q^2}$$

It has been shown[12,13,14] that the antiscreening due to the "Coulomb" gluon is twelve times stronger than the screening due to the transverse gluons.

Using renormalization-group techniques[15,16,17,18] both the bare coupling constant and the cut-off paramater L can be eliminated and the so called running coupling constant can be written as

$$\bar{\alpha}_s(Q^2) = \frac{\bar{\alpha}_s(Q_0^2)}{1 + (11-2f/3)[\bar{\alpha}_s(Q_0^2)/4\pi]\ln(Q^2/Q_0^2)} \qquad (1.4.16)$$

where $\bar{\alpha}_s(Q^2)$ is cutoff independent and Q_0^2 is a suitable reference momentum transfer where $\bar{\alpha}_s(Q_0^2)$ is known from experiment.

Perturbation theory cannot be applied in the regime of small energies as the coupling constant may be rather large, but at high energies (large momentum transfers) as $Q^2 \to \infty$ the coupling constant approaches zero provided $(11 - {}^2/_3 f) > 0$ or $f < 16$. This phenomenon is called asymptotic freedom. It is interesting to note here that an upper limit is placed on the number of quark flavours which are allowed if asymptotic freedom holds.

From (1.4.16) we see that vaccuum polarization in QCD

leads to a logarithmic increase in the force between coloured constituents. This implies that the colour flux lines between two coloured sources are more collimated than they would be in a Coulomb field. Fig. 1.9 illustrates a simple interpretation of this flux line collimation where the flux lines are drawn together by the exchange of coloured transverse gluons.

The fact that in QCD the colour flux lines are more collimated than in a pure Coulomb potential may imply that the force between two coloured objects does not fall off with distance rapidly enough to lead to a finite ionization energy. An intuitive picture (see fig. 1.10) may be drawn where as the distance between a quark-antiquark pair increases, the attraction between the colour flux lines becomes so strong that at large distances the field lines tend to be parallel and the force between the quark-antiquark pair becomes constant. The energy of the system then grows linearly with the separation and the system breaks up as soon as there is enough energy available to create a new quark-antiquark pair and form two colour singlets. If this picture of chromodynamics at large distances is correct colour would be confined and hadrons would exist only as colour singlet states.

Eq. (1.4.16) is valid only in the limit $Q^2 >> m_q^2$, where m_q is the effective quark mass. If $Q^2 << m_q^2$, the quark

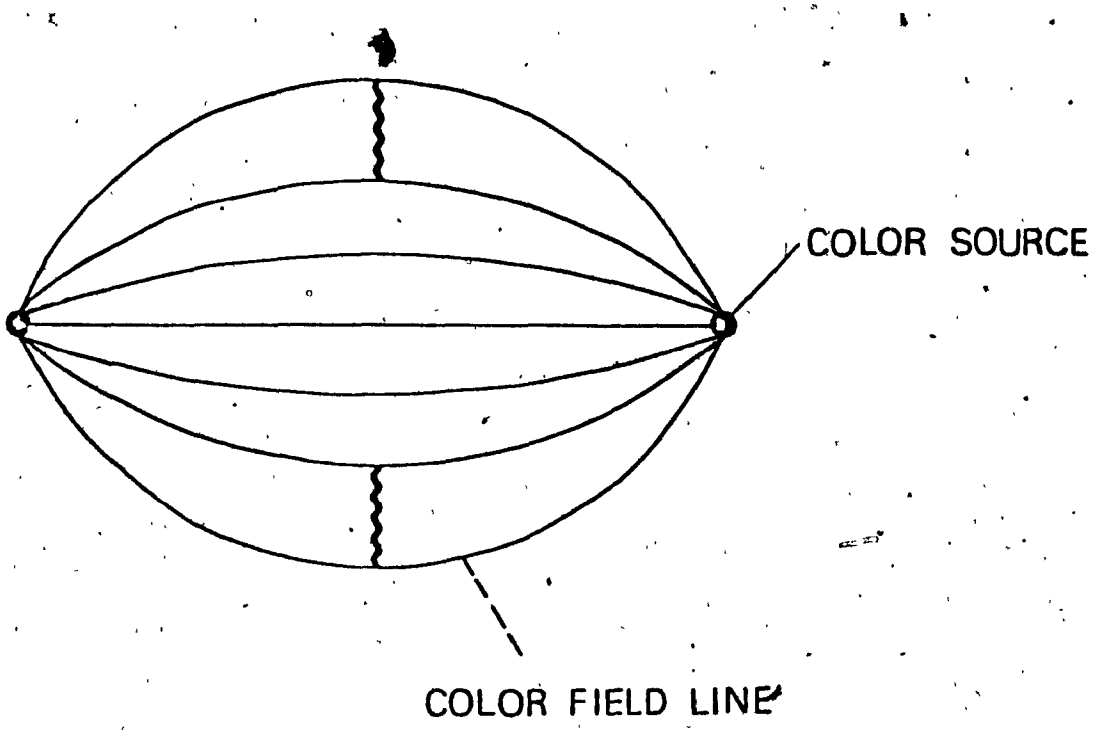

Fig. 1.9 Logarithmic flux line collimation in QCD due to the chromomagnetic attraction of the cromoelectic fieldlines.

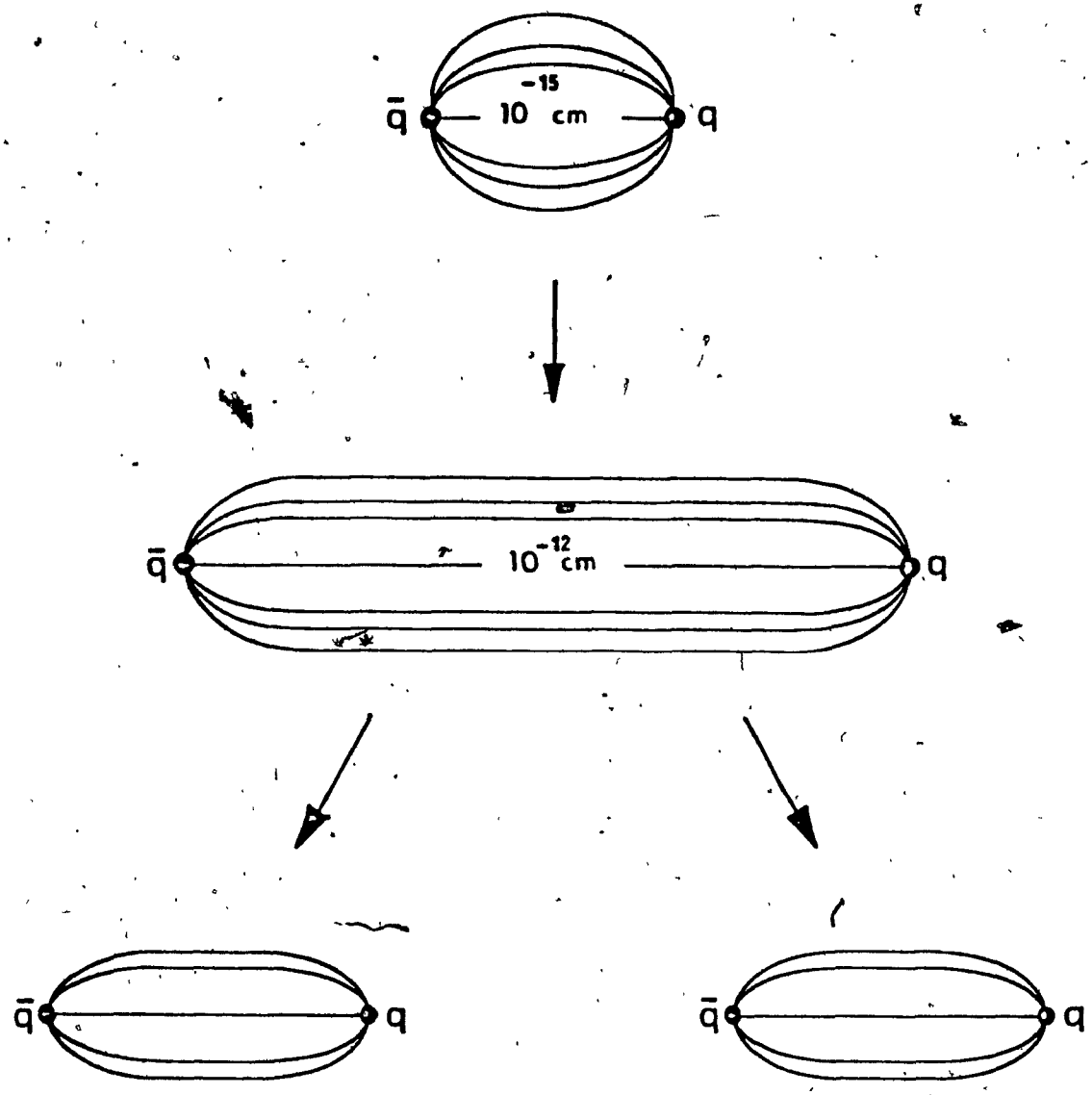

Fig. 1.10 Hypothetical collimation of the flux lines in QCD due to the chromoelectric Meissner effect. If the field energy exceeds the threshold for quark pair production the string breaks.

contributions to vaccuum polarization are suppressed by powers of (Q^2/m_q^2). As a result, in the renormalization of $\bar{\alpha}_s(Q^2)$ only quark flavours with $Q^2 > m_q^2$ are significant, the other quark flavours being "turned off". This implies that at low Q^2 (large distances) the coupling constant is independent of the masses and is determined only by gluon contributions to vaccuum polarization.

It is possible to express $\bar{\alpha}_s(Q^2)$ by the renormalization-group invariant parameter Λ given by

$$\Lambda^2 = Q_0^2 \exp\left[- \frac{1}{\frac{33-2f}{12\pi}\,\bar{\alpha}_s(Q_0^2)} \right] \qquad (1.4.17)$$

and thus eliminate the dependence of $\bar{\alpha}_s$ on an arbitrary renormalization point Q_0. We can write (1.4.16) as

$$\bar{\alpha}_s(Q^2) = \left[\frac{33-2f}{12\pi} \ln \frac{Q^2}{\Lambda^2} \right]^{-1} \qquad (1.4.18)$$

The scale parameter Λ characterizes the strength of the coupling constant. It is interesting to note from (1.4.18) that when $Q^2 = \Lambda^2$ the coupling constant becomes singular. This occurs at about .5 fm for $\Lambda \simeq 500$ MeV as determined from deep inelastic neutrino scattering experiments. The Q dependence of the effective quark gluon coupling constant from (1.4.18) is shown in fig. 1.11.

The appearance of a scale parameter Λ in QCD is an interesting phenomenon. We associate the critical length Λ^{-1} with the typical size of a hadron ($\simeq$ 1 fm), which is

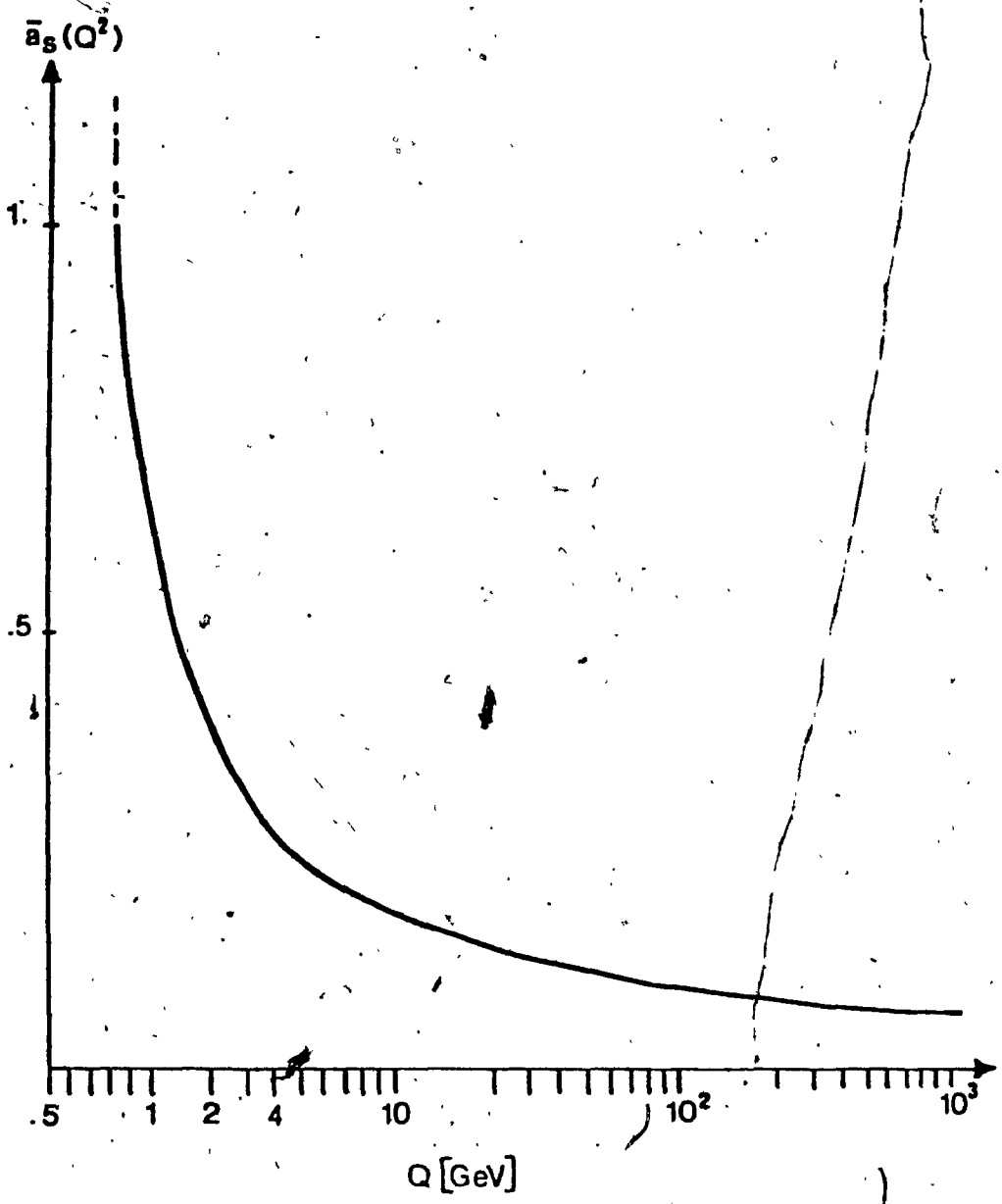

Fig. 1.11 Q-dependence of the effective quark gloun coupling constant $\bar{a}_s(Q^2)$. The flavour number f starts with 3 and increases by one at every flavour threshold. Experimentally one finds for the scale parameter $\Lambda \simeq 0.5$ GeV.

consistent with a measured value of Λ of $\simeq$ 500 MeV, and note that quarks confined within a region of extension Λ^{-1} have a typical momentum of the order of Λ. The light quarks m_q<500MeV will thus be moving relativistically inside the hadron while since $m_c > \Lambda$ (m_c is the charmed quark mass) we can consider charm-anticharm bound states to be non-relativistic bound states.

CHAPTER 2

HADRON SPECTROSCOPY IN QCD

2.1 Models for Hadron Specroscopy

"Once upon a time, there was a controversy in particle physics. There were some physicists who denied the existence of structures more elementary than hadrons, and searched for a self consistent interpretation wherein all hadron states stable or resonant, were equally elementary. Others appalled by the teeming democracy of hadrons, insisted on the existence of a small number of fundamental constituents and a simple underlying force law. In terms of these more fundamental things, hadron spectroscopy should be qualitatively described and essentially understood just as are atomic and nuclear physics." Having said this De Rújula, Georgi and Glashow[19] went on to demonstrate how it should be done. Arguing that colour gauge couplings produce a long range spin-independent force leading to the appearance of $SU(6)_q \otimes SU(6)_q \otimes O(3)$ supermultiplets of hadrons, that only the short range force between quarks (arising from one-gluon exchange) is spin dependent and allowing the different quark flavours to acquire different masses as the sole mechanism for SU(3) symmetry breaking, they wrote the Hamiltonian for hadrons in the form

$$H = L(\vec{r}_1,\vec{r}_2,\ldots) + \sum_i \left(m_i + \frac{\vec{p}_i^{\,2}}{2m_i} + \ldots\right)$$

$$+ \sum_{i>i} (\alpha Q_i Q_j + k\alpha_s) S_{ij} \qquad (2.1.1)$$

where r_i, m_i, $\vec{p}_i$ and Q_i are respectively the position, mass, momentum and electric charge of the i th quark. α is the fine structure constant, α_s is the colour interaction coupling constant and k is the colour factor ($-\,{}^4/_3$ for $q\bar{q}$ pairs in a meson and $-\,{}^2/_3$ for qq pairs in a baryon). L is the "universal" interaction responsible for quark binding, the second term in the Hamiltonian is the classical free particle Hamiltonians for the constituent quarks and the third term is the two body Coulombic interaction which has the form

$$S_{ij} = \frac{1}{|\vec{r}|} - \frac{1}{2m_i m_j}\left[\frac{\vec{p}_i.\vec{p}_j}{|\vec{r}|} + \frac{\vec{r}.(\vec{r}.\vec{p}_j)\vec{p}_i}{|\vec{r}|^3}\right] -$$

$$\frac{\pi}{2}\delta^3(\vec{r})\left[\frac{1}{m_i^2} + \frac{1}{m_j^2} + \frac{16\vec{S}_j.\vec{S}_i}{3m_i m_j}\right] - \frac{1}{2|\vec{r}|^3}$$

$$\left\{\frac{1}{m_1^2}\vec{r}\times\vec{p}_i.\vec{S}_i - \frac{1}{m_j^2}\vec{r}\times\vec{p}_j.\vec{S}_j + \frac{1}{m_i m_j}\left[2\vec{r}\times\vec{p}_i.\vec{S}_j -\right.\right.$$

$$\left.\left.2\vec{r}\times\vec{p}_j.\vec{S}_i - 2\vec{S}_i.\vec{S}_j + \frac{6(\vec{S}_i.\vec{r})(\vec{S}_j.\vec{r})}{|\vec{r}|^2}\right]\right\} + \ldots, \qquad (2.1.2)$$

where $\vec{r} = \vec{r}_i - \vec{r}_j$ and ..... denotes neglected relativistic corrections.

In essence, what De Rújula, Georgi and Glashow did was to put together within the framework of QCD and the quark

model a general Hamiltonian of the Fermi-Breit type, and, show how with a minimal number of plausible assumptions and fits to observed particle masses a model could emerge based on "a simple underlying force law" and " a small number of fundamental constituents" which both qualitatively and quantitatively provide a solid basis for describing hadron spectroscopy.

They suggested that the principal binding forces of hadrons are the long range confining forces arising from the idea of infrared slavery, where the colour force coupling becomes stronger at large distance (low Q^2). These forces were assumed to be independent of quark masses and spins, depending strictly on the spatial separation of interacting quarks and form the L term in the Hamiltonian.

The concept of asymptotic freedom, the small α_s at short distance (large Q^2) and the decrease of α_s with increasing energy, was used to justify a perturbative approach based on the existence of short range forces depending on quark masses and spins and arising from one gluon exchange, hence the Fermi-Breit term.

The observed hadron mass splittings were attributed to splittings among the quark masses and these quark mass differences were applied as the mechanism for SU(3) symmetry breaking.

Non-relativistic $SU(6)_{FS}$ (where the subscripts FS represent flavour and spin) zeroth-order wavefunctions were then used to generate the hadron states.

The model was then applied to the S-wave baryons to give the first order mass formula

$$M = M_0 + \sum_i \left[\Delta m_i + a\left(\frac{1}{m_i} - \frac{1}{m_u}\right) \right] + \sum_{i>j} \left(\alpha Q_i Q_j - \tfrac{2}{3}\alpha_s\right)$$

$$\left[b - \frac{C}{m_i m_j} - d \left[\frac{1}{m_i^2} + \frac{1}{m_j^2} + \frac{16\, \vec{S_i}\cdot\vec{S_j}}{3 m_i m_j} \right] \right] \qquad (2.1.3)$$

where $\Delta m_i = m_i - m_u$; m_u is the u-quark mass

$H_0 |\psi_0\rangle = M_0 |\psi_0\rangle$; $|\psi_0\rangle$ is the completely symmetric function $\psi_0(r_1, r_2, r_3)$ of the positions of the quarks.

$$a = \frac{1}{2} \langle \psi_0 | p_i^2 | \psi_0 \rangle$$

$$b = \langle \psi_0 | \frac{1}{|\vec{r}_{12}|} | \psi_0 \rangle$$

$$c = \frac{1}{2} \langle \psi_0 | \frac{r_{12}^2\, \vec{p}_1\cdot\vec{p}_2 + \vec{r}_{12}\cdot(\vec{r}_{12}\cdot\vec{p}_1)\vec{p}_2}{|\vec{r}_{12}|^3} | \psi_0 \rangle$$

and $$d = \frac{\pi}{2} \langle \psi_0 | \delta^3(\vec{r}_{12}) | \psi_0 \rangle$$

The spin-orbit and tensor force expectation values vanish because the relative orbital angular momentum of each two quark subsystem is zero in S-wave.

They then proceeded to expand (2.1.3) to first order in Δm, justifying the neglect of higher order terms by the effect of the mass difference between the strange and

non-strange quarks. The resulting mass formula describes the eight masses of the 56-plet $(N,\Lambda,\Sigma,\Xi,\Delta,\Sigma^*,\Xi^*,\Omega)$ in terms of four parameters A,B,C and $(\frac{\Delta m_s}{m_u})$.

$$M = A + B\sum_i \frac{\Delta m_i}{m_u} + C\sum_{i>j} \vec{S}_i.\vec{S}_j\left(1 - \frac{\Delta m_i+\Delta m_j}{m_u}\right) \quad (2.1.4)$$

where

$$A = M_0 - 2\alpha_s [\ b - (c+2d)/m_u^2\ ]$$

$$B = m_u - a/m_u - 4\alpha_s(c+2d)/3m_u^2$$

$$C = 32\alpha_s d/9m_u^2$$

Because in an attractive Coulomb potential two fermions in an L=0 state have a higher energy when their spins are aligned than when their spins are opposite, the above formulation was able to give at least a natural qualitative explanation of both the decuplet-octet and the Σ-Λ mass splittings. These mass splittings are related by

$$\Sigma - \Lambda = \tfrac{2}{3}(1 - \frac{m_u}{m_s})\ (\Delta - N) \quad (2.1.5)$$

and are a manifestation of hyperfine splitting.

Using Eq. (2.1.3) they were also able to obtain octet electromagnetic mass differences satisfying the Coleman-Glashow relation

$$\Sigma^+ - \Sigma^- = p-n + \Xi^0 - \Xi^- \quad (2.1.6)$$

and to predict decuplet electromagnetic mass splittings.

The mass difference between the strange and non-strange quarks was used to confirm the successful non-relativistic

quark model prediction of the magnetic moments of baryons

$$\mu(n) = -{}^{2}/_{3}\,\mu(p) \qquad (2.1.7)$$

and resulted in a prediction of $\mu(\Lambda) = -0.6$ which is in better agreement with experiment than the SU(3) prediction of -0.93. Then assuming that the anomalous magnetic moments of quarks are negligible they obtained values for the quark masses

$$m_u = P/\mu(p) = 336 \text{ MeV}$$

and
$$m_s = \frac{2\Sigma^*+\Sigma-3\Lambda}{2(\Sigma^*-\Sigma)}\, m_u = 540 \text{ MeV}$$

The P-wave baryons posed a more serious problem since it was difficult to parameterize $\langle S_{ij} \rangle$ in any model independent way. So without a model to provide the required wavefunctions, the authors could only give a qualitative sketch, which in broad outline was consistent with observation.

For the S-wave mesons the first-order mass formula was written as

$$M = M_0 + \Delta m_1 + \Delta m_2 + a'(m_1^{-1} + m_2^{-1} - 2m_u^{-1}) + (\alpha Q_1 Q_2 - \tfrac{4}{3}\alpha_s)\left[b' - \frac{c'}{m_1 m_2} - d'\left(\frac{1}{m_1^2} + \frac{1}{m_2^2} + \frac{16\vec{S}_1\cdot\vec{S}_2}{3m_1 m_2} \right) \right] + X \qquad (2.1.8)$$

where the parameters are as previously defined with ψ_0 replacing ψ_0, x being an annihilation correction term

relevant to the I = 0 states.

Again expanding to first order they obtained (for I≠0 states)

$$M = A + B\left(\frac{\Delta m_1+\Delta m_2}{m_u}\right) + C\,\vec{S}_1.\vec{S}_2\left(1-\frac{\Delta m_1+\Delta m_2}{m_u}\right) \qquad (2.1.9)$$

and the masses π, K, ρ and K* were obtained in terms of three new parameters and the ratio $(\frac{\Delta m_s}{m_u})$ previously determined from baryon masses. This resulted in the relation

$$\frac{K^* - K}{\rho - \pi} = \frac{m_u}{m_s} \qquad (2.1.10)$$

which is satisfied by observation. The K*-K and the ρ-π mass differences can be explained qualitatively as being hyperfine splittings inversely proportional to the product of the masses of the constituent quarks. Further analysis of the light mesons system ran into problems associated with annihilation channels in the neutral isoscalar mesons.

De Rujula, Georgi and Glashow went on to interpret the resonance at 3.105 GeV as being a vector meson (the J/ψ) and predicted a charm quark mass of 1690 MeV>m_c>1630MeV. They then offered predictions for the levels of charmonium and the masses of charmed mesons and bayrons.

The De Rujula, Georgi, Glashow model is truly impressive, both in the quality of its predictions and in

the scope of its applicability. But what makes it unique is best said in their own words. "Our approach is unique because it is partially dynamical insofar as the form of the force is precisely prescribed by the underlying theoretical structure: There is only SU(3) - singlet exchange, the Fermi term varies with the inverse product of the quark masses, the co-efficients of the spin-orbit and tensor forces are related, etc."

What was now needed was a more detailed model which would explicitly define the form of the confining potential and provide a set of wavefunctions with which to extract information from the Hamiltonian. A number of potential models[20-24] were proposed with varying degrees of success. One of these, the Isgur-Karl model, was particularily successful in dealing with the baryon system and provides the framework for this research.

2.2 The Isgur-Karl Model

In a series of papers[26,27] on baryons in the quark model, published between 1977 and 1980, Isgur and Karl developed in great detail a model describing the interaction of colour confined, point like, constituent quarks through a one gluon exchange mechanism. The remarkable success of this model in describing the baryon system, both in terms of the spectroscopic evidence and the predicted internal

structure of the eigenstates from decay amplitude analysis, is unique. This success has motivated its application to other systems such as mesons[26,29,30] and multiquark states.

Due to the centrality of this model to the present research we describe it below in some detail.

The Isgur-Karl Hamiltonian in its general form may be written

$$H = \sum_i m_i + H_0 + H_{hyp} + H_{so} \qquad (2.2.1)$$

where, m_i is the constituent quark mass

H_0 is the non-relativistic quark Hamiltonian in a colour dependent confining potential

H_{hyp} is the colour hyperfine (magnetic dipole - magnetic dipole) interaction

H_{so} is the interaction of the magnetic moment of a moving quark in colour electric fields.

2.2.1 The Quark Masses

The constituent quark masses in this model are not the so called current quark masses of the QCD lagrangrian. Quarks appear with different masses when we probe hadron structure at different momentum transfer. At high momentum transfers in deep inelastic scattering, quark masses are small and of the order of the current quark masses. At low momentum transfers, appropriate to the study of the

spectroscopy and static properties of hadrons the constituent quark masses appear larger than the current quark masses. This can be expressed as

$$m_q = M_q + a_0$$

where, m_q are the constituent quark masses

M_q are the current quark masses

a_0 are the mass corrections due to gluon couplings, the zero point energy of the quarks and other effects such as our ignorance about the potential, relativistic corrections, etc.

The ground state meson and baryon masses are then roughly equal to the sum of their constituent quark masses.

The constituent quark masses can also be defined using the additivity of the quark magnetic moments inside a hadron. The proton magnetic moment μ_p is given by the sum of its constituent quarks. Since the proton contains two up and one down quark ($|p\rangle = |uud\rangle$) we have

$$\mu_p = 2\mu_u + \mu_d = \frac{2.79e}{M_p} \qquad (2.2.2)$$

where $-e$ is the electron charge and M_p the proton mass.

Since $\mu_q = \frac{Q}{2m_q}$

where Q is the quark electric change and m_q the quark constituent mass. Therefore,

$$\mu_u = \frac{2e/3}{2m_u} \qquad \mu_d = \frac{-e/3}{2m_d}$$

and $$m_u \simeq m_d \simeq \frac{M_p}{2.79} = 336 \text{ MeV} \qquad (2.2.3)$$

The importance of the masses lies in the fact that they are at the origin of flavour symmetry breaking in the model. Typically these are of the order of

$$m_u \simeq m_d \simeq 330 \text{ MeV}$$

$$m_d - m_u \simeq 6 \text{ MeV}$$

$$m_s \simeq 550 \text{ MeV}$$

2.2.2 The Non-relativistic Quark Hamiltonian in a Colour Dependent Confining Potential

This Hamiltonian is written as

$$H_0 = \sum_i \frac{P_i^2}{2m_i} + V_{conf} \qquad (2.2.4)$$

where $\vec{P}_i$ is the constituent quark momentum

m_i is the constituent quark mass

V_{conf} is a confining potential which is assured to be a flavour-independent function of the relative quark separation.

The confining potential is written as the sum of two body potentials $\left[V_{conf} = \sum_{i<j} V_{conf}^{ij} \right]$ of the form

$$V_{conf}^{ij} = \tfrac{1}{2}Kr_{ij}^2 + U(\vec{P}_{ij}) \qquad (2.2.5)$$

where $U(\vec{P}_{ij})$ is some unknown potential and $\frac{1}{2}Kr_{ij}^2$ is a harmonic oscillator potential, K is the spring constant and $\vec{P}_{ij}$ the interparticle separation.

Isgur and Karl do not suggest that the "true" confining potential is of the harmonic oscillator type. In their own words "There is of course no reason..... to assume that the 'true' confining potential is harmonic; a linear potential would be a much more popular choice....". However a confining potential was needed to generate the wavefunctions required to solve the problem and since the non-relativistic three body problem with two particle forces can only be solved for the harmonic oscillator potential, it seemed a good choice. The success met when dealing with the negative parity baryons reinforced the choice, but when it came to applying a harmonic potential to the positive parity baryons a problem arose. While the P-wave baryons are all contained within a single SU(6) multiplet, the positive parity excited baryons are to be found in five distinct SU(6) multiplets and a harmonic oscillator potential would make these multiplets degenerate.

Significantly the inclusion of an anharmonic term in the confining potential allows us to justify the "physics" of the problem by providing us with a vehicle for introducing the effects deriving from QCD (a short range attractive OGE potential and a long range confining potential) and at the same time resolves the degeneracy issue. In first order perturbation theory any potential U will split the harmonic oscillator spectrum into exactly the same pattern. This is shown in fig. (2.1) for the N = 2 supermultiplets. The

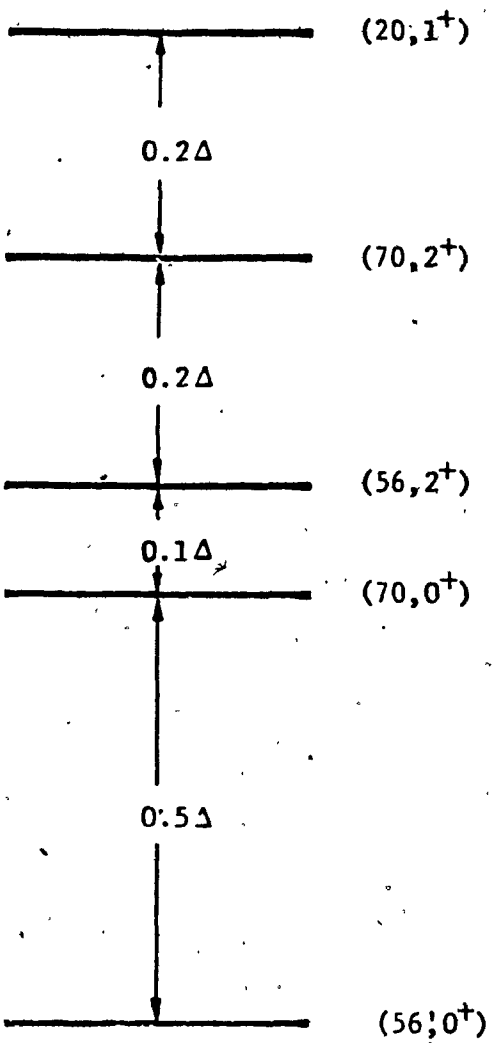

Fig. 2.1 The zeroth-order pattern of N= 2 supermultiplets.

energies of the five multiplets are now written as

$$E(S_S) = E(56,0^+) = E_0 - \Delta \qquad (2.2.6)$$

$$E(S_M) = E(70,0^+) = E_0 - {}^1/_2\Delta \qquad (2.2.7)$$

$$E(D_S) = E(56,2^+) = E_0 - {}^3/_5\Delta \qquad (2.2.8)$$

$$E(D_M) = E(70,2^+) = E_0 - {}^2/_5\Delta \qquad (2.2.9)$$

$$E(P_A) = E(20,1^+) = E_0 \qquad (2.2.10)$$

where we have used the notations

$E(L_\pi)$, where L is the orbital angular momentum state, S,P,D,F....etc. and π is the particular permutation symmetry S,A or M.

$E(\mu,J^R)$, where μ is the SU(6) multiplicity, J is the total angular momentum and p the parity of the state.

and where the two parameters E_0 and Δ are defined as follows

$$E_0 = 5\hbar\omega + \frac{2}{3}b \qquad (2.2.11)$$

$$\Delta = -\frac{5}{4}a + \frac{5}{3}b - \frac{1}{3}c \qquad (2.2.12)$$

where,

$$a = \frac{3\alpha^3}{\pi^{3/2}} \int d^3\vec{\rho}\, U(\sqrt{2}\,\vec{\rho})\, e^{-\alpha^2\rho^2} \qquad (2.2.13)$$

$$b = \frac{3\alpha^5}{\pi^{3/2}} \int d^3\vec{\rho}\, U(\sqrt{2}\,\vec{\rho})\, \rho^2 e^{-\alpha^2\rho^2} \qquad (2.2.14)$$

$$c = \frac{3\alpha^7}{\pi^{3/2}} \int d^3\vec{\rho}\, U(\sqrt{2}\,\vec{\rho})\, \rho^4 e^{-\alpha^2\rho^2} \qquad (2.2.15)$$

and where, $\hbar$ is the Planck constant

ω is the angular frequency of the harmonic oscillator given by $\omega = (3K/m_i)^{1/2}$

α is given by $\alpha = (3km_1)^{1/4}$

$\vec{\rho}$ is a relative co-ordinate given by $\vec{\rho} = \frac{1}{\sqrt{2}} (\vec{r}_1 - \vec{r}_2)$ and arising from the separation of the centre of mass motion in the harmonic oscillator problem.

having reduced the problem to two parameters, the next step was to fit them empirically. This gives

$$E_0 \simeq 2020 \text{ MeV} \quad , \quad \Delta \simeq 420 \text{ MeV}$$

It is interesting to note that an attractive potential such as the Coulomb type potential expected from QCD makes the $(56,0^+)$ multiplet low lying while pushing the unobserved $(20,1^+)$ multiplet very high.

Having introduced the anharmonic term in the confining potential it was no longer possible to obtain exact solutions for the zeroth order eigenstates but a satisfactory description could be obtained by treating the Hamiltonian as a composite of an exactly solvable harmonic oscillator term and a perturbation term.

$$H_0 = \tilde{H}_0 + U \qquad (2.2.16)$$

The Isgur and Karl treatment of the non-strange (S=0) sector; where $m_1=m_2=m_3=m_U$, is followed here in some detail

due to its relevance to this research. The S=-1 sector; where $m_1=m_2=m_u$, $m_3=m_s$ and $m_u \neq m_s$, is outlined only insofar as the more important features of this sector are presented.

In the S=0 sector the Hamiltonian $\tilde{H}_0$ after separating out the centre of mass motion gives

$$\tilde{H}_0 = \frac{P_\lambda^2}{2m_u} + \frac{P_\rho^2}{2m_u} + \frac{3K}{2}(\rho^2+\lambda^2) \qquad (2.2.17)$$

where,

$$\vec{\rho} = \frac{1}{\sqrt{2}}(\vec{r}_1-\vec{r}_2) \quad , \quad \vec{P}_\rho = m_u\frac{d\vec{\rho}}{dt} \qquad (2.2.18)$$

$$\vec{\lambda} = \frac{1}{\sqrt{6}}(\vec{r}_1+\vec{r}_2-2\vec{r}_3) \quad , \quad \vec{P}_\lambda = m_u\frac{d\vec{\lambda}}{dt} \qquad (2.2.19)$$

An illustration of the relative co-ordinate $\vec{\rho}$ and $\vec{\lambda}$ is shown in fig. 2.2. This leads to two uncoupled three dimensional harmonic oscilators which in the equal mass limit have the same spring constant k.

Before going any further it should be pointed out that these potentials depend only on the colour and not on the flavour of the quarks. This means that the eigenstates of the confining potential alone, before the introduction of spin dependent effects, exhibit flavour symmetry breaking only through the appearance of the quark mass in the kinetic energy term. In the equal mass case, no flavour symmetry breaking is included. The colour dependence of the confining potential is obtained by calculating the colour averaged quark-quark potential. The colour wavefunction for

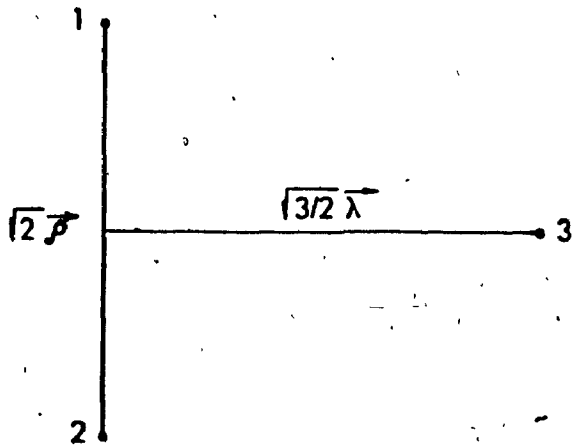

Fig. 2.2 The relative coordinates in the baryon problem.

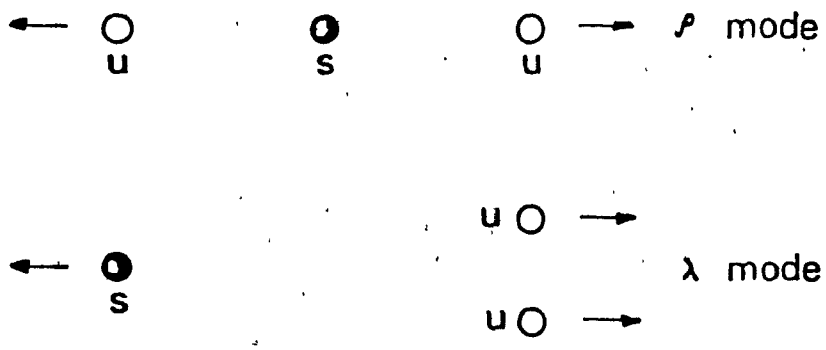

Fig. 2.3 The ρ and λ modes in the baryon problem.

baryons can be written as

$$|B\rangle = \frac{1}{\sqrt{6}} \epsilon^{\alpha\beta\gamma} |q^{\alpha} q^{\beta} q^{\gamma}\rangle \qquad (2.2.20)$$

where, $\epsilon^{\alpha\beta\gamma}$ is the completely antisymmetric unit tensor of rank 3

α, β, γ are the quark colours r,b,g

Using the colour dependent two body potential given by

$$V_{qq}(\vec{r}_{12}) = -V(\vec{r}_{12}) \sum_i \frac{\lambda_1^i}{2} \cdot \frac{\lambda_2^i}{2} \qquad (2.2.21)$$

the colour factor K is found to be

$$K = \langle \Sigma \frac{\lambda^i_1}{2} \cdot \frac{\lambda^i_2}{2} \rangle = \frac{2}{3}$$

for qq pair in a baryon. In the Isgur and Karl formulation, this factor is included in the spring constant K and in the anharmonic potential.

The two orbital angular momenta L_λ and L_ρ corresponding to the oscillators add vectorially to give the total orbital angular momentum

$$\vec{L} = \vec{L}_\lambda + \vec{L}_\rho \qquad (2.2.22)$$

for the bound state. The total space wavefunction is the product of the space wavefunctions of the oscillators. The parity of the bound state is then given by

$$P = (-1)^{\ell_\lambda + \ell_\rho} \qquad (2.2.23)$$

The total angular momentum of the baryon is given by

$$\vec{J} = \vec{L} + \vec{S} \qquad (2.2.24)$$

where $\vec{S}$ is the total quark spin. The bound states can be

labeled by the quantum numbers ℓ_λ and ℓ_ρ and by the number of radial excitations n_λ and n_ρ of the oscillators ($n_{\lambda,\rho}=0,1,2...$). The principal quantum number n for the baryon is then

$$n = 2n_\lambda + 2n_\rho + \ell_\lambda + \ell_\rho \qquad (2.2.25)$$

The space wavefunctions with definite permutation symmetry S,M or A are given by

$$\psi^S_{000} = \frac{\alpha^3}{\pi^{3/2}} e^{-1/2\alpha^2(\rho^2+\lambda^2)} \qquad (2.2.26)$$

$$\psi^{M_\rho}_{111} = \frac{\alpha^4}{\pi^{3/2}} \rho_+ e^{-1/2\alpha^2(\rho^2+\lambda^2)} \qquad (2.2.27)$$

$$\psi^{M_\lambda}_{111} = \frac{\alpha^4}{\pi^{3/2}} \lambda_+ e^{-1/2\alpha^2(\rho^2+\lambda^2)} \qquad (2.2.28)$$

$$\psi^S_{200} = \frac{1}{\sqrt{3}} \frac{\alpha^5}{\pi^{3/2}} (\rho^2+\lambda^2-3\alpha^{-2}) e^{-1/2\alpha^2(\rho^2+\lambda^2)} \qquad (2.2.29)$$

$$\psi^{M_\rho}_{200} = \frac{2}{\sqrt{3}} \frac{\alpha^5}{\pi^{3/2}} \vec{\rho}.\vec{\lambda} e^{-1/2\alpha^2(\rho^2+\lambda^2)} \qquad (2.2.30)$$

$$\psi^{M_\lambda}_{200} = \frac{1}{\sqrt{3}} \frac{\alpha^5}{\pi^{3/2}} (\rho^2-\lambda^2) e^{-1/2\alpha^2(\rho^2+\lambda^2)} \qquad (2.2.31)$$

$$\psi^S_{222} = \frac{1}{2} \frac{\alpha^5}{\pi^{3/2}} (\rho_+^2+\lambda_+^2) e^{-1/2\alpha^2(\rho^2+\lambda^2)} \qquad (2.2.32)$$

$$\psi^{M_\rho}_{222} = \frac{\alpha^5}{\pi^{3/2}} \rho_+\lambda_+ e^{-1/2\alpha^2(\rho^2+\lambda^2)} \qquad (2.2.33)$$

$$\psi^{M_\lambda}_{222} = \frac{1}{2} \frac{\alpha^5}{\pi^{3/2}} (\rho_+^2-\lambda_+^2) e^{-1/2\alpha^2(\rho^2+\lambda^2)} \qquad (2.2.34)$$

$$\psi^A_{211} = \frac{\alpha^5}{\pi^{3/2}} (\rho_+\lambda_z-\rho_z\lambda_+) e^{-1/2\alpha^2(\rho^2+\lambda^2)} \qquad (2.2.35)$$

where we display only the highest state of an orbital

angular momentum multiplet. We use the notation $\Psi^{\pi}_{n\ell m}$ for the wavefunction, where π is the permutation symmetry and n,ℓ,m are the principal and orbital momentum quantum numbers.

The eigenvalues of $\tilde{H}_0$ are given by

$$\tilde{E}_0 = (n+3)\omega \qquad (2.2.36)$$

In the S = -1 sector the degeneracy between the normal modes of the ρ and the λ oscillators is broken. This is because the mass of the λ oscillator (see fig. 2.3) is now

$$m_\lambda = \frac{3m_u m_s}{2m_u+m_s} \qquad (2.2.37)$$

and the angular frequency now given by

$$\omega_\lambda = \left(\frac{3k}{m_\lambda} \right)^{1/2}$$

is lower than the angular frequency ω_ρ which remains unchanged. In addition the permutation symmetry of the wavefunctions is lost. Because of the frequency splitting, the states which in the degenerate case (equal mass quarks) have permutation symmetry S, M_ρ and M_λ, respectively break into $\lambda\lambda$, $\lambda\rho$ and $\rho\rho$ excitations. The lowest eigenstate is the $\lambda\lambda$ excitation. Isgur and Karl have introduced another basis to represent states in the S = -1 sector. In the so called "uds" basis the strange quark is singled out due to its different mass and the only remaining relevant symmetry is that of the u and d quarks.

2.2.3 The Quark Hyperfine Interactions

The confining potentials alone are not sufficient to lift the Δ-N, ρ-π, D*-D, etc. degeneracies. These splittings arise in QCD from the interaction of colour magnetic forces analogous to the magnetic dipole interactions in QED.

The quark hyperfine Hamiltonian is written as

$$H_{hyp} = \sum_{i<j} \frac{k\alpha_s}{m_i m_j} \left\{ \frac{8\pi}{3} \vec{S}_i \cdot \vec{S}_j \delta^3(\vec{r}_{ij}) + \frac{1}{r_{ij}^3} \left[\frac{3\vec{S}_i \cdot \vec{r}_{ij} \vec{S}_j \cdot \vec{r}_{ij}}{r_{ij}^2} - \vec{S}_i \cdot \vec{S}_j \right] \right\} \qquad (2.2.38)$$

The first term is the Fermi contact term and may be visualized as arising from the interaction of the colour magnetic dipole of one quark with the colour magnetic field internal to the other quark ($\vec{\mu}_i \cdot \vec{B}^j_{internal}$). The second term is the tensor term and represents the interaction of the colour magnetic dipole of one quark with the external colour magnetic field of the other ($\vec{\mu}_i \cdot \vec{B}^j_{external}$). These effects are illustrated in fig. 2.4. It is important to point out that if hyperfine interactions exist between quarks, then both Fermi contact and tensor effects must be present and must have the correct relative strength of $\frac{8\pi}{3}$.

The Fermi contact term has a non-zero expectation value only in S-wave, while the tensor term has zero expectation

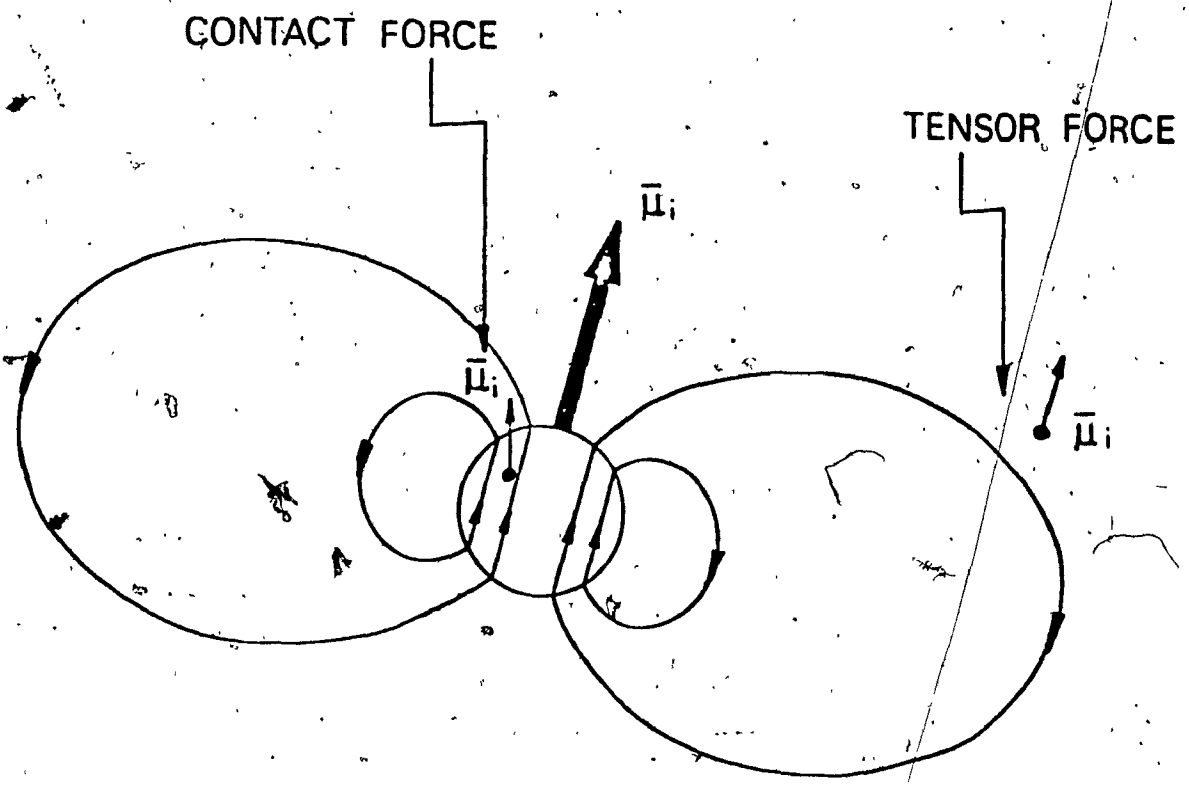

Fig. 2.4 A representation of the origin of the tensor and contact parts of the hyperfine interaction.

value in S-wave. An interesting qualitative observation may be made using a QED analogy to illustrate an important feature of the colour hyperfine interaction and to highlight the fundamental differences between QED and QCD.

In the positronium system in S-wave the configuration with the lowest energy is the one where the spins are antiparallel (parapositronium). If we suppose that the chromomagnetic interaction between quarks is dominated by one gluon exchange forces, then similarly the $q\bar{q}$ states where the spins are aligned should be heavier than the $q\bar{q}$ states where the spins are opposite to each other. This explains why the ρ meson is heavier than the π meson, demonstrating that this SU(6) breaking is analogous to the 21 cm line in hydrogen ground states caused by the Fermi contact interaction.

In the qqq system then we expect a qq pair with parallel spin to be lower in mass than a pair with antiparallel spin. This would result in the Δ mass being lower than the N mass. This is not what happens, and the reason is the non-abelian nature of the chromomagnetic forces. A q in the Δ sees the other two quarks as a $\bar{q}$ and so the chromomagnetic effect is the same as that for a $q\bar{q}$ pair. This explains why the Δ mass is greater than the N mass.

2.2.4 The Spin-Orbit Interaction

Once we accept the analogy with QED, it follows that we should expect to observe other QED-like effects. In particular a colour magnetic dipole moving in a colour electric field should see a colour magnetic field in its rest frame. The interaction of a quark colour magnetic dipole with the colour magnetic field produced in its rest frame by the colour electric field of another quark should produce a torque proportional to $\vec{L}.\vec{S}$., i.e. a spin-orbit effect.

The spin-orbit Hamiltonian for the equal mass case is written as

$$H_{so} = \frac{3}{4m_q^2\rho}\frac{d(V-S/3)}{d\rho}\left[3(\vec{\rho}\times\vec{P}_\rho)(\vec{S}_1+\vec{S}_2) - \frac{1}{\sqrt{3}}(\vec{\rho}\times\vec{P}_\lambda)(\vec{S}_1-\vec{S}_2)\right] \qquad (2.2.39)$$

where, V is the vector potential from one gluon exhange

S is the scalar confining potential.

Isgur and Karl obtained a good fit of the P-wave baryon spectrum by ignoring the spin-orbit interaction; this they attributed to the near cancellation of the one gluon exchange contribution to spin orbit by the Thomas precession in the confining potential. They estimated that spin orbit forces were reduced to less than 10% of the expectation from one gluon exchange in the P-wave baryons and less than about

20% for the positive parity baryons. A further source of error is the anharmonic character of the confining potential. In their paper on the positive parity baryons they state "...the calculation of the spin orbit effects due to Thomas precession in the confining potential becomes doubly uncertain: not only can we not calculate the three body contributions, but even the two body contributions are largely uncertain. Without further understanding of the confinement forces, it is therefore very difficult to know whether this mechanism is still viable...".

In the meson system which comprises the first phase of this research, we cannot ignore the spin-orbit effect as has been pointed out by Schnitzer[31]. We postulate a pure O.G.E. (1/r) potential and calculate the reduction in the $\vec{L}\cdot\vec{S}$ Lorentz spin orbit interaction by Thomas precession in the 1/r and harmonic potentials.

2.2.5 Baryons as a Testing Ground

It is interesting that Isgur and Karl first applied their model to the baryon system. It would seem that a two body system like the meson is simpler to treat theoretically. Perhaps the most important reason is that at the time the baryons were much better known experimentally. Not only were more baryon resonances known, but their masses, widths and decay amplitudes were also better known

than those of the mesons. The P-wave mesons in particular were very poorly known (only the $A_2(1320)2^{++}$ and $B(1230)1^{++}$ were well established), while all seven P-wave baryons in the S=0 sector were well established and had a wealth of measured decay amplitudes (in all there are twenty reasonably well established P-wave baryons). In addition the I=0 light meson data is unreliable due to the annihilation interaction in the isoscalar mesons. It also appears that quarks in a baryon are somewhat more nonrelativistic than quarks in a meson and it is possible that the existence of three quarks in a baryon makes the effective potential seen by each quark less sensitive to precise knowledge of the interquark potential.

Recently published[32] meson data, in particular for the $c\bar{c}$ (charmonium) and $b\bar{b}$ (bottomonium) systems, shown in figs. 1.4 and 2.5 provides us now with a sufficient number of well established states to justify a treatment of mesons.

2.2.6 Results and Conclusions

The success of the Isgur and Karl model lies in its ability to accurately predict with relatively few free parameters, seven at most, a wealth of data. The predictions of the model are not limited to masses and composition of states. Koniuk and Isgur[27] have successfully predicted the decay rates and branching ratios for a large

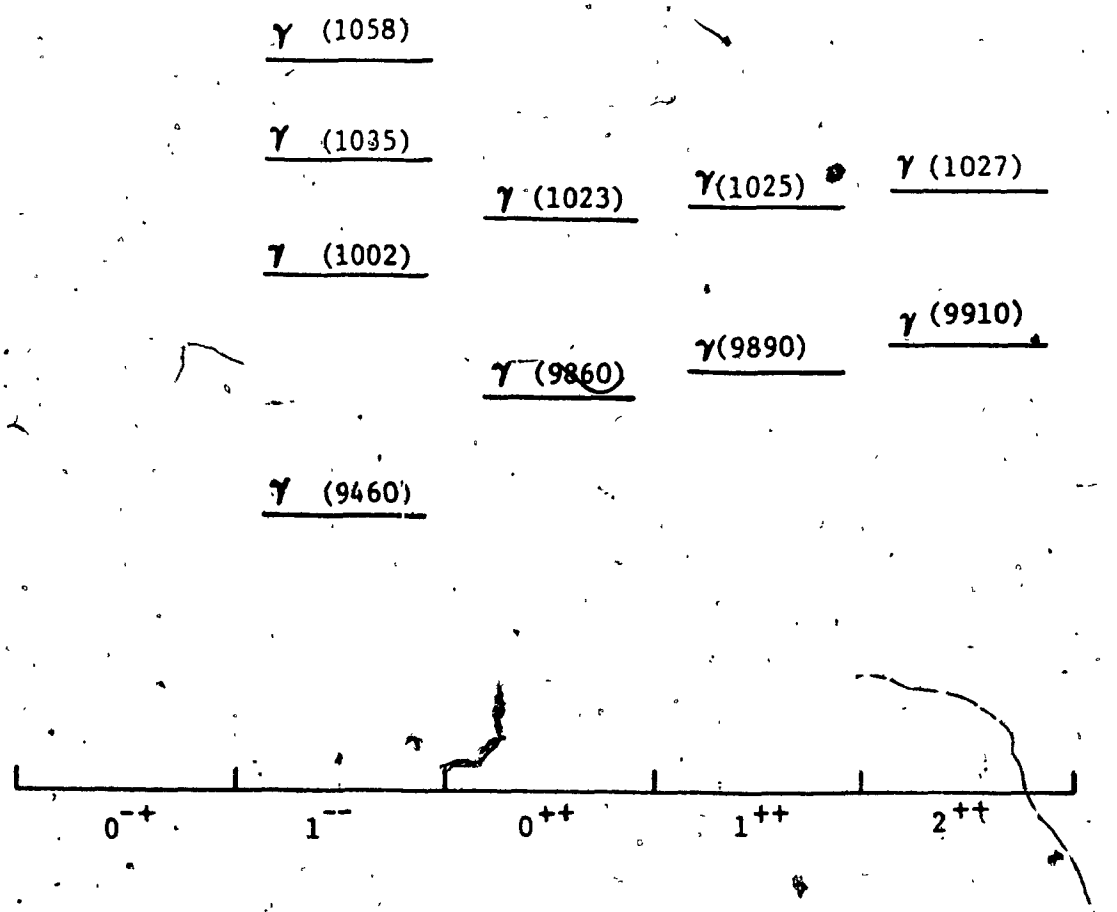

Fig. 2.5 Low lying energy states of bottomonium.

number of baryons. It is a measure of its success, that no other model predicts masses, compositions and decay rates, all in such good agreement with observation. Some predictions of the model together with comparisons to experiment are illustrated in figs. 2.6 to 2.8 and tables 2.1 to 2.2.

In addition the model explains certain features of the baryon spectrum which had hitherto remained a puzzle. The $\Sigma^{*5/2^-} - \Delta^{5/2^-}$ mass splitting is such a case. The hyperfine interactions try to make the $\Sigma^{5/2^-}$ heavier than the $\Delta^{5/2^-}$ by about 25 MeV. The non-degeneracy of the normal modes of the ρ and λ oscillators in the S=-1 sector ($\omega_\rho > \omega_\lambda$) makes a λ excitation (Σ) 75 MeV less massive than a ρ excitation (Δ), this results in the mass of the $\Delta^{5/2^-}$ being $\simeq$50 MeV larger than that of the $\Sigma^{5/2^-}$, in good agreement with observation.

The suppression of the decay

$$\Delta^{5/2^-} \longrightarrow \bar{K}N, \bar{K}^*N$$

is also explained in the model. This decay, illustrated in in fig. 2.9, provides no mechanism for the removal of the orbital angular momentum of the ρ oscillator. The $\Sigma^{5/2^-}$, on the other hand, is a λ excitation and the angular momentum of the λ oscillator can be carried away by the meson.

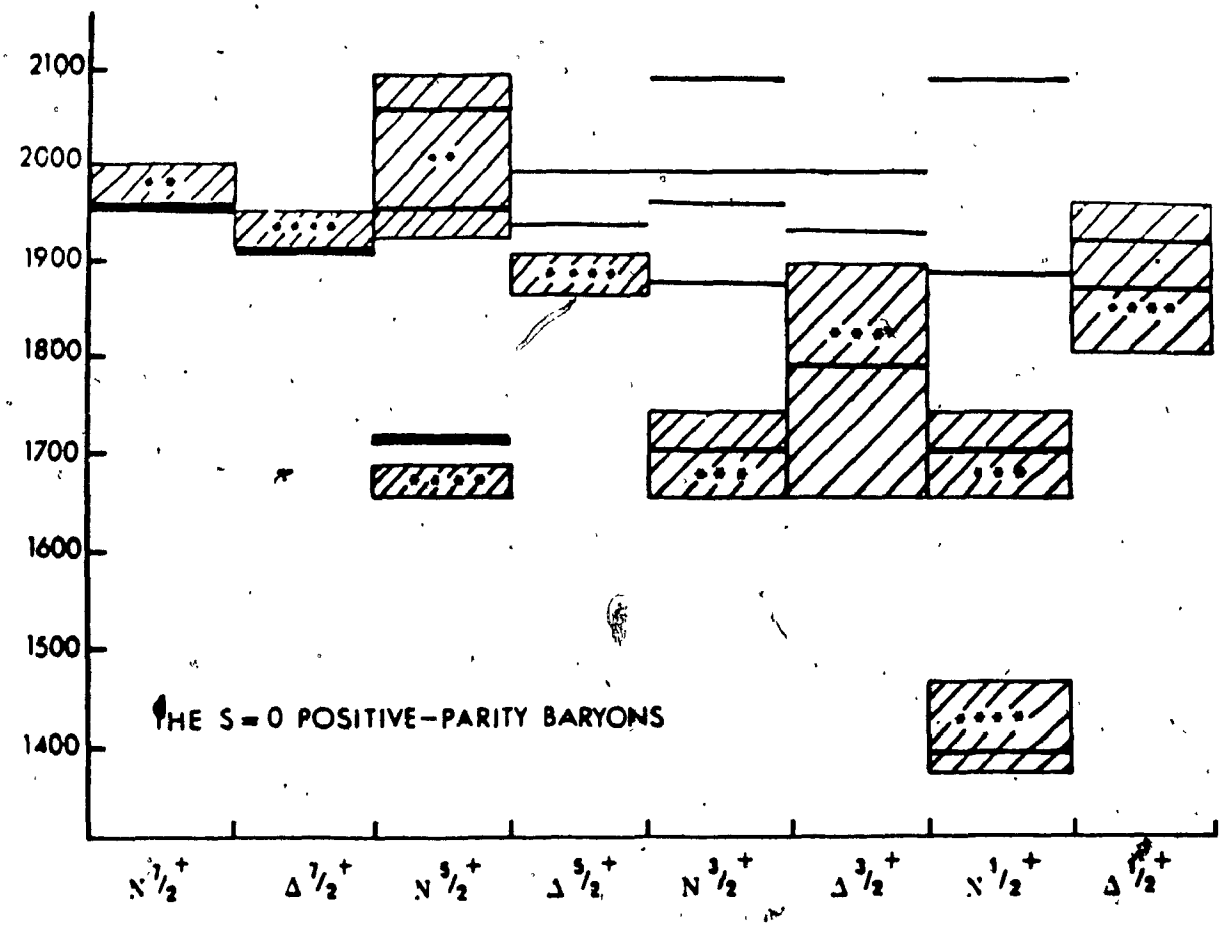

Fig. 2.6 Comparison of the predicted and observed spectrum of low-lying S 0 positive-parity excited baryons (mass in MeV). The solid bars are the predictions of the text. The shaded regions give the likely mass range for those resonances.

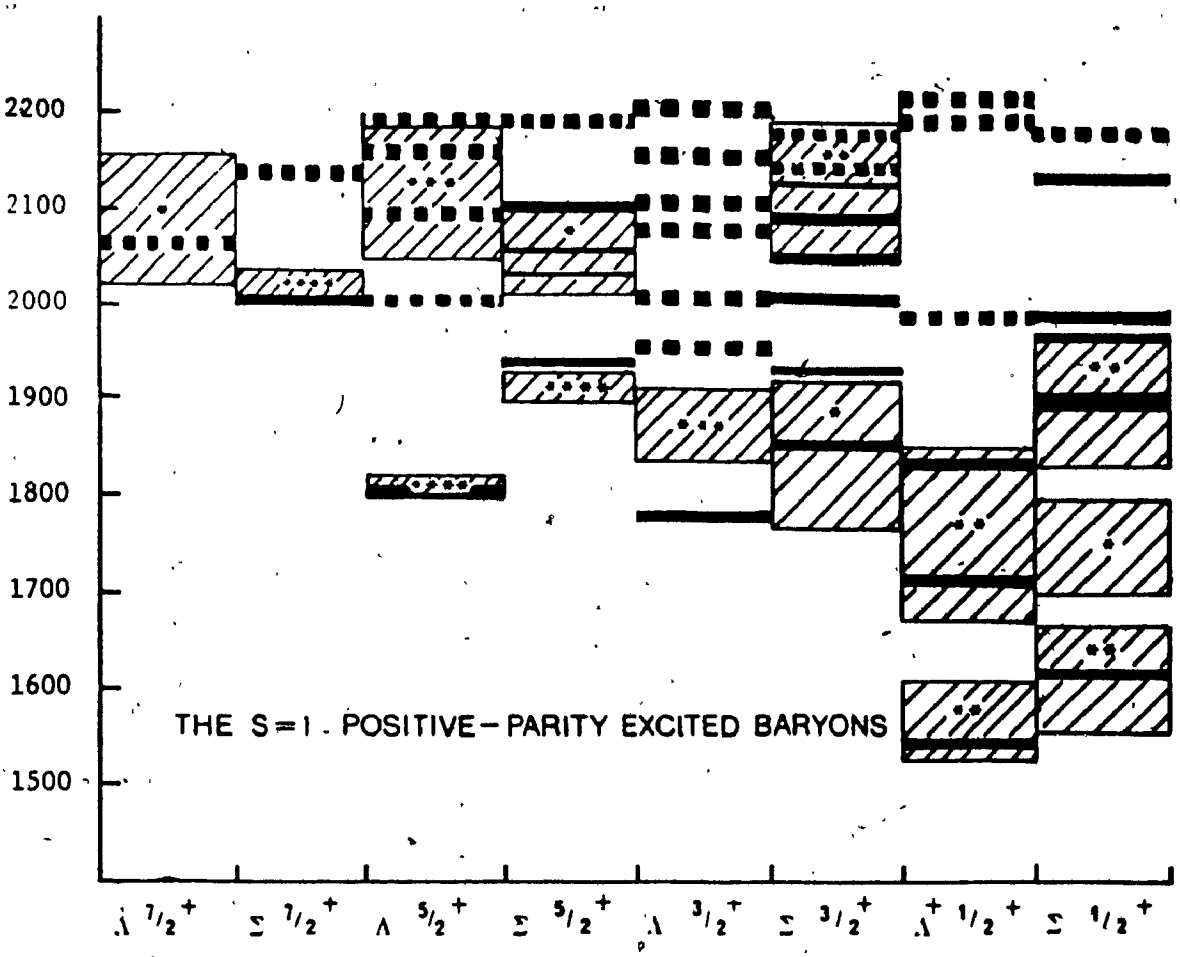

Fig 2.7 Comparison of the predicted and observed spectrum of low-lying S=1 positive-parity excited baryons (mass in MeV). The solid (dotted) bars are those resonances predicted by the model to be strongly (weakly) coupled to $\bar{K}N$.

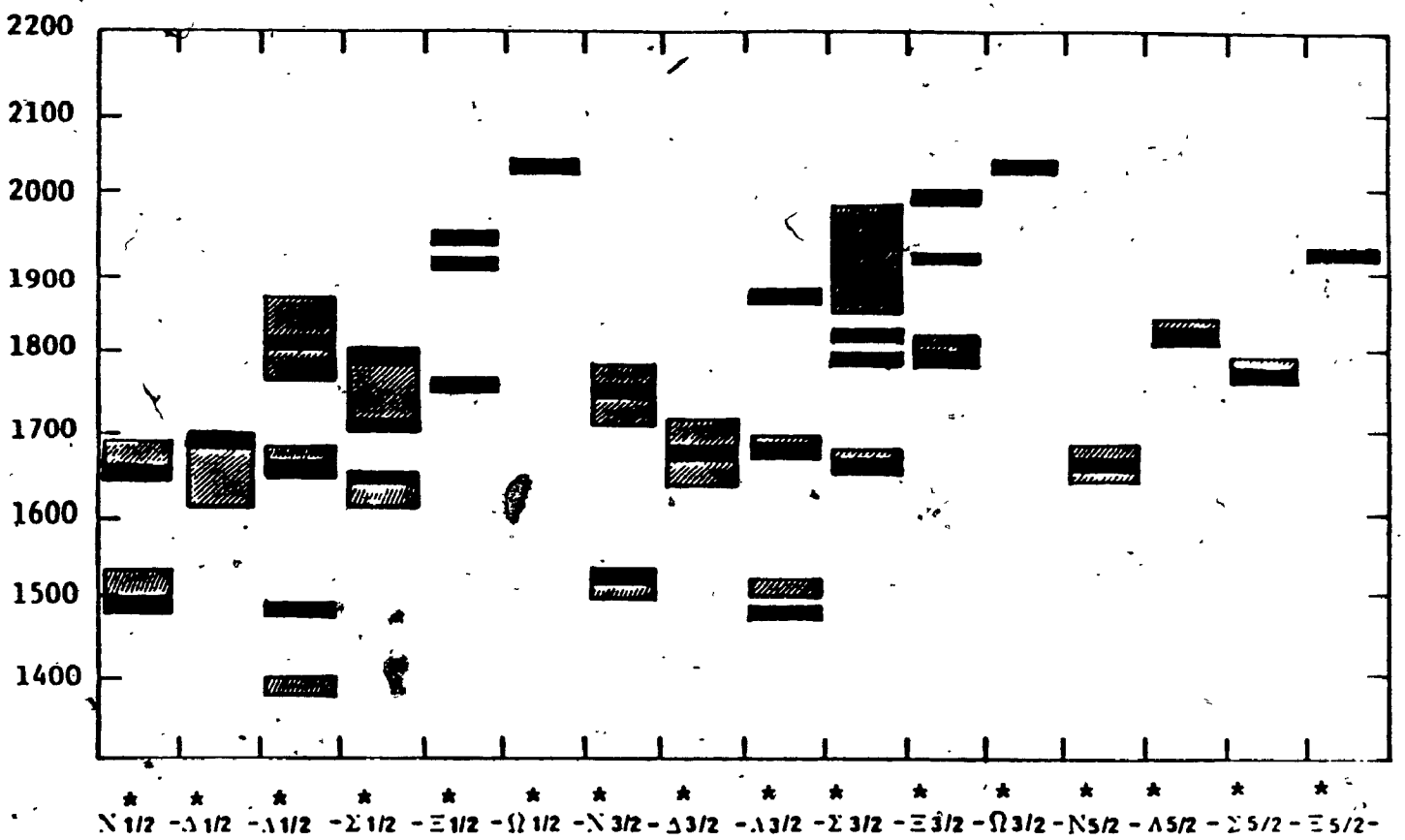

Fig. 2.8 Comparison of the predicted and observed spectrum of negative-parity baryons. The shaded regions corrspond to the likely mass values of resonances; the solid bars are the predictions.

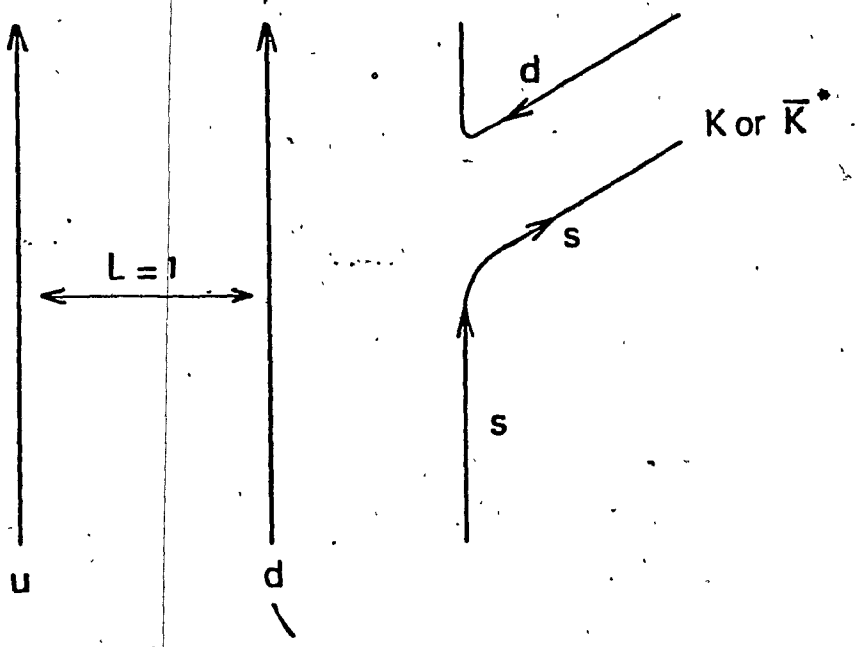

Fig. 2.9 Decay $\Lambda\ ^5/2^- \rightarrow \bar{K}N, \bar{K}^*N$

TABLE 2.1

The calculated spectrum and composition in the S=0 sector.

State	Mass MeV	Composition					
$N\frac{7}{2}^+$	1955	1.00					$N^4D_M\frac{7}{2}^+$
$\Delta\frac{7}{2}^+$	1915	1.00					$\Delta^4D_S\frac{7}{2}^+$
$N\frac{5}{2}^+$	1715	0.88	-0.48	0.01			$N^2D_S\frac{5}{2}^+$
$N\frac{5}{2}^+$	1955	0.48	0.84	0.27			$N^2D_M\frac{5}{2}^+$
$N\frac{5}{2}^+$	2025	-0.13	-0.23	0.96			$N^4D_M\frac{5}{2}^+$
$\Delta\frac{5}{2}$	1940	0.94	0.38				$\Delta^4D_S\frac{5}{2}^+$
$\Delta\frac{5}{2}$	1975	-0.38	0.94				$\Delta^2D_M\frac{5}{2}^+$
$N\frac{3}{2}^+$	1710	-0.17	0.84	-0.52	0.03	0.00	$N^4S_M\frac{3}{2}^+$
$N\frac{3}{2}^+$	1870	0.75	0.34	0.28	-0.46	0.16	$N^2D_S\frac{3}{2}^+$
$N\frac{3}{2}^+$	1955	0.59	-0.05	-0.23	0.61	-0.48	$N^2D_M\frac{3}{2}^+$
$N\frac{3}{2}^+$	1980	-0.23	0.41	0.77	0.28	-0.34	$N^4D_M\frac{3}{2}^+$
$N\frac{3}{2}^+$	2060	0.11	0.08	0.12	0.58	0.79	$N^2P_A\frac{3}{2}^+$
$\Delta\frac{3}{2}^+$	1780	0.98	0.18	-0.10			$\Delta^4S_S\frac{3}{2}^+$
$\Delta\frac{3}{2}^+$	1925	-0.18	0.92	-0.36			$\Delta^4D_M\frac{3}{2}^+$
$\Delta\frac{3}{2}^+$	1975	0.03	0.36	0.94			$\Delta^2D_M\frac{3}{2}^+$
$N\frac{1}{2}^+$	1405	0.99	0.17	0.01	0.00		$N^2S_S\frac{1}{2}^+$
$N\frac{1}{2}^+$	1705	-0.15	0.94	-0.31	-0.07		$N^2S_M\frac{1}{2}^+$
$N\frac{1}{2}^+$	1890	-0.06	0.30	0.83	0.46		$N^4D_M\frac{1}{2}^+$
$N\frac{1}{2}^+$	2055	0.02	-0.08	-0.45	0.89		$N^2P_A\frac{1}{2}^+$
$\Delta\frac{1}{2}^+$	1875	0.64	0.77				$\Delta^2S_M\frac{1}{2}^+$
$\Delta\frac{1}{2}^+$	1925	0.77	-0.64				$\Delta^4D_S\frac{1}{2}^+$

TABLE 2.2

Predicted masses and compositions of negative-parity baryons

State	Predicted splitting[a] from unperburbed mass in units of σ	Predicted mass (MeV)		Predicted (**) and measured composition[b] ^{2}1	^{2}8	^{4}8	^{2}10
$N^*\frac{1}{2}^-$	−0.40	1490	**	...	+0.85	+0.53	...
			HLC	...	+0.85	+0.53	...
			FP	...	+0.73	+0.68	...
$N^*\frac{1}{2}^-$	+0.15	1655	**	...	+0.53	−0.85	...
			HLC	...	+0.53	−0.85	...
			FP	...	+0.68	−0.73	...
$\Delta^*\frac{1}{2}^-$	+0.25	1685	**	...			
$\Delta^*\frac{1}{2}^-$	−0.69[c]	1490	**	+0.90	+0.43	+0.06	...
			HLC	+0.85	+0.46	+0.25	...
			FP1	+0.79	+0.61	−0.04	...
			FP2	+0.72	+0.68	+0.14	...
$\Delta^*\frac{1}{2}^-$	−0.16	1650	**	−0.39	+0.75	+0.58	...
			HLC	−0.30	+0.04	+0.95	...
			FP1	−0.44	+0.63	+0.64	...
			FP2	−0.32	+0.15	+0.94	...
$\Delta^*\frac{1}{2}^-$	+0.34	1800	**	−0.18	+0.50	−0.85	...
			HLC	−0.43	+0.89	−0.17	...
			FP1	−0.41	+0.49	−0.77	...
			FP2	−0.62	+0.71	−0.32	...

In the S = -1 sector the model predicts many more states than are observed experimentally, but this is explained when one takes into account the decoupling of the ρ excitations. The $\Lambda^{3}/_{2}{}^{+}$ is an example. Six of the seven states predicted by the model are decoupled from $\vec{K}N$ decay and the one remaining coupled state is observed experimentally.

2.3 A Consistent Model

In calculating the zeroth order energies of the supermultiplets in the s= -1 sector, Isgur and Karl had to modify the U term matrix elements by a factor $\left(\frac{m_u}{m_s}\right)^{1/2}$ to accomodate the lower energy of a λ excitation relative to a ρ excitation. Kalman, Hall and Misra[33] proposed a method for incorporating quark mass dependence in the matrix elements of the U term. They defined the parameters

$$a(s) = \frac{3\alpha^3 s^{3/2}}{\pi^{3/2}} \int d^3\rho \; U(\sqrt{2}\,\vec{\rho}) \exp(-s\alpha^2\rho) \qquad (2.3.1)$$

$$b(s) = \frac{3\alpha^5 s^{5/2}}{\pi^{3/2}} \int d^3\rho \; U(\sqrt{2}\,\vec{\rho}) \rho^2 \exp(-s\alpha^2\rho) \qquad (2.3.2)$$

$$c(s) = \frac{3\alpha^7 s^{7/2}}{\pi^{3/2}} \int d^3\rho \; U(\sqrt{2}\,\vec{\rho}) \rho^4 \exp(-s\alpha^2\rho^2) \qquad (2.3.3)$$

which when s=1 reduce to the a,b and c parameters defined by Isgur and Karl in the SU(3) limit. In an oscillator model with different oscillators having the same spring constant K, they related the α and ω parameters of the

oscillators by

$$\alpha'^2 = \rho\alpha^2 s \quad , \quad \omega'^2 = \omega^2 s \qquad (2.3.4)$$

where s is some known function of the mass ratio and colour factors. They then represented the matrix elements of the U term as functions of a(s), b(s), c(s) and higher order moments where applicable. Next by constructing quadratic and high order approximations about s=1 they were able to determine values for a(s), b(s) c(s), etc. and thus evaluate the U terms. The importance of this contribution is twofold.

First, it allows us to apply the Isgur and Karl model to different mass sectors in the baryon system without having to indroduce new parameters, as was done by Isgur and Karl for the S=-1 sector of the positive parity baryons. A case in point is $\Sigma^{5/2^-} - \Delta^{5/2^-}$ mass difference, which when calculated in the SU(3) limit gives $\simeq$ 15 MeV but when calculated in the consistent model gives $\simeq$ 50 MeV in agreement with observation. In a further extension to this, Kalman and Pfeffer[34] successfully computed the energy levels of baryons with one charm quark and those with one bottom quark.

Second, it allows us to use parameters derived in one hadron system to evaluate another hadron system. Thus the baryon parameters of Isgur and Karl were used by Kalman, Hall and Misra[33] to calculate the ground state of baryonium,

the baryon parameters of Kalman[35] were used by Kalman and Barbari[36] to compute meson masses in the $s\bar{s}$, $c\bar{c}$ and $b\bar{b}$ systems and to evaluate dibaryon ground states in this research.

A further refinement was introduced to the consistent quark model by Kalman and Sood[37] when they applied the Lagrange method to obtain an exact evaluation of the cross terms in the intercluster matrix elements of the U term.

Armed with a consistent quark model we investigate in this research whether the same forces occur in both mesons and baryons, and having confirmed that this is the case, we go on to calculate hyperfine splitting in the ground state of dibaryons.

CHAPTER 3

MESONS FROM BARYON PARAMETERS: A TEST OF THE IDENTITY OF FORCES

3.1 Introduction

The first phase of this research consisted of testing the consistent quark model by applying baryon parameters to calculate the low lying states of the ϕ, ψ and Υ systems. The objective was to answer the question as to whether within this model, a consistent parameter set can be applied to both mesons and baryons, i.e., whether the same forces occur in both mesons and baryons. It was assumed that the harmonic oscillator strength is the same in mesons and baryons. The baryon parameters were taken from the earlier baryon calculations of Kalman and Hall[38] and Kalman[35]. With the sole exception of the effective quark masses which were obtained by fitting to meson masses, the quarkonium spectra were calculated using baryon parameters.

3.2 The Meson Hamiltonian

The Hamiltonian for the equal mass $q\bar{q}$ system may be written as

$$H = 2m_q + H_0 + H_{hyp} + H_{so} \qquad (3.2.1)$$

where m_q is the common constituent quark mass.

As before,

$$H_o = \sum_i P_i^2/2m_i + \sum_{i<j} V^{ij}_{conf} - \Big(\sum_i P_i\Big)^2/2\sum_i m_i \qquad (3.2.2)$$

Therefore,

$$H_o = \frac{P_1^2}{2m_q} + \frac{P_2^2}{2m_q} + V^{12}_{conf}\ (\vec{P}_1+\vec{P}_2)^2/2m_q \qquad (3.2.3)$$

The confining potential is

$$V^{12}_{conf} = \vec{\lambda}_1.\vec{\lambda}_2\ \left[\tfrac{1}{2}kr^2_{12} + U(\vec{r}_{12})\right] \qquad (3.2.4)$$

and $\langle\vec{\lambda}_1.\vec{\lambda}_2\rangle_{meson} = \frac{4}{3} = 2\langle\vec{\lambda}_1.\vec{\lambda}_2\rangle_{baryon}$

Therefore,

$$V^{12}_{conf} = Kr^2_{12} + 2U(\vec{r}_{12}) \qquad (3.2.5)$$

where we have multiplied the baryon potential by two since the baryon colour factors (2/3) were included in the spring constant K and the anharmonic potential U as previously discussed. The hyperfine term is

$$H_{hyp} = \frac{4}{3}\frac{\alpha_s}{m_q^2}\left\{\frac{8\pi}{3}\vec{S}_1.\vec{S}_2\delta^3(\vec{r}_{12}) + \frac{1}{r^3_{12}}\left[\frac{3\vec{S}_1.\vec{r}_{12}\vec{S}_2.\vec{r}_{12}}{r^2_{12}} - \vec{S}_1.\vec{S}_2\right]\right\} \qquad (3.2.6)$$

and the spin orbit term is

$$H_{so} = H_{so(1G)} + H_{so(HO)} \qquad (3.2.7)$$

where $H_{so(1G)} = \left(\frac{2\alpha_s}{m_q^2 r^3_{12}}\right)\vec{L}.\vec{S}$ (3.2.8)

and $H_{so(HO)} = -\left(\frac{2K}{m_q^2}\right)\vec{L}.\vec{S}$ (3.2.9)

3.2.1 The Harmonic Oscillator Potential

In the centre of mass system the reduced mass harmonic oscillator Hamiltonian is

$$\tilde{H}_o = \frac{P^2}{2\mu} + Kr_{12}^2 \qquad (3.2.10)$$

where

$$r_{12} = |\vec{r}_1 - \vec{r}_2|$$

$$\vec{P} = \mu \frac{d\vec{r}_{12}}{dt}$$

and the reduced mass $\mu = \frac{m_{q_1} m_{q_2}}{m_{q_1} + m_{q_2}} = \frac{m_q}{2}$, $(m_{q_1} = m_{q_2} = m_q)$

For a harmonic oscillator Hamiltonian of the form

$$\tilde{H}_o = \frac{P^2}{2\mu} + \frac{1}{2}\mu\omega^2 r_{12}^2 \qquad (3.2.11)$$

The eigenvalues and eigenfunctions are given by

$$E_n = (n + \tfrac{3}{2})\omega \qquad (3.2.12)$$

where,

$$n = \ell + 2k$$

ℓ is the orbital angular momentum quantum number and k is the number of radial excitations (k=0,1,2,etc.).

$$\Psi_{n\ell m} = N_{n\ell}(\beta r_{12})^{\ell} L_n^{\ell+1/2}(\beta^2 r_{12}^2)\exp(-\tfrac{1}{2}\beta^2 r_{12}^2) Y_{\ell}^{m}(\theta,\phi) \qquad (3.2.13)$$

where $N_{n\ell}$ is a normalization constant given by

$$|N_{n\ell}|^2 = \frac{2\beta^3 k!}{\pi^{1/2}(k+1+1/2)(k+1-1/2)\ldots 3/2 \cdot 1/2}$$

$$\beta^2 = \mu\omega = \frac{m_q\omega}{2}$$

L is the Laguerre polynomial of half-integral order

$Y_\ell^m(\theta,\phi)$ are the spherical harmonics

We then write

$$K = \frac{1}{2}\mu\omega^2$$

Therefore,

$$\beta^2 = \frac{2K}{\omega} \qquad (3.2.14)$$

Next we establish the correspondence between our parameters and the baryon parameters of Isgur and Karl.

Since, $\alpha = (3Km_u)^{1/4}$, $\omega_u = \left[\frac{3K}{m_u}\right]^{1/2}$

therefore with the same spring constant k we get

$$\omega_q = \left[\frac{4}{3}\left[\frac{m_u}{m_q}\right]\right]^{1/2}\omega_u \qquad (3.2.15)$$

and

$$\beta^2 = \left[3\left[\frac{m_u}{m_q}\right]\right]^{-1/2}\alpha^2 \qquad (3.2.16)$$

Where we have labelled the angular frequency ω by the quark flavour since in our research we use different masses.

The eigenvalues of the reduced mass harmonic oscillator Hamiltonian are then give in terms of the baryon parameters

as

$$E_n = (n + \frac{3}{2}) \left[\frac{4}{3} \left(\frac{m_u}{m_q}\right)\right]^{1/2} \omega_u$$

therefore for the ground state and the n = 2 states we get

$$E_0 = \frac{3}{2} \left[\frac{4}{3} \left(\frac{m_u}{m_q}\right)\right]^{1/2} \omega_u \qquad (3.2.17)$$

and

$$E_2 = \frac{7}{2} \left[\frac{4}{3} \left(\frac{m_u}{m_q}\right)\right]^{1/2} \omega_u \qquad (3.2.18)$$

The low lying eigenfunctions for the S and D states are written in terms of β for convenience.

$$\Psi_{000} = \frac{\beta^{3/2}}{\pi^{3/4}} \exp\left(\frac{1}{2} \beta^2 r_{12}^2\right) \qquad (3.2.19)$$

$$\Psi_{200} = \sqrt{\frac{2}{3}} \frac{\beta^{7/2}}{\pi^{3/4}} \left(\frac{3}{2} \beta^{-2} - r_{12}^2\right) \exp\left(-\frac{1}{2} \beta^2 r_{12}^2\right) \qquad (3.2.20)$$

$$\Psi_{222} = \frac{1}{\sqrt{2}} \frac{\beta^{7/2}}{\pi^{3/4}} r_{12}^2 \sin^2\theta e^{2i\phi} \exp\left(-\frac{1}{2} \beta^2 r_{12}^2\right) \qquad (3.2.21)$$

$$\Psi_{221} = -\sqrt{2} \frac{\beta^{7/2}}{\pi^{3/4}} r_{12}^2 \cos\theta \sin\theta e^{i\phi} \exp\left(\frac{1}{2} - \beta^2 r_{12}^2\right) \qquad (3.2.22)$$

$$\Psi_{220} = \frac{1}{\sqrt{3}} \frac{\beta^{7/2}}{\pi^{3/4}} r_{12}^2 (3\cos^2\theta - 1) \exp\left(-\frac{1}{2} \beta^2 r_{12}^2\right) \qquad (3.2.23)$$

$$\Psi_{22-1} = \sqrt{2} \frac{\beta^{7/2}}{\pi^{3/4}} r_{12}^2 \cos\theta \sin\theta e^{-i\phi} \exp\left(-\frac{1}{2} \beta^2 r_{12}^2\right) \qquad (3.2.24)$$

$$\Psi_{22-2} = \frac{1}{\sqrt{2}} \frac{\beta^{7/2}}{\pi^{3/4}} r_{12}^2 \sin^2\theta e^{-2i\phi} \exp\left(\frac{1}{2} \beta^2 r_{12}^2\right) \qquad (3.2.25)$$

3.2.2. The Nonharmonic Potential

Using the baryon parameters of Kalman[35]

m_s = 664.98 MeV, x = 0.58, ω_u= 274.02, δ = 265 MeV,

a(1) = -847.08, b(1) = -705.54, c(1) = -1313.28

where,

$$x = \frac{m_u}{m_s} \quad \text{and} \quad \delta = \frac{4\alpha_s\alpha^3}{3\sqrt{2\pi}\, m_u^2} \quad \text{(the } \Delta\text{-N mass difference)}$$

we solve the quadratic approximations from Kalman, Hall and Misra[33]

$$a(s) \simeq A + Bs + Cs^2 \qquad (3.2.26)$$

$$b(s) \simeq (3A + Bs - Cs^2)/2 \qquad (3.2.27)$$

$$c(s) \simeq (15A + 3Bs - Cs^2)/4 \qquad (3.2.28)$$

for A, B and C.

We have A = -198, B = -733 and C = 84 MeV.

Next we calculate the matrix elements of the anharmonic potential. For example we have

$$\langle\Psi_{000}|2U(\vec{r}_{12})|\Psi_{000}\rangle = \frac{8\beta^3}{\pi^{1/2}}\int_0^\infty r_{12}^2 U(\vec{r}_{12})\exp(-\beta^2 r_{12}^2)\,dr_{12}$$

expressing β in terms of α

$$\langle\Psi_{000}|2U(\vec{r}_{12})|\Psi_{000}\rangle = \frac{2^{3/2}\alpha^3 s^{3/2}}{\pi^{1/2}}\int_0^\infty r_{12}^2 U(r_{12})\exp\left[-\frac{1}{2}s\alpha^2 r_{12}^2\right]dr_{12}$$

where,

$$s = \frac{2}{\sqrt{3}}\left(\frac{m_q}{m_u}\right)^{1/2}$$

From Kalman and Barbari[34] we have the general form

$$a_n(s) = \left[3(\alpha s^{1/2})^{2n+1}/\pi^{3/2}\right]\int d^3\vec{\rho}\,\rho^{2n}\,U(\sqrt{2}\,\vec{\rho})\exp(-s\alpha^2\rho^2)$$

$$= \left\{12\left[\alpha\left(\frac{s}{2}\right)^{1/2}\right]^{2n+1}/\sqrt{\pi}\right\}\int_0^\infty d\vec{r}\,r^{2n}U(\vec{r})\exp\left(-\frac{s}{2}\alpha^2 r^2\right) \qquad (3.2.29)$$

where,

$\vec{r} = \sqrt{2}\,\vec{\rho}$, $n = 1,2,3,$ etc. and $a_n = a,b,c,$ etc.

Using (3.2.29) we get

$$\langle\Psi_{000}|2U(\vec{r}_{12})|\Psi_{000}\rangle = \frac{2}{3}\,a(s) \qquad (3.2.30)$$

similarily,

$$\langle\Psi_{000}|2U(\vec{r}_{12})|\Psi_{200}\rangle = \sqrt{\tfrac{2}{3}}\,a(s) - \frac{2}{3}\sqrt{\tfrac{2}{3}}\,b(s) \qquad (3.2.31)$$

$$\langle\Psi_{200}|2U(\vec{r}_{12})|\Psi_{200}\rangle = a(s) - \frac{4}{3}b(s) + \frac{4}{9}\,c(s) \qquad (3.2.32)$$

$$\langle\Psi_{222}|2U(\vec{r}_{12})|\Psi_{222}\rangle = \frac{8}{45}\,c(s) \qquad (3.2.33)$$

where $a(s)$, $b(s)$ and $c(s)$ are functions of some as yet undetermined quark mass m_q. It follows then from (3.2.1), (3.2.17), (3.2.18), (3.2.30), (3.2.32), (3.2.33) that

$$E_0(S) = 2m_q + \frac{3}{2}\left[\frac{4}{3}\left(\frac{m_1}{m_q}\right)\right]^{1/2}\omega_u + \frac{2}{3}\,a(s) \qquad (3.2.34)$$

$$E_0(S') = 2m_q + \frac{7}{2}\left[\frac{4}{3}\left(\frac{m_1}{m_q}\right)\right]^{1/2}\omega_u + a(s) - \frac{4}{3}b(s) + \frac{4}{9}c(s) \qquad (3.2.35)$$

$$E_0(D) = 2m_q + \frac{7}{2}\left[\frac{4}{3}\left(\frac{m_1}{m_q}\right)\right]^{1/2}\omega_u + \frac{8}{45}\,c(s) \qquad (3.2.36)$$

3.2.3. The Hyperfine Interaction

In S-wave the only spin dependent one gluon exchange interaction present is due to the Fermi contact term. We write $H_{hyp} = H_{cont} + H_{tensor}$ and evaluate the matrix elements of the contact term as follows.

For example,

$$\langle \Psi_{000} X | \frac{32\alpha_s \pi}{9m_q^2} \vec{S}_1 . \vec{S}_2 \delta^3(\vec{r}_{12}) | \Psi_{000} X \rangle$$

$$= \frac{32\alpha_s \pi}{9m_q^2} \langle X | \vec{S}_1 . \vec{S}_2 | X \rangle \langle \Psi_{000} | \delta^3(\vec{r}_{12}) | \Psi_{000} \rangle \qquad (3.2.37)$$

using,

$$\langle X | \vec{S}_1 . \vec{S}_2 | X \rangle = \begin{cases} \frac{1}{4} & \text{for the symmetric spin triplet} \\ -\frac{3}{4} & \text{for the antisymmetric spin singlet} \end{cases}$$

and

$$\langle \Psi | \delta^3(\vec{r}_{12}) | \Psi \rangle = |\Psi(0)|^2$$

Therefore,

$$\langle \Psi_{000} | \delta^3(\vec{r}_{12}) | \Psi_{000} \rangle = \frac{\beta^3}{\pi^{3/2}}$$

we have

$$\langle {}^3S_1 | H_{cont} | {}^3S_1 \rangle = \frac{1}{4} \left[\frac{2^{1/2}}{3^{1/4}}\right]^7 \left[\frac{m_1}{m_q}\right]^{5/4} \delta \qquad (3.2.38)$$

$$\langle {}^1S_0 | H_{cont} | {}^1S_0 \rangle = -\frac{3}{4} \left[\frac{2^{1/2}}{3^{1/4}}\right]^7 \left[\frac{m_1}{m_q}\right]^{5/4} \delta \qquad (3.2.39)$$

similarily,

$$\langle {}^3S_1 | H_{cont} | {}^3S_1 \rangle = \frac{2}{3^{5/4}} \left[\frac{m_1}{m_q}\right]^{5/4} \delta \qquad (3.2.40)$$

$$\langle {}^1S_0 | H_{cont} | {}^1S_0 \rangle = -\frac{2}{3^{1/4}} \left(\frac{m_u}{m_q}\right)^{5/4} \delta \qquad (3.2.41)$$

$$\langle {}^3S_1 | H_{cont} | {}^3S_1 \rangle = \frac{\sqrt{2}}{3^{1/4}} \left(\frac{m_u}{m_q}\right)^{5/4} \delta \qquad (3.2.42)$$

$$\langle {}^1S_0 | H_{cont} | {}^1S_0 \rangle = -\sqrt{2}\, 3^{1/4} \left(\frac{m_u}{m_q}\right)^{5/4} \delta \qquad (3.2.43)$$

The D states on the other hand have one gluon contributions from both the tensor and spin orbit terms and no contributions from the Fermi contact term.

As noted by Isgur and Karl[24] the tensor term is easily evaluated from the identity

$$\langle LSJ | r_{12}^{-3} (3\vec{S}_1 \cdot \vec{r}_{12} \vec{S}_2 \cdot \vec{r}_{12} - \vec{S}_1 \cdot \vec{S}_2) | L'S'J \rangle$$

$$= (-)^{J-L-S} \left[(2L+1)(2S+1)\right]^{1/2} W(LL'SS';2J)$$

$$\langle L \| \frac{\sqrt{3}}{2} r_{12}^{-3} \vec{r}_{12_+} \cdot \vec{r}_{12_+} \| L' \rangle \langle S \| \frac{\sqrt{3}}{2} \vec{S}_{1_-} \cdot \vec{S}_{2_-} \| S' \rangle \qquad (3.2.44)$$

where $W(LL'SS';2J)$ is the Racah co-efficient,

$\langle L \| \frac{\sqrt{3}}{2} r_{12}^{-3} \vec{r}_{12_+} \cdot \vec{r}_{12_+} \| \rangle$ and $\langle S \| \frac{\sqrt{3}}{2} \vec{S}_{1_-} \cdot \vec{S}_{2_-} \| S' \rangle$

are the reduced matrix elements, L is the total orbital angular momentum quantum number, S is the total spin quantum number and J is the total angular momentum quantum number. In appendix A we illustrate a calculation of the tensor term matrix elements. Below we list the results.

$$\langle {}^3D_1 | H_{tensor} | {}^3D_1 \rangle = -\frac{4\sqrt{2}}{5 \times 3^{1/4}} \left(\frac{m_u}{m_q}\right)^{5/4} \delta \qquad (3.2.45)$$

$$\langle {}^3D_2 | H_{tensor} | {}^3D_2 \rangle = \frac{4\sqrt{2}}{5\times 3^{7/4}} \left(\frac{m_u}{m_q}\right)^{5/4} \delta \qquad (3.2.46)$$

$$\langle {}^3D_3 | H_{tensor} | {}^3D_3 \rangle = \frac{-8\sqrt{2}}{35\times 3^{7/4}} \left(\frac{m_u}{m_q}\right)^{5/4} \delta \qquad (3.2.47)$$

In addition the tensor interaction mixes the $^3D_1$ state with the $^3S_1$ and $^3S_1'$ states.

$$\langle {}^3D_1 | H_{tensor} | {}^3S_1 \rangle = \frac{4}{3^{5/4}\sqrt{5}} \left(\frac{m_u}{m_q}\right)^{5/4} \delta \qquad (3.2.48)$$

$$\langle {}^3D_1 | H_{tensor} | {}^3S_1' \rangle = \frac{2\sqrt{2}}{3^{7/4}\sqrt{5}} \left(\frac{m_u}{m_q}\right)^{5/4} \delta \qquad (3.2.49)$$

3.2.4 The Spin-Orbit Interaction

Using (3.2.7) - (3.2.9) we can write the spin-orbit interaction as

$$H_{so} = \frac{2}{m_q^2}\left[\frac{a_s}{r_{12}^3} - K\right] \vec{L}.\vec{S} \qquad (3.2.50)$$

$$= f(r_{12})\, \vec{L}.\vec{S} \qquad (3.2.51)$$

In the coupled representation

$$\langle LSJM | \vec{L}.\vec{S} | L'S'J'M' \rangle = \frac{1}{2}\left[J(J+1)-L(L+1)-S(S+1)\right]\delta_{LL'}\delta_{SS'}\delta_{MM'} \qquad (3.2.52)$$

where M is the total angular momentum projection quantum number.

In appendix B we illustrate a calculation of the spin-orbit matrix elements. Below we list the results.

$$\langle {}^3D_2 | H_{SO} | {}^3D_2 \rangle = 0 \qquad (3.2.53)$$

$$\langle {}^3D_1 | H_{SO} | {}^3D_1 \rangle = -4\sqrt{2}\left(\frac{3}{5}\right)^{1/4}\left(\frac{m_u}{m_q}\right)^{5/4}\delta^- + 2m_u\omega_0^2/m_q^2 \qquad (3.2.54)$$

$$\langle {}^3D_2 | H_{SO} | {}^3D_2 \rangle = \frac{-4\sqrt{2}}{5\times 3^{3/4}}\left(\frac{m_u}{m_q}\right)^{5/4}\delta + 2m_u\omega_0^2/3m_q^2 \qquad (3.2.55)$$

$$\langle {}^3D_3 | H_{SO} | {}^3D_3 \rangle = \frac{8\sqrt{2}}{5\times 3^{3/4}}\left(\frac{m_u}{m_q}\right)^{5/4}\delta - 4m_u\omega_0^2/3m_q^2 \qquad (3.2.56)$$

3.3 Results and Conclusions

Next, we obtain the effective quark masses by fitting to the known meson masses $\phi(1020)$, $\psi(3097)$ and $\Upsilon(9460)$.

In S-wave there are no tensor nor spin orbit interactions, the splitting is caused only by the contact term. So we write the mass mixing matrix for the (ϕ,ϕ'), (ψ,ψ'), and (Υ,Υ') as

$$\begin{bmatrix} 2m_q+E_0+\langle \Psi_{000}|2U(\vec{r}_{12})|\Psi_{000}\rangle+\langle {}^3S_1|H_C|{}^3S_1\rangle & \langle {}^3S_1|H_C|{}^3S_1'\rangle \\ \langle {}^3S_1|H_C|{}^3S_1'\rangle & 2m_q+E_2+\langle \Psi_{200}|2U(\vec{r}_{12})|\Psi_{200}\rangle+\langle {}^3S_1'|H_C|{}^3S_1'\rangle \end{bmatrix} \qquad (3.3.1)$$

we have

$$\begin{bmatrix} E_0(S) + \frac{1}{4}\left(\frac{2}{\sqrt{3}}\right)^{7/2}\left(\frac{m_u}{m_q}\right)^{5/4}\delta & 2\left(\frac{m_u}{3m_q}\right)^{5/4}\delta \\ 2\left(\frac{m_u}{3m_q}\right)^{5/4}\delta & E_0(S') + \frac{\sqrt{2}}{3^{3/4}}\left(\frac{m_u}{m_q}\right)^{5/4}\delta \end{bmatrix} \qquad (3.3.2)$$

The mixing matrix for the (η,η'), (η_c,η_c') and (η_b,η_b') is given by

$$\begin{bmatrix} 2m_q+E_0+\langle\Psi_{000}|2U(\vec{r}_{12})|\Psi_{000}\rangle+\langle {}^1S_0|H_C|{}^1S_0\rangle & \langle {}^1S_0|H_C|{}^1S_0\rangle \\ \langle {}^1S_0|H_C|{}^1S_0\rangle & 2m_q+E_2+\langle\Psi_{200}|2U(\vec{r}_{12})|\Psi_{200}\rangle+\langle {}^1S_0|H_C|{}^1S_0\rangle \end{bmatrix} \tag{3.3.3}$$

we have

$$\begin{bmatrix} E_0(S)-\frac{3}{4}\left(\frac{2}{\sqrt{3}}\right)^{7/2}\left(\frac{m_u}{m_q}\right)^{5/4}\delta & -\frac{2}{3^{1/4}}\left(\frac{m_u}{m_q}\right)^{5/4}\delta \\ -\frac{2}{3^{1/4}}\left(\frac{m_u}{m_q}\right)^{5/4}\delta & E_0(S')-3^{1/4}\sqrt{2}\left(\frac{m_u}{m_q}\right)^{5/4}\delta \end{bmatrix} \tag{3.3.4}$$

where $E_0(S)$ and $E_0(S')$ are given by (3.2.34) and (3.2.35) respectively.

Fitting to the masses of ϕ, ψ and Υ yields m_s = 687 MeV, m_c = 1948 MeV and m_b = 5263 MeV. These effective quark masses are then used to calculate the masses of the other low lying states of the ϕ, ψ and Υ systems as shown in table (3.1). We include for the D states one gluon exchange contributions from the tensor and spin-orbit interactions while noting that there is no contribution from the Fermi contact term.

The fitting to meson masses was prompted by an argument by Lipkin[39] that the effective quark mass may be different in mesons and baryons. So even though a value for m_s was available from the baryon fit of Kalman[35] and a value for m_c

TABLE 3.1 Masses of the low-lying states of ϕ, ψ, and Υ systems. Input parameters are underlined.

ϕ				ψ				Υ			
	Mass (MeV)		%		Mass (MeV)		%		Mass (MeV)		%
State	Experiment	Calculation	Deviation	State	Experiment	Calculation	Deviation	State	Experiment	Calculation	Deviation
ϕ	<u>1020</u>	1020		ψ	<u>3097</u>	3097		Υ	<u>9460</u>	9460	
ϕ'	1684	1798	1 4	ψ'	3685	3890	5 6	Υ'	10020	10194	1 7
η_s	958	757	21 0	η_c	2984	3036	1 7	η_b		9444	
η_s'		1450		η_c'	3592	3807		η_b'		10068	
$^1D_2$		1833		$^1D_2$	3768	3937	4 5	$^1D_2$		10093	

was obtained from a fit of charmed baryons by Kalman and Pfeffer[34], it was decided to leave the quark mass as a free parameter.

The results show that the deviation from experimental value is small enough except for the case of the η' labelled as η_s in table (3.1). This state is known to have a large u and d quark admixture so this result is not surprising. We conclude that the results indicate that the same forces occur in both mesons and baryons and that the consistent quark model provides a suitable framework for relating the two systems.

CHAPTER 4

DIBARYONS IN A CONSISTENT QUARK MODEL

4.1 Multiquark States

As a consequence of $SU(3)_C$ colour confinement, observable hadron states must be colour singlet states. Some years ago experimentalists believed they had found evidence for new kinds of resonances in the nucleon-antinucleon decay channel[40-43] which were named baryonium. They attempted to explain the narrow widths of these states ($\Gamma<20$MeV) by describing them as colour singlet bound states of a diquark and an antidiquark, each having opposite colour charge and separated by an angular momentum barrier. The possibility has since been raised by Weinstein[44], Weinstein and Isgur[45] and Kalman and Misra[46] that these states would spontaneously split up into two mesons as a result of strong internal colour mixing. However, other multiquark colour singlet states can be formed. These so-called quark molecules, may open a whole new field of hadron spectroscopy for which the name "colour chemistry" has been suggested[47,48]. If such states are confirmed experimentally, this would provide strong support for the notion of colour charge. A list of some possible multiquark states is given in table (4.1)

TABLE (4.1)

List of the simplest quark molecules and their decay signature. The lower index is the dimension of the color representation.

Quark moelecule	Suggested name	Decay signature
$(qq)_3(\bar{q}\bar{q})_3$	T-Diquonium	Baryon+antibaryon
$(qq)_6(\bar{q}\bar{q})_{\bar{6}}$	M-Diquonium	Meson+M-diquonium (cascade)
$(q\bar{q})_8(q\bar{q})_8$	Mesonium	Multimesons
$(q\bar{q})(qqq)_8$	Mesobaryon	Baryon+mesons
$(qq)_{\bar{3}}(qq\bar{q})_3$	3-Pseudobaryon	Baryon+Mesons
$(qq)_6(qqq)_{\bar{6}}$	6-Pseudobaryon	Baryon+M-diquonium
$(qqq)_8(qqq)_8$	Dibaryon	Baryon+baryon
$(qqq)_8(\bar{q}\bar{q}\bar{q})_8$	8-Baryonium	Meson cascade
$(qqq)_{10}(\bar{q}\bar{q}\bar{q})_{10}$	10-Baryonium	Meson cascade

Theoretical calculations of the baryonium system in the MIT bag model and in the Isgur-Karl model have been performed by a number of researchers[49,50,44,45]. Kalman, Hall and Misra[33], Kalman and Misra[46] and Kalman and Sood[37] have performed calculations in the consistent quark model.

Six quark configurations have also aroused considerable experimental interest[51-54]. Theoretically, they have been examined both in the context of the NN interaction and as resonant q^6 states or dibaryons. The NN interaction has been investigated by DèTar[55], Libermann[56], Ribiero[57], Maltman and Isgur[29], and others[58]. Bag model calculations for dibaryon resonances in $(q^2)(q^4)$ and $(q^3)(q^3)$ clustering have been performed by Jaffe[59], Aerts and Dover[60], Högaasen and Sorba[61], and others[62]. QCD based potential models have been applied by Maltman[30], Oka and Yazaki[63] and Cvetič[64].

In this research we apply the consistent quark model to dibaryons in $(q^3)(q^3)$ clustering. This is motivated by the success of the model in describing baryon structures and by its success in describing other quark systems in terms of baryon parameters.

4.2 The Dibaryon Hamiltonian

In the ground state there are no tensor nor spin orbit interactions and the Isgur-Karl Hamiltonian is written as

$$H = \sum_{i=1}^{6} m_i + H_0 + H_{contact} \qquad (4.2.1)$$

where $m_i = m$ is the common constituent quark mass.

The H_0 term includes the harmonic oscillator confining potential together with the anharmonic U potential. This is written as

$$H_0 = \sum_{i=1}^{6} \frac{P_i^2}{2m} + \sum_{i<j} V_{conf}^{ij} - \frac{\left(\sum_{i=1}^{6} \vec{P_i}\right)^2}{12m} \qquad (4.2.2)$$

where

$$V_{conf}^{ij} = \vec{\lambda}_i \cdot \vec{\lambda}_j V_{ij} \qquad (4.2.3)$$

and

$$V_{ij} = \left[\frac{1}{2} K r_{ij}^2 + U(\vec{r}_{ij}) \right] \qquad (4.2.4)$$

The Fermi contact term is written as

$$H_{contact} = \frac{8\pi\alpha_s}{3m^2} \sum_{\alpha} \sum_{i<j} (\vec{S}_i \cdot \vec{S}_j) \lambda_i^{\alpha} \lambda_j^{\alpha} \delta^{(3)}(\vec{r}_{ij}) \qquad (4.2.5)$$

where $\alpha = 1,2,\ldots,8$, $i = 1,2,3$ and $j = 4,5,6$

In the following sections we evaluate each of the terms of the Hamiltonian, but before we do this we examine the colour factors.

4.3 The Colour Factors for Three Quark Clustering

If we consider a dibaryon to be made up of two clusters

of three quarks each, then for each cluster in colour $SU(3)_C$

$$3 \otimes 3 \otimes 3 = 1 \oplus 8_{M_A} \oplus 8_{M_S} \oplus 10 \qquad (4.3.1)$$

and

$$\begin{aligned}(3 \otimes 3 \otimes 3) \otimes (3 \otimes 3 \otimes 3) = {} & 1 \otimes 1 + 1 \otimes 8_{M_A} \\ & + 1 \otimes 8_{M_S} + 1 \otimes 10 + 8_{M_A} \otimes 1 + 8_{M_A} \otimes 8_{M_A} + 8_{M_A} \otimes 8_{M_S} \\ & + 8_{M_A} \otimes 10 + 8_{M_S} \otimes 1 + 8_{M_S} \otimes 8_{M_A} + 8_{M_S} \otimes 8_{M_S} \\ & + 8_{M_S} \otimes 10 + 10 \otimes 1 + 10 \otimes 8_{M_A} + 10 \otimes 8_{M_S} + 10 \otimes 10\end{aligned} \qquad (4.3.2)$$

We find that colour singlets arise only from the $1 \otimes 1$ and $8 \otimes 8$ terms. The singlet arising from the $1 \otimes 1$ leads to in-cluster colour factors similar to those of baryons and no inter-cluster colour coupling. The singlet in the

$$8 \otimes 8 = 1 \oplus 8_{M_S} \oplus 8_{M_S} \oplus 10 + \overline{10} + 27 \qquad (4.3.3)$$

can arise from one of three possible cases

$$8_{M_S} \otimes 8_{M_S}$$

$$8_{M_A} \otimes 8_{M_A}$$

$$8_{M_S} \otimes 8_{M_A}$$

and each case corresponds to a different set of colour factors. The composite state must be a colour singlet.

$$\sum_{i=1}^{6} \vec{\lambda}_i^2 = 0 \qquad (4.3.4)$$

We label the clusters as A and B, where cluster A is made up

of quarks 1, 2 and 3, and cluster B is made up of quarks 4, 5 and 6. Each cluster is a colour octet.

$$(\vec{\lambda}_1 + \vec{\lambda}_2 + \vec{\lambda}_3)^2 = (\vec{\lambda}_4 + \vec{\lambda}_5 + \vec{\lambda}_6)^2 = 3 \qquad (4.3.5)$$

and each quark is a colour triplet

$$\lambda_i^2 = \frac{4}{3} \quad , \quad i = 1, 2, 3, 4, 5, 6 \qquad (4.3.6)$$

We decompose (4.3.1) to show the origins of the 8_{M_A} and 8_{M_S}

$$3 \otimes 3 = 6 \oplus \bar{3} \qquad (4.3.7)$$

and

$$3 \otimes (6 \oplus \bar{3}) = (3 \otimes 6) \oplus (3 \otimes \bar{3}) .$$

$$= (8_{M_S} \oplus 10) \oplus (1 \oplus 8_{M_A}) \qquad (4.3.8)$$

We see that the 8_{M_S} arises from the $3 \otimes 6$ and the 8_{M_A} form the $3 \otimes \bar{3}$. Therefore in the 8_{M_S} a quark "sees" the other two quarks in a 6 of colour, while in the 8_{M_A} they appear as a $\bar{3}$.

Next we calculate the colour factors for the three types of octet combinations.

1. $8_{M_S} \otimes 8_{M_S}$

A 3 in one cluster sees the other two quarks in that cluster as a 6. Therefore within each cluster

$$(\vec{\lambda}_i + \vec{\lambda}_j)^2_{i \neq j} = \frac{10}{3} \quad i,j = 1,2,3 \text{ or } 4,5,6 \qquad (4.3.9)$$

$$\vec{\lambda}_i . \vec{\lambda}_j{}_{i \neq j} = \frac{1}{2} \left\{ \frac{10}{3} - \frac{4}{3} - \frac{4}{3} \right\} = \frac{1}{3} \qquad (4.3.10)$$

From the condition that the composite state be a colour singlet

$$(\vec{\lambda}_1 + \vec{\lambda}_2 + \vec{\lambda}_3 + \vec{\lambda}_4 + \vec{\lambda}_5 + \vec{\lambda}_6)^2 = 0 \qquad (4.3.11)$$

$$\sum_{i=1}^{6} \vec{\lambda}_i^2 + 2 \left[\sum_{\substack{i<j \\ i,j=1,2,3}} \vec{\lambda}_i . \vec{\lambda}_j + \sum_{\substack{i<j \\ i,j,=4,5,6}} \vec{\lambda}_i . \vec{\lambda}_j + \sum_{i=1}^{3} \sum_{j=4}^{6} \vec{\lambda}_i . \vec{\lambda}_j \right] = 0 \qquad (4.3.12)$$

Due to the symmetry of the dibaryon we can write

$$\sum_{i=1}^{3} \sum_{j=4}^{6} \vec{\lambda}_i . \vec{\lambda}_j = 9\, \vec{\lambda}_A . \vec{\lambda}_B \qquad (4.3.13)$$

where A = 1,2,3 and B = 4,5,6. From (4.3.12) and (4.3.13) we have

$$\vec{\lambda}_A . \vec{\lambda}_B = -\frac{2}{3} \qquad (4.3.14)$$

which is the inter-cluster colour coupling factor.

2. $8_{M_A} \otimes 8_{M_A}$

In this case a 3 in one cluster sees the other two quarks in that cluster as a $\bar{3}$. Therefore within each cluster

$$(\vec{\lambda}_i + \vec{\lambda}_j)^2_{i \neq j} = \frac{4}{3} \quad i,j = 1,2,3 \text{ or } 4,5,6 \qquad (4.3.15)$$

and $$\vec{\lambda}_i . \vec{\lambda}_{j\, i \neq j} = -\frac{2}{3} \qquad (4.3.16)$$

And as in the previous case we evaluate the inter-cluster coupling. We have

$$\vec{\lambda}_A . \vec{\lambda}_B = 0 \qquad (4.3.17)$$

3. $8_{M_S} \otimes 8_{M_A}$

The colour factors within each cluster are different and have previously been evaluated. The inter-cluster colour factors are

$$\vec{\lambda}_A . \vec{\lambda}_B = -\frac{1}{3} \tag{4.3.18}$$

Next we observe that the symmetry of the dibaryon system requires that the spatial expectation values of the potential be such that

$$V_I = \langle V_{12} \rangle = \langle V_{13} \rangle = \langle V_{23} \rangle = \langle V_{45} \rangle = \langle V_{54} \rangle = \langle V_{46} \rangle \tag{4.3.19}$$

and

$$V_{II} = \langle V_{14} \rangle = \langle V_{15} \rangle = \langle V_{16} \rangle = \langle V_{24} \rangle = \langle V_{25} \rangle$$

$$= \langle V_{26} \rangle = \langle V_{34} \rangle = \langle V_{35} \rangle = \langle V_{36} \rangle \tag{4.3.20}$$

Therefore for the four colour compositions of dibaryons $(\Sigma\, V^{ij}_{conf})$ is given by

$$\begin{aligned} &\text{(a)} \quad 1 \otimes 1 \longrightarrow -4V_I \\ &\text{(b)} \quad 8_{M_S} \otimes 8_{M_S} \longrightarrow 2V_I - 6V_{II} \\ &\text{(c)} \quad 8_{M_A} \otimes 8_{M_A} \longrightarrow -4V_I \\ &\text{(d)} \quad 8_{M_A} \otimes 8_{M_S} \longrightarrow -V_I - 3V_{II} \end{aligned} \tag{4.3.21}$$

4.4 The Harmonic Oscillator Term

We separate out the anharmonic potential U for treatment in the next section and we write the harmonic oscillator Hamiltonian

(4.4.1)

$$H_{HO} = \frac{1}{2m}\sum_{i=1}^{6} P_i^2 - \frac{1}{2m}\left[\sum_{i=1}^{6}\vec{P}_i\right]^2 + \frac{1}{2} f_A K\left[r_{12}^2 + r_{13}^2 + r_{23}^2\right]$$
$$+ \frac{1}{2} f_B K\left[r_{45}^2 + r_{46}^2 + r_{56}^2\right] + \frac{1}{2} f_C K\left[r_{14}^2 + r_{15}^2 + r_{16}^2\right.$$
$$\left. + r_{24}^2 + r_{25}^2 + r_{26}^2 + r_{34}^2 + r_{35}^2 + r_{36}^2\right]$$

where f_A, f_B and f_C are colour factors.

We incorporate a $-\frac{2}{3}$ factor in the spring constant K for ease of comparison with the Isgur-Karl baryon model and we write the colour factors (f_A, f_B, f_C) as follows

(4.4.2)

(a) $1 \otimes 1 \longrightarrow (1, 1, 0)$

(b) $8_{M_S} \otimes 8_{M_S} \longrightarrow (-\frac{1}{2}, -\frac{1}{2}, 1)$

(c) $8_{M_A} \otimes 8_{M_A} \longrightarrow (1, 1, 0)$

(d) $8_{M_A} \otimes 8_{M_S} \longrightarrow (1, -\frac{1}{2}, \frac{1}{2})$

The Hamiltonian H_{HO} separates in terms of a set of orthogonal relative co-ordinates[65]

(4.4.3)

$$\begin{pmatrix} \vec{\rho}_2 \\ \vec{\rho}_3 \\ \vec{\rho}_4 \\ \vec{\rho}_5 \\ \vec{\rho}_6 \end{pmatrix} = \begin{pmatrix} \frac{1}{\sqrt{2}} & \frac{-1}{\sqrt{2}} & 0 & 0 & 0 & 0 \\ \frac{1}{\sqrt{6}} & \frac{1}{\sqrt{6}} & \frac{-2}{\sqrt{6}} & 0 & 0 & 0 \\ 0 & 0 & 0 & \frac{1}{\sqrt{2}} & \frac{-1}{\sqrt{2}} & 0 \\ 0 & 0 & 0 & \frac{1}{\sqrt{6}} & \frac{1}{\sqrt{6}} & \frac{-2}{\sqrt{6}} \\ \frac{1}{\sqrt{6}} & \frac{1}{\sqrt{6}} & \frac{1}{\sqrt{6}} & \frac{-1}{\sqrt{6}} & \frac{-1}{\sqrt{6}} & \frac{-1}{\sqrt{6}} \end{pmatrix} \begin{pmatrix} \vec{r}_1 \\ \vec{r}_2 \\ \vec{r}_3 \\ \vec{r}_4 \\ \vec{r}_5 \\ \vec{r}_6 \end{pmatrix}$$

with the corresponding relative mementa $\pi_i = i\hbar\frac{\partial}{\partial \rho_i}$ and

$$H_{HO} = \frac{1}{2m}\left(\vec{\pi}_2^2 + \vec{\pi}_3^2 + \vec{\pi}_4^2 + \vec{\pi}_5^2 + \vec{\pi}_6^2 \right) + \frac{3}{2} K(f_A + f_C)(\rho_2^2 + \rho_3^2) + \frac{3}{2} K (f_B + f_C)(\rho_4^2 + \rho_5^2) + 3f_C K \rho_6^2 \qquad (4.4.4)$$

H_{HO} is now diagonal and we may write down the energies and corresponding eigenstates. First however we relate the dibaryon parameters to the Isgur-Karl baryon parameters. We write

$$\begin{aligned} \alpha_1^2 &= \alpha^2 S_1 \quad , \quad \omega_1 = \omega S_1 \\ \alpha_2^2 &= \alpha^2 S_2 \quad , \quad \omega = \omega S_2 \\ \alpha_3^2 &= \alpha^2 S_3 \quad , \quad \omega_3 = \omega S_3 \end{aligned} \qquad (4.4.5)$$

where $\alpha^2 = (3mK)^{1/2}$, $\omega = \left(\frac{3K}{m}\right)^{1/2}$ and

$$\begin{aligned} S_1 &= (f_A + f_C)^{1/2} \\ S_2 &= (f_B + f_C)^{1/2} \\ S_3 &= (2f_C)^{1/2} \end{aligned} \qquad (4.4.6)$$

The ground state eigenfunction can now be written as

$$\Psi_{000}(\vec{\rho}_2, \vec{\rho}_3, \vec{\rho}_4, \vec{\rho}_5, \vec{\rho}_6) = \frac{\alpha_1^3 \alpha_2^3 \alpha_3^3}{\pi^{15/2}} \exp\left[-\frac{1}{2}\left(\alpha_1^2 \rho_2^2 + \alpha_1^2 \rho_3^2 + \alpha_2^2 \rho_4^2 + \alpha_2^2 \rho_5^2 + \alpha_3^2 \rho_6^2 \right)\right] \qquad (4.4.7)$$

And the ground state energy is

$$\begin{aligned} E_{HO} &= 3\left(\omega_1 + \omega_2 + \frac{1}{2}\omega_3\right) \\ &= 3\omega\left(s_1 + s_2 + \frac{s_3}{2}\right) \end{aligned} \qquad (4.4.8)$$

The factor (s_1, s_2, s_3) are given by

$$\begin{aligned}
&\text{(a)} \quad 1 \otimes 1 \longrightarrow (1, 1, 0) \\
&\text{(b)} \quad 8_{M_S} \otimes 8_{M_S} \longrightarrow \left(\frac{1}{\sqrt{2}}, \frac{1}{\sqrt{2}}, \sqrt{2}\right) \\
&\text{(c)} \quad 8_{m_A} \otimes 8_{M_A} \longrightarrow (1, 1, 0) \\
&\text{(d)} \quad 8_{M_A} \otimes 8_{M_S} \longrightarrow \left(\sqrt{\tfrac{3}{2}}, 0, 1\right)
\end{aligned} \tag{4.4.9}$$

Using the baryon parameters of Kalman[35] we obtain for $\omega = 274.02$ MeV

$$\begin{aligned}
E_{HO}(1 \otimes 1) &= 6\omega = 1644 \text{ MeV} \\
E_{HO}(8_{M_S} \otimes 8_{M_S}) &= \frac{9\omega}{\sqrt{2}} = 1744 \text{ MeV} \\
E_{HO}(8_{M_A} \otimes 8_{M_A}) &= 6\omega = 1644 \text{ MeV} \\
E_{HO}(8_{M_A} \otimes 8_{M_S}) &= 3\omega\left[\sqrt{\tfrac{3}{2}} + \tfrac{1}{2}\right] = 1418 \text{ MeV}
\end{aligned} \tag{4.4.10}$$

4.5 The Anharmonic Potential

From (4.2.2)-(4.2.4) the anharmonic U potential is given by

$$\begin{aligned}
U = {} & f_A\left[U(\vec{r}_{12}) + U(\vec{r}_{13}) + U(\vec{r}_{23})\right] \\
& + f_B\left[U(\vec{r}_{45}) + U(\vec{r}_{46}) + U(\vec{r}_{56})\right] \\
& + f_C\left[U(\vec{r}_{14}) + U(\vec{r}_{15}) + U(\vec{r}_{16}) + U(\vec{r}_{24})\right. \\
& \quad + U(\vec{r}_{25}) + U(\vec{r}_{26}) + U(\vec{r}_{34}) + U(\vec{r}_{35}) \\
& \quad \left. + U(\vec{r}_{36})\right]
\end{aligned} \tag{4.5.1}$$

The first order contribution of U to the energy is $\langle\Psi_{000}|U|\Psi_{000}\rangle$. We evaluate the in-cluster contributions $\langle\Psi_{000}|U(\vec{r}_{12})|\Psi_{000}\rangle$ and $\langle\Psi_{000}|U(\vec{r}_{45})|\Psi_{000}\rangle$.

$$\langle\Psi_{000}|U(\vec{r}_{12})|\Psi_{000}\rangle = \frac{\alpha_1^4\alpha_2^4\alpha_3^3}{\pi^{15/2}}\int d^3\rho_2 d^3\rho_3 d^3\rho_4 d^3\rho_5 d^3\rho_6 U(\sqrt{2}\rho_2)$$

$$\times \quad \exp\left[-(\alpha_1^2\rho_2^2+\alpha_1^2\rho_3^2+\alpha_2^2\rho_4^2+\alpha_2^2\rho_5^2+\alpha_3^2\rho_6^2)\right]$$

$$= \frac{\alpha^3 s_1^{3/2}}{\pi^{3/2}}\int d^3\rho_2 U(\sqrt{2}\rho_2)\exp\left[-s_1\alpha^2\rho_2^2\right]$$

$$= \frac{a(s_1)}{3} \qquad (4.5.2)$$

where a(s) is given by (3.2.29). Similarily we find

$$\langle\Psi_{000}|U(\vec{r}_{45})|\Psi_{000}\rangle = \frac{a(s_2)}{3} \qquad (4.5.3)$$

In order to evaluate the inter-cluster contributions we transform to a new set of relative co-ordinates $(\vec{\sigma}_2,\vec{\sigma}_3,\vec{\sigma}_4,\vec{\sigma}_5,\vec{\sigma}_6)$ given by

$$\begin{bmatrix}\vec{\rho}_2\\ \vec{\rho}_3\\ \vec{\rho}_4\\ \vec{\rho}_5\\ \vec{\rho}_6\end{bmatrix} = \begin{bmatrix} \frac{1}{2} & -\frac{1}{2} & 0 & \frac{1}{\sqrt{2}} & 0\\ \frac{1}{2\sqrt{3}} & \frac{1}{2\sqrt{3}} & -\frac{1}{\sqrt{3}} & 0 & \sqrt{\frac{2}{3}}\\ -\frac{1}{2} & \frac{1}{2} & 0 & \frac{1}{\sqrt{2}} & 0\\ -\frac{1}{2\sqrt{3}} & -\frac{1}{2\sqrt{3}} & \frac{1}{\sqrt{3}} & 0 & \sqrt{\frac{2}{3}}\\ \frac{1}{\sqrt{3}} & \frac{1}{\sqrt{3}} & \frac{1}{\sqrt{3}} & 0 & 0\end{bmatrix}\begin{bmatrix}\vec{\sigma}_2\\ \vec{\sigma}_3\\ \vec{\sigma}_4\\ \vec{\sigma}_5\\ \vec{\sigma}_6\end{bmatrix}$$

where,

$\vec{r}_{14} = \sqrt{2}\,\vec{\sigma}_2$, $\vec{r}_{25} = \sqrt{2}\,\vec{\sigma}_3$, $\vec{r}_{36} = \sqrt{2}\,\vec{\sigma}_4$,

$\frac{1}{2}(\vec{r}_{12} + \vec{r}_{45}) = \vec{\sigma}_5$ and $\frac{1}{4}(\vec{r}_{13} + \vec{r}_{23} + \vec{r}_{46} + \vec{r}_{56}) = \vec{\sigma}_6$

We substitute the new set of relative co-ordinates in the exponent of the ground state wavefunction and then using the Lagrange method remove the cross-product terms by suitable transformations and we express the quadratic form as a sum of squares. The calculations are too lengthy to show here but we write the results below.

The exponent $-\frac{1}{2}(\alpha_1^2\rho_2^2 + \alpha_1^2\rho_3^2 + \alpha_2^2\rho_4^2 + \alpha_2^2\rho_5^2 + \alpha_3^2\rho_6^2)$ transforms to $-\frac{1}{2}(\beta_1^2\sigma_2^2 + \beta_2^2\Omega_3^2 + \beta_3^2\Omega_4^2 + \beta_4^2\Omega_5^2 + \beta_5^2\Omega_6^2)$ where $\vec{\Omega}_3$, $\vec{\Omega}_4$, $\vec{\Omega}_5$ and $\vec{\Omega}_6$ are a new set of relative co-ordinates and β_1^2, β_2^2, β_3^2, β_4^2, β_5^2 are co-efficients given by

$$\beta_1^2 = \frac{3\alpha^2 s_1 s_2 s_3}{(s_1 s_3 + s_2 s_3 + s_1 s_2)} \qquad (4.5.4)$$

$$\beta_2^2 = \frac{4\alpha^2 s_1 s_2 (s_1 s_3 + s_2 s_3 + s_1 s_2)}{(s_1 + s_2)(s_1 s_3 + s_2 s_3 + 4 s_1 s_2)} \qquad (4.5.5)$$

$$\beta_3^2 = \frac{\alpha^2 (s_1 s_3 + s_2 s_3 + 4 s_1 s_2)}{3(s_1 + s_2)} \qquad (4.5.6)$$

$$\beta_4^2 = \frac{\alpha^2 (s_1 + s_2)}{2} \qquad (4.5.7)$$

$$\beta_5^2 = \frac{2\alpha^2 (s_1 + s_2)}{3} \qquad (4.5.8)$$

We then write the ground state wavefunction in terms of the new co-ordinates

$$\Psi_{000}(\vec{\sigma}_2,\vec{\Omega}_3,\vec{\Omega}_4,\vec{\Omega}_5,\vec{\Omega}_6) = \frac{\alpha^{15/2}s_1^{3/2}s_2^{3/2}s_3^{3/2}}{\pi^{15/2}}$$

$$\exp\left[-\frac{1}{2}(\beta_1^2\sigma_2^2+\beta_2^2\Omega_3^2+\beta_3^2\Omega_4^2+\beta_4^2\Omega_5^2+\beta_5^2\Omega_6^2)\right] \qquad (4.5.9)$$

and we evaluate $\langle\Psi_{000}|U(\vec{r}_{14})|\Psi_{000}\rangle$ to get

$$\langle\Psi_{000}|U(\vec{r}_{14})|\Psi_{000}\rangle = \frac{\alpha^{15}s_1^3s_2^3s_3^{3/2}}{\pi^{15/2}}\int d^3\sigma_2 d^3\Omega_3 d^3\Omega_4 d^3\Omega_5 d^3\Omega_6$$

$$\times U(\sqrt{2}\vec{\sigma}_2)\exp\left[-(\beta_1^2\sigma_2^2+\beta_2^2\Omega_3^2+\beta_3^2\Omega_4^2+\beta_4^2\Omega_5^2+\beta_5^2\Omega_6^2\right]$$

$$\langle\Psi_{000}|U(\vec{r}_{14})|\Psi_{000}\rangle = \left(\frac{3\alpha}{2}\right)^3\left[\frac{s_1s_2s_3}{\pi(s_1s_2+s_2s_3+s_1s_3)}\right]^{3/2}$$

$$\int d^3\sigma_2 U(\sqrt{2}\vec{\sigma}_2)\exp\left[-\beta_1^2\sigma_2\right]$$

Therefore,

$$\langle\Psi_{000}|U(\vec{r}_{14})|\Psi_{000}\rangle = \frac{\sqrt{3}}{8}a\left[\frac{3s_1s_2s_3}{s_1s_2+s_2s_3+s_1s_3}\right] \qquad (4.5.10)$$

From the permutation symmetry of the ground state we have from (4.5.1)

$$\langle\Psi_{000}|U|\Psi_{000}\rangle = 3f_a\langle\Psi_{000}|U(\vec{r}_{12})|\Psi_{000}\rangle$$
$$+ 3f_b\langle\Psi_{000}|U(\vec{r}_{45})|\Psi_{000}\rangle$$
$$+ 9f_c\langle\Psi_{000}|U(\vec{r}_{14})|\Psi_{000}\rangle \qquad (4.5.11)$$

Using (3.2.26) - (3.2.28) we evaluate the matrix elements of the anharmonic potential. We have in MeV

	$\langle f_A U(\vec{r}_{12})\rangle$	$\langle f_B U(\vec{r}_{45})\rangle$	$\langle f_C U(\vec{r}_{16})\rangle$
$1 \otimes 1$	-282	-282	0
$8_{M_S} \otimes 8_{M_S}$	112	112	-164
$8_{M_A} \otimes 8_{M_A}$	-282	-282	0
$8_{M_A} \otimes 8_{M_S}$	-323	33	- 21

The total energy in S-wave excluding hyperfine interaction is given by

$$E_{TOTAL} = 6m + E_{HO} + \langle \Psi_{000} | U | \Psi_{000} \rangle \qquad (4.5.13)$$

and we have for m= 385.69 MeV (Kalman[35])

(a) $1 \otimes 1 = 2264$ MeV

(b) $8_{M_S} \otimes 8_{M_S} = 3252$ MeV

(c) $8_{M_A} \otimes 8_{M_A} = 2264$ MeV

(d) $8_{M_A} \otimes 8_{M_S} = 2668$ MeV

4.6 The Hyperfine Interaction

The one gluon exchange interaction between quarks in a dibaryon gives rise to a Fermi contact interaction in the ground state. The Hamiltonian has the form

$$H_{contact} = -\frac{8\pi\alpha_s}{3m^2} \sum_{\alpha} \sum_{i<j} (\vec{s}_i \cdot \vec{s}_j) \lambda_i^{\alpha} \lambda_j^{\alpha} \delta^{(3)}(\vec{r}_{ij})$$

The spatial integrals required for the contact term are reduced to three by the spatial symmetry of the dibaryon system. We have

$$\langle \delta^{(3)}_{12} \rangle = \langle \delta^{(3)}_{13} \rangle = \langle \delta^{(3)}_{23} \rangle \qquad (4.6.1)$$

$$\langle \delta(\vec{r}_{45}) \rangle = \langle \delta(\vec{r}_{46}) \rangle = \langle \delta(\vec{r}_{56}) \rangle \qquad (4.6.2)$$

$$\begin{aligned} \langle \delta(\vec{r}_{14}) \rangle &= \langle \delta(\vec{r}_{15}) \rangle = \langle \delta(\vec{r}_{16}) \rangle = \langle \delta(\vec{r}_{24}) \rangle \\ &= \langle \delta(\vec{r}_{25}) \rangle = \langle \delta(\vec{r}_{26}) \rangle = \langle \delta(\vec{r}_{34}) \rangle \\ &= \langle \delta(\vec{r}_{35}) \rangle = \langle \delta(\vec{r}_{36}) \rangle \end{aligned} \qquad (4.6.3)$$

We can then write the Hamiltonian as

$$\begin{aligned} H_{cont} = &- \frac{8\pi\alpha_s}{2m^2} \langle \delta^{(3)}(\vec{r}_{14}) \rangle \sum_{\alpha} \sum_{i<j} \vec{s}_i \cdot \vec{s}_j \, \lambda_i^{\alpha} \cdot \lambda_j^{\alpha} \\ &- \frac{8\pi\alpha_s}{2m^2} (\vec{\lambda}_1 \cdot \vec{\lambda}_2) \left[\langle \delta^{(3)}(\vec{r}_{12}) \rangle - \langle \delta^{3}(\vec{r}_{14}) \rangle \right] \\ &\left[\vec{S}_1 \cdot \vec{S}_2 + \vec{S}_1 \cdot \vec{S}_3 + \vec{S}_2 \cdot \vec{S}_3 \right] \\ &- \frac{8\pi\alpha_s}{2m^2} (\vec{\lambda}_4 \cdot \vec{\lambda}_5) \left[\langle \delta^{(3)}(\vec{r}_{45}) \rangle - \langle \delta^{3}(\vec{r}_{14}) \rangle \right] \\ &\left[\vec{S}_4 \cdot \vec{S}_5 + \vec{S}_4 \cdot \vec{S}_6 + \vec{S}_5 \cdot \vec{S}_6 \right] \end{aligned} \qquad (4.6.4)$$

since $\vec{r}_{12} = \sqrt{2}\vec{\beta}$ and $\vec{r}_{14} = \sqrt{2}\vec{\beta}'$ we can write

$$\delta^{(3)}(\vec{r}_{12}) = 2^{-3/2}\delta^{(3)}(\vec{r}) \qquad (4.6.5)$$

and

$$\delta^{(3)}(\vec{r}_{14}) = 2^{-3/2}\delta^{(3)}(\vec{r}) \qquad (4.6.6)$$

From (4.6.5) and (4.4.7) we have

$$\langle\delta^{(3)}(\vec{r}_{12})\rangle = \frac{s_1^{3/2}\alpha^3}{(2\pi)^{3/2}} \qquad (4.6.7)$$

and from the symmetry of the clusters we can write

$$\langle\delta^{(3)}(\vec{r}_{45})\rangle = \frac{s_1^{3/2}\alpha^3}{(2\pi^{3/2}} \qquad (4.6.8)$$

From (4.6.7) and (4.5.9) we have

$$\langle\delta^{(3)}(\vec{r}_{14})\rangle = \left[\frac{9}{4}\right]^{3/2}\frac{\alpha^3}{(2\pi)^{3/2}}\left[\frac{s_1s_2s_3}{s_1s_2+s_2s_3+s_1s_3}\right]^{3/2} \qquad (4.6.9)$$

In general $\langle\delta^3(\vec{r}_{ij})\rangle$ can be written as

$$\langle\delta^3(\vec{r}_{ij})\rangle = f(s_1,s_2,s_3)\frac{\alpha^3}{(2\pi)^{3/2}} \qquad (4.6.10)$$

Also $\left[\frac{8\pi\alpha_s}{3m^2}\right]$ can be written as

$$\left[\frac{8\pi\alpha_s}{3m^2}\right] = \delta\frac{(2\pi)^{3/2}}{\alpha^3} \qquad (4.6.11)$$

where δ is the Δ - N mass difference

Therefore from (4.6.10) and (4.6.11) we have

$$\frac{8\pi\alpha_s}{3m^2}\langle\delta^{(3)}(\vec{r}_{ij})\rangle = f(s_1s_2s_3)\delta \qquad (4.6.12)$$

Using δ = 265 (Kalman[35]) we tabulate below the products $f(s_1s_2s_3)\delta$ for the different colour symmetry configurations in MeV.

	$\frac{8\pi\alpha_s}{3m^2}\langle\delta^{(3)}(\vec{r}_{12})$	$\frac{8\pi\alpha_s}{3m^2}\langle\delta^{(3)}(\vec{r}_{45})\rangle$	$\frac{8\pi\alpha_s}{3m^2}\langle\delta^{(3)}(\vec{r}_{14})\rangle$
$1 \otimes 1$	265	265	0
$8_{M_S} \otimes 8_{M_S}$	158	158	135
$8_{M_A} \otimes 8_{M_A}$	265	265	0
$8_{M_A} \otimes 8_{M_S}$	359	0	0

Next we tabulate the colour factor products appearing in the second term of (4.6.4)

	$\vec{\lambda}_1.\vec{\lambda}_2$	$\vec{\lambda}_4.\vec{\lambda}_5$
$1 \otimes 1$	$-\frac{2}{3}$	$-\frac{2}{3}$
$8_{M_S} \otimes 8_{M_S}$	$\frac{1}{3}$	$\frac{1}{3}$
$8_{M_A} \otimes 8_{M_A}$	$-\frac{2}{3}$	$-\frac{2}{3}$
$8_{M_A} \otimes 8_{M_S}$	$-\frac{2}{3}$	$\frac{1}{3}$

The spin states for each cluster are given in $SU(2)_S$ by

$$2 \otimes 2 \otimes 2 = 4_S + 2_{M_S} + 2_{M_A}$$

where the 4_S is a symmetric spin $3/2$ multiplet and the 2_{M_S} and 2_{M_A} are mixed symmetry spin $1/2$ doublets.

The SU(2) Casimir operator S^2 for three quarks (a,b,c) in a cluster may be written as

$$S^2 = (\vec{S}_a+\vec{S}_b+\vec{S}_c)^2 = S_a^2 + S_b^2 + S_c^2 + 2(\vec{S}_a\cdot\vec{S}_b+\vec{S}_a\cdot\vec{S}_c+\vec{S}_b\cdot\vec{S}_c)$$

where $S_a^2 = S_b^2 = S_c^2 = \frac{1}{2} (\frac{1}{2} + 1) = \frac{3}{4}$

therefore

$$\vec{S}_a\cdot\vec{S}_b + \vec{S}_a\cdot\vec{S}_c + \vec{S}_b\cdot\vec{S}_c = \frac{1}{2} (S(S+1) - \frac{9}{4}) \qquad (4.6.13)$$

and we have the following table

	$S(S+1)$	$\frac{1}{2} (S(S+1)- \frac{9}{4})$
4_S	$\frac{15}{4}$	$\frac{3}{4}$
2_{M_S}	$\frac{3}{4}$	$-\frac{3}{4}$
2_{M_A}	$\frac{3}{4}$	$-\frac{3}{4}$

Following Jaffe[59] and Høgaasen and Sorba[61] we note that the products $\Lambda^a S^i$ are among the generators of colour-spin $SU(6)_{CS}$. The generators of $SU(6)_{CS}$ are defined as follows

$$\{\Omega\} = \begin{cases} 2\left(\frac{2}{3}\right)^{1/2} S^k, & k = 1,2,3 \\ \Lambda^\alpha, & \alpha = 1,2,\ldots,8 \\ 2\Lambda^\alpha S^k \end{cases} \qquad (4.6.14)$$

The 35 generators are normalized to $Tr\Omega^2 = 4$.

We then express the colour-spin products of the Fermi contact interaction in terms of the quadratic Casimir operators of $SU(3)_C$, $SU(2)_S$ and $SU(6)_{CS}$.

$$-4 \sum_\alpha \sum_{i<j} (\vec{S}_i \cdot \vec{S}_j)\, \Lambda_i^\alpha\, \Lambda_j^\alpha = 48 + \frac{4}{3} S(S+1) + \frac{1}{2} C_{3_C} - \frac{1}{2} C_{6_{CS}} \qquad (4.6.15)$$

The Casimir operators are defined as follows:

$$C_{6_{CS}} = \sum_{u=1}^{35} \left(\sum_{i=1}^{6} \Omega_i^u \right)^2 ,$$

$$C_{3_C} = \sum_{\alpha=1}^{8} \left(\sum_{i=1}^{6} \Lambda_i^\alpha \right)^2 ,$$

$$S(S+1) = \sum_{k=1}^{3} \left(\sum_{i=1}^{6} S_i^k \right)^2 .$$

For colour singlets $C_{3_C} = 0$ and (4.6.15) becomes

$$-\sum_\alpha \sum_{i<j} (\vec{S}_i \cdot \vec{S}_j)\, \Lambda_i^\alpha\, \Lambda_j^\alpha = 12 + \frac{1}{3} S(S+1) - \frac{1}{8} C_{6_{CS}} \qquad (4.6.16)$$

In S-wave the product of the colour-spin and flavour representations is antisymmetric as a result of the generalized Pauli principle. A rotation by 90° of the Young tableaux of the colour-spin representation gives us the

associated (conjugate) Young tableaux for the flavour representation. A symmetry (antisymmetry) in the colour-spin indices then induces the corresponding antisymmetry (symmetry) in flavour. Table (4.2) shows the six quark $SU(6)_{CS}$ representations, their dimensions, the value of the $SU(6)_{CS}$ Casimir operator, the colour singlet spin content and the corresponding flavour representaions with their dimensions for different numbers of flavours.

We note from (4.6.16) and table (4.2) that the contact interaction is most attractive (negative) for states in which the quarks are in the largest possible representations of $SU(6)_{CS}$.

Following an argument suggested by Högaasen and Sorba[41] we can approximately express the contact interaction as being proportional to $(8N + {}^{8}/_{3}\, S(S+1) - {}^{1}/_{2}C_{6})$ where N is the number of quarks. We calculate the lowest (most attractive) value this interaction can have for different numbers of flavours and find the following

Number of flavours	Lowest Eigenvalue of H_{cont}	Total Spin	CS representation
1	48K	0	[1]
2	$\frac{8}{3}$ K	1	[175]
3	- 24K	0	[490]

where K is the proportionality constant.

TABLE 4.2

Spin	Flavour Dim. F=1	F=2	F=3	F=4	F=6	SU(6)$_{CS}$	Val. of C_4(CS)
0	1	7	28	84	462	1	0
1	0	5	35	140	1050	35	48
1 and 3	0	1	$\overline{10}$	50	490	175	96
0 and 2	0	3	27	126	1134	189	80
1	0	0	10	70	840	280	96
1 and 2	0	0	8	64	896	896	120
0	0	0	1	$\overline{10}$	175	490	144
0	0	0	0	10	280	840	144
1	0	0	0	6	189	1134	160

Flavour and colour spin representation of six q states.

We note that for one and two flavours the interaction is repulsive. The six quarks will experience a repulsive core effect and will separate into groups to minimize the energy. It is interesting that the state with the lowest energy in the two flavour case has the same quantum numbers as the deuteron.

For three or more flavours the interaction is attractive. This is not sufficient for obtaining bound dibaryon states. The criterion for the stability of a dibaryon is that the mass of the dibaryon be smaller than the masses of all the states it can decay into. If the dibaryon decays into two spin $^1/_2$ baryons, the eigenvalue of H_{cont} will be $-8k'$. If the wavefunction overlap is assumed to be the same for both the three quark and six quark systems then $k' = k$.

We write a simple mass formula for a multiquark system with quarks in S-wave

$$M = \sum_{i=1}^{N} m_i + \langle H_{cont} \rangle \qquad (4.6.17)$$

where M is the total multiquark system mass, and m_i are the effective constituent quark masses.

If we further assume that the effective constituent quark masses are the same in a dibaryon and in a baryon, we can write the stability criterion as follows,

$$\langle H_{cont} \rangle_{6q} \quad > \quad 2 \langle H_{cont} \rangle_{3q} = -.16 \text{ K}$$

This suggests that stable dibaryons would exist only in the [490] and higher dimensional representations of $SU(6)_{CS}$. It also suggests that no stable dibaryons can be constructed with less than three quark flavours.

Next we consider the symmetry requirements. In S-wave an N-quark state must be assigned to the completely antisymmetric representation of the group $SU(T)_{CS}$ of dimension $\frac{N(N-1)(N-2)}{6}$. In addition the state must be a colour singlet. Here T=6F, where F is the number of quark flavours.

A quark is a [6] in $SU(6)_{CS}$ and thus a three quark cluster is given by,

$$6 \otimes 6 \otimes 6 = 56_S + 70_{M_S} + 70_{M_A} + 20_A$$

The $SU(3)_C \times SU(2)_S$ decompositions of the three quark $SU(6)_{CS}$ multiplets are as follows,

$$56 = (10,4) + (8,2)$$

$$70 = (10,2) + (8,4) + (8,2) + (1,2)$$

$$20 = (1,4) + (8,2)$$

Here we use the notation (d_C, d_S), where d_C is the dimension of the $SU(3)_C$ representation and d_S is the dimension of the $SU(2)_S$ representation.

The isospin group $SU(2)_F$ allows the following representations for three quarks

$$2 \otimes 2 \otimes 2 = 4_S \oplus 2M_S \oplus 2M_A$$

The antisymmetric colour-spin-flavour combinations of the two three quark clusters are then limited to,

$([20]_{CS}\ [4]_F)\ ([20]_{CS}\ [4]_F)$

$([20]_{CS}\ [4]_F)\ ([70]_{CS}\ [2]_F)$

$([70]_{CS}\ [2]_F)\ ([70]_{CS}\ [2]_F)$

The $SU(6)_{CS}$ colour-spin representations are shown below

$$20 \otimes 20 = 1 + 35 + 175 + 189$$

$$20 \otimes 20 = 35 + 189 + 280 + 896$$

$$70 \otimes 70 = 175 + 189 + 280 + 490 + 840 + 896 + 896 + 1134$$

The $SU(3)_C \otimes SU(2)_S$ decompositions of the six quark $SU(6)_{CS}$ multiplets are as follows,

$$1 = (1,1)$$

$$35 = (8,1) + (8,3) + (1,3)$$

$$175 = (27,3)+(8,5)+(1,7)+(10,1)+(\overline{10},1)+(8,3)+(1,3)$$

$$189 = (1,1)+(1,5)+(8,1)+(8,5)+(8,3)+(8,3)+(10,3)+(\overline{10},3)+(27,1)$$

$$280 = (27,3)+(10,5)+(10,3)+(8,5)+(10,1)+(\overline{10},1)+(8,3)+(8,3)+(8,1)+(1,3)$$

$$490 = (\overline{10},7)+(27,5)+(8,5)+(35,3)+(10,3)+(\overline{10},3)+(8,3)+(28,1)+(27,1)+(1,1)$$

$$840 = (35,5)+(35,3)+(10,7)+(27,5)+(27,3)+(10,5)+(27,1)$$
$$+(10,3)+(10,3)+(\overline{10},3)+(8,5)+(10,1)+(8,3)+(8,3)$$
$$+(8,1)+(1,1)$$

$$896 = (35,3)+(35,1)+(27,5)+(27,3)+(27,3)+(10,5)+(\overline{10},5)$$
$$+(8,7)+(27,1)+(10,3)+(10,3)+(\overline{10},3)+(8,5)+(8,5)$$
$$+(10,1)+(8,3)+(8,3)+(8,3)+(8,1)+(8,1)+(1,5)$$
$$+(1,3)$$

$$1134 = (28,3)+(27,7)+(35,5)+(35,3)+(27,5)+(10,5)+(35,1)$$
$$+(\overline{10},5)+(8,5)+(27,3)+(27,3)+(10,3)+(8,3)+(8,3)$$
$$+(10,1)+(\overline{10},1)+(8,1)+(1,3)$$

We now proceed to construct the eigenstates of H_{cont} for each of the allowed cluster combinations.

A. $([20]_{CS}[4]_F)([20]_{CS}[4]_F)$

The $SU(6)_{CS}$ representations for these 16 dimensional flavour multiplets contain the following colour singlets,

(1,1) c 1

(1,3) c 35

(1,3), (1,7) c 175

(1,1), (1,5) c 189

Only the (1,4) ⊠ (1,4) colour-spin decompositions of the three quark clusters can contribute to the J=3 and J=2 dibaryons. The wavefunctions are then given by

$$| \, 3^+, 16[175] \, \rangle = | \, (1,4)4; \; (1,4)4; \; (1,7) \, \rangle$$

and,

$$|\ 2^+,16[189]\ \rangle = |\ (1,4)4;\ (1,4)4;\ (1,5)\ \rangle$$

The J=1 wavefuctions are orthogonal linear combinations of (1,4) ■ (1,4) and (8,2) ■ (8,2).

$$|\ 1^+,\ 16[35]\ \rangle = \left(\frac{1}{5}\right)^{1/2} |\ (1,4)4;\ (1,4)4;\ (1,3)\ \rangle + \left(\frac{4}{5}\right)^{1/2} |\ (8,2)4;\ (8,2)4;\ (1,3)\ \rangle$$

and,

$$|\ 1^+,\ 16[175]\rangle = \left(\frac{4}{5}\right)^{1/2} |\ (1,4)4;\ (1,4)4;\ (1,3)\ \rangle - \left(\frac{1}{5}\right)^{1/2} |\ (8,2)4;\ (8,2)4;\ (1,3)\ \rangle$$

Since both these states arise from the same combinations of colour-spin representations and since they both have the same total spin, H_{cont} mixes these two states and the eigenstates are given by

$$|\ 1^+,\ 16\ \rangle = .601\ |\ 1^+,16[35]\rangle - .798\ |\ 1^+,16[175]\rangle$$

and,

$$|\ 1^+,\ 16^*\rangle = .798\ |\ 1^+,16[35]\rangle + .601\ |\ 1^+,16[175]\rangle$$

Similarily the J=0 wavefunctions are orthogonal linear combinations of (1,4) ■ (1,4) and (8,2) ■ (8,2)

$$|\ 0^+,\ 16\ [1]\ \rangle = \left(\frac{1}{5}\right)^{1/2} |\ (1,4)4;\ (1,4)4;\ (1,1)\ \rangle + \left(\frac{4}{5}\right)^{1/2} |\ (8,2)4;\ (8,2)4;\ (1,1)\ \rangle$$

and,

$$| \ 0^+, \ 16[189]\rangle = \left(\frac{4}{5}\right)^{1/2} | \ (1,4)4; \ (1,4)4; \ (1,1) \ \rangle$$

$$- \left(\frac{1}{5}\right)^{1/2} | \ (8,2)4; \ (8,2)4; \ (1,1) \ \rangle$$

Again H_{cont} mixes these two states and the eigenstates are

$$| \ 0^+, \ 16 \ \rangle = .928 \ | \ 0^+,16 \ [1]\rangle + .373 \ | \ 0^+,16[189]\rangle$$

and,

$$| \ 0^+, \ 16^* \rangle = .373 \ | \ 0^+,16 \ [1]\rangle - .928 \ | \ 0^+,16[189]\rangle$$

The Eigenvalues are shown in table (4.3).

We note here that in evaluating the matrix elements of H_{cont} we require an expression for the contact interaction which is independant of the total colour-spin Casimir operator. This is because the off-diagonal terms of the matrix mix states of different total colour-spin representations. It is easy to define an expression equivalent to (4.6.16) which is a function only of the in-cluster and intercluster colour factors and the cluster and total spin Casimir operators. This is given by,

$$- \sum_{\alpha} \sum_{i<j} (\vec{S}_i . \vec{S}_j) \ \Lambda_i^{\alpha} \ \Lambda_j^{\alpha} = -\frac{1}{2} \Big[\ \Lambda_1 . \Lambda_2 \ (S_{123}(S_{123}+1) - \frac{9}{4})$$

$$+ \Lambda_4 . \Lambda_5 (S_{456}(S_{456}+1) - \frac{9}{4})$$

$$+ \Lambda_1 . \Lambda_4 (S_{tot}(S_{tot}+1) - S_{123}(S_{123}+1) - S_{456}(S_{456}+1)) \Big]$$

(4.6.18)

B. $([20]_{CS}[4]_F)$ $([70]_{CS}[2]_F)$

The $SU(6)_{CS}$ representations for these flavour octets contain the following colour singlets,

$$(1,3) \subset 35$$

$$(1,1),\ (1,5) \subset 189$$

The 280 and 896 dimensional $SU(6)_{CS}$ representations are ignored because for two flavours it is impossible to make a sufficiently antisymmetric flavour combination to correspond to the conjugate of the $SU(6)_{CS}$ Young tableaux.

The wavefunction of the J=2 dibaryons is constructed from linear combinations of (1,4) ⊗ (1,2) and (8,2) ⊗ (8,4) we write,

$$|\ 2^+,\ 8[189]\ \rangle = \left(\frac{1}{9}\right)^{1/2} |\ (1,4)4;\ (1,2)2;\ (1,5)\ \rangle$$

$$+ \left(\frac{8}{9}\right)^{1/2} |\ (8,2)4;\ (8,4)2;\ (1,5)\ \rangle$$

For the J=1 dibaryons we have

$$|\ 1^+,\ 8\ [35]\ \rangle = \left(\frac{3}{43}\right)^{1/2} |\ (1,4)4;\ (1,2)2;\ (1,3)\ \rangle$$

$$+ \left(\frac{24}{43}\right)^{1/2} |\ (8,2)4;\ (8,4)2;\ (1,3)\ \rangle$$

$$+ \left(\frac{16}{43}\right)^{1/2} |\ (8,2)4;\ (8,2)2;\ (1,3)\ \rangle$$

And for the J=0 dibaryons

$$|\ 0^+,\ 8[189]\rangle = |\ (8,2)4;\ (8,2)2;\ (1,1)\ \rangle$$

The Eigenvalues are shown in table (4.3).

C. $([70]_{CS}[2]_F)\ ([70]_{CS}[2]_F)$

The $SU(6)_{CS}$ representation for these four dimensional flavour multiplets contain the following colour singlets,

(1,3), (1,7) ⊂ 175

(1,1), (1,5) ⊂ 189

As before the higher dimensional $SU(6)_{CS}$ representations are ignored. The wavefunctions are

$$|\ 3^+,\ 4[175]\rangle = |\ (8,4)2;\ (8,4)2;\ (1,7)\ \rangle$$

$$|\ 2^+,\ 4[189]\rangle = \left(\frac{4}{7}\right)^{1/2} |\ (8,4)2;\ (8,4)2;\ (1,5)\ \rangle + \left(\frac{3}{7}\right)^{1/2} |\ (8,4)2;\ (8,2)2;\ (1,5)\ \rangle$$

$$|\ 1^+,\ 4[175]\rangle = \left(\frac{16}{37}\right)^{1/2} |\ (8,4)2;\ (8,4)2;\ (1,3)\ \rangle + \left(\frac{12}{37}\right)^{1/2} |\ (8,4)2;\ (8,2)2;\ (1,3)\ \rangle + \left(\frac{8}{37}\right)^{1/2} |\ (8,2)2;\ (8,2)2;\ (1,3)\ \rangle + \left(\frac{1}{37}\right)^{1/2} |\ (1,2)2;\ (1,2)2;\ (1,3)\ \rangle$$

$$|\ 0^+,\ 4[189]\rangle = \left(\frac{16}{25}\right)^{1/2} |\ (8,4)2;\ (8,4)2;\ (1,1)\ \rangle + \left(\frac{8}{25}\right)^{1/2} |\ (8,2)2;\ (8,2)2;\ (1,1)\ \rangle + \left(\frac{1}{25}\right)^{1/2} |\ (1,2)2;\ (1,2)2;\ (1,1)\ \rangle$$

Again the Eigenvalues are shown in table (4.3).

4.7 Results and conclusion

The magnetic interaction energies, the masses and the baryonic content of the dibaryon states are listed in table (4.3) below. It is difficult to compare these results with other theoretical calculations since there are very few published calculated dibaryon masses in the (u,d) sector. One such calculation by Hwang, Lichtenberg and Namgund[44] predicts two different masses for a 0^+ dibaryon composed of a diquark and a quadriquark. These are 2540 MeV using a Krolikowski-type equation and 2950 MeV using a Tadorov-type equation. They suggest that the true mass of a dibaryon resonance of this type lies between the values calculated with the two different wave equations. We predict several 0^+ states in this mass range. The calculations by Maltman[30] and Maltman and Isgur[29] using a variational method offer no predictions for masses. Maltman and Isgur[29] specialize to a system of 3u and 3d quarks and are concerned mainly with the NN nuclear interaction. Maltman[30] investigates the possibility of deeply bound dibaryon resonances but presents no mass calculations. The bag model calculations by Jaffe[59] and Aerts and Dover[60] all deal with the H dibaryon (strongeness=-2). An analysis of our results suggests the following,

a) No stable dibaryons exist in the u,d sector. The predicted masses are large enough to permit strong decay.

b) ΔΔ dibaryons experience a short range repulsion due to the magnetic interaction.

c) NN and ΔN dibaryons in mixed symmetric states experience a weak short range attractive magnetic interaction.

TABLE 4.3

Masses and magnetic interaction energies of S-wave dibaryons

STATE	MAGNETIC INTERACTION	MASS	BARYONIC CONTENT
$I3^+,16[175]\rangle$	265	2529	ΔΔ
$I2^+,16[189]\rangle$	265	2529	ΔΔ
$I1^+,16\ \rangle$	134	2580	ΔΔ
$I1^+,16^*\rangle$	322	2842	ΔΔ
$I0^+,16\rangle$	438	3024	ΔΔ
$I0^+,16^*\rangle$	150	2542	ΔΔ
$I2^+,8[189]\ S\rangle$	−160	2722	ΔN
$I2^+,8[189]\ A\rangle$	80	2523	ΔN
$I1^+,8[\ 35]\ S\rangle$	−127	2692	ΔN
$I1^+,8[\ 35]\ A\rangle$	− 8	2536	ΔN
$I0^+,8[189]\ S\rangle$	41	2754	ΔN
$I0^+,8[189]\ S\rangle$	2	2715	ΔN
$I3^+,4[175]SS\rangle$	−551	2700	NN
$I3^+,4[175]SA\rangle$	179	2847	NN
$I3^+,4[175]AS\rangle$	179	2847	NN
$I3^+,4[175]AA\rangle$	265	2529	NN
$I2^+,4[189]SS\rangle$	−235	2892	NN
$I2^+,4[189]SA\rangle$	− 51	2742	NN
$I2^+,4[189]AS\rangle$	64	2645	NN
$I2^+,4[189]AA\rangle$	190	2540	NN
$I1^+,4[175]SS\rangle$	− 63	2951	NN
$I1^+,4[175]SA\rangle$	17	2778	NN

TABLE 4.3 (CONTINUED)

STATE	MAGNETIC INTERACTION	MASS	BARYONIC CONTENT
$11^+,4[175AS\rangle$	31	2632	NN
$11^+,4[175]AA\rangle$	99	2525	NN
$10^+,4[189]SS\rangle$	-204	2836	NN
$10^+,4[189]SA\rangle$	104	2770	NN
$10^+,4[189]AS\rangle$	104	2770	NN
$10^+,4[189]AA\rangle$	88	2495	NN

The notation we use to describe the states is $|J^P,D_F[CS]M_1M_2\rangle$, where

J is the angular momentum

p is the parity

D_F is the dimension of the flavour multiplet

[CS] is the colour-spin representation

M_1M_2 are the type of mixed symmetry colour-spin representations of the clusters.

CHAPTER 5

CONCLUSIONS

In their work on the hyperfine splitting of the ground state of baryonium, Kalman, Hall and Misra[3.3] expressed the hope that their work would "lead to the establishment of a quark-quark pair potential which would enable one to predict the spectra of multiquark systems". In this research we have followed along this path, first by using the rich and accurate baryon data to predict meson masses and to confirm the identity of forces in both systems, then by applying this same data to calculating dibaryon masses.

A quark in a dibaryon is expected to be less relativistic than a quark in a meson or in a baryon due to the greater size of the dibaryon. This means that the model Hamiltonian should offer reasonable predictions without requiring additional relativistic correction terms. The parameters used in evaluating the dibaryon system were derived from a baryon fit and it is reasonable to expect that they contain some relativistic contributions at the "relativistic level" of the baryon. Since these same parameters have been used with some success in describing the meson system, which is at a different relativistic level, we may conclude that the parameters are not

excessively sensitive to the relativistic level of the system. Therefore the relativistic contributions implicit in the baryon parameters should not constitute a major source of error when these parameters are applied to a less relativistic system such as the dibaryon.

Moreover our treatment of the dibaryon system is based on three quark clustering. Each cluster is essentially a baryon, albeit in some cases a coloured baryon. The above leads us to believe that the application of baryon data to the dibaryon system should result in a better fit than that obtained in the meson case.

Experimentally the situation is rather obscure. Several candidates for dibaryon resonances have been found[32,42] in the strangeness zero sector. These resonances vary from 2170 to 2600 MeV and appear mainly as NN or ΔN composites.

Our model predicts masses that are 5% to 20% higher than the observed resonances. This difference between predicted and observed mass is not surprising considering that,

- The "real" potential is not necessarily a harmonic oscillator potential.
- The anharmonic contribution is in some cases as large as 65% of the predicted dibaryon mass.
- The dynamics of a six body system are expected to be more complex than those of a two or three body system.

- Above all the experimental situation is in a state of flux. Present results contain large errors and ultimate results may very well approach the predicted values.

We conclude that the consistent model is in reasonable agreement with experiment and provides a strong foundation upon which to build.

REFERENCES

1. Gell-Mann, M., 1964, Phys. Lett. 8, 214.
2. Zweig, G, 1964, CERN Report No. 8182/TH401 (unpublished)
3. LaRue, G., Fairbank, W.M. and Hebard, A.F., 1977, Phys. Rev. Lett. 38, 1011-4.
4. Goldhaber, A.S. and Smith, J., 1975, Rep. Prog. Phys. 38, 731-70.
5. Jones, L.W., 1977, Rev. Mod. Phys. 49, 717-52.
6. Wilson, K.G., 1974, Phys. Rev. D10, 2445-59.
7. Kogut, J. and Susskind, L., 1975, Phys. Rev. D11, 395-408.
8. Greenberg, O.W., 1964, Phys. Rev. Lett. 13, 598.
9. Han, M.Y. and Nambu, Y., 1965, Phys. Rev. 139B, 1006.
10. Adler, S.L., 1969, Phys. Rev. 177, 2426.
11. Fritzsch, H., Gell-Mann, M. and Lentwyler, H., Phys. Lett. 47B, 365(1971).
12. Khriplovich, I.B., 1969, Yad. Fiz. 10, 409; 1970, Sov. J. Nucl. Phys. 10, 235.
13. Ali, A. and Bernstein, J., 1975, Phys Rev. D12, 503.
14. Novikov, V.A. et al., 1978, Phys. Rep. 41C, 1.
15. Politzer, H.D., 1974, Phys. Rep. 14C, 129.
16. Nash, C., 1978, Relativistic Quantum Fields, Academic Press, London.
17. Gross, D.J. and Wilczek, F., 1973, Phys. Rev. D8, 3633.
18. Politzer, H.D., 1973, Phys. Rev. Lett. 30, 1346.

19. DeRújula, A., Georgi, H. and Glashow, S.L., 1975, Phys. Rev. D12, 147.

20. Appelquist, T. and Politzer, H.D., 1975, Phys. Rev. Lett. 34, 43.

21. Eichlen, E. et al., 1975, Phys. Rev. Lett. 34, 369.

22. Kang, J.S. and Schnitzer, H.J., 1975, Phys. Rev. D12, 841.

23. Barbieri, R. et al., 1976, Nucl. Phys. B105, 125.

24. Celmaster, W. et al., 1978, Phys. Rev. D17, 879; D18, 1688.

25. Lichtenberg, D.B. and Wills, J.G., 1978, Nuovo Cim. 47A, 483.

26. Isgur, N. and Karl, G., 1977, Phys. Lett. 72B, 109; 1978_a, Phys. Lett. 74B, 353; 1978_b, Phys. Rev. D18, 4187; 1979_a, Phys. Rev. D19, 2653; 1979_b, Phys. Rev. D20, 1191.

27. Koniuk, R. and Isgur, N., 1980_a, Phys. Rev. D21, 1868; 1980_b, Phys. Rev. Lett. 44, 845.

28. Isgur, N., Low Energy Hadron Physics with Chromodynamics, Lectures presented at XVI International School of Subnuclear Physics. Erice, August 1978 (unpublished).

29. Maltman, K. and Isgur, N., 1984, Phys. Rev. D29, 952.

30. Maltman, K., 1984, On the possibility of deeply bound di-baryon resonances, University of California pre-print, LBL-17652.

31. Schnitzer, H.J., 1981, Spin-Dependence and Gluon Mixing in Ordinary Meson Spectroscopy, Brandeis University report (unpublished).

32. Particle Data Grdup, 1982, Review of Particle Properties, LBL-100 Revised.

33. Kalman, C.S., Hall, R.L. and Misra, S.K., 1980, Phys. Rev. D21, 1908.

34. Kalman, C.S. and Pfeffer, D., 1983, Phys. Rev. D27, 1648; 1983, Phys. Rev. D28, 2324.

35. Kalman, C.S., 1982, Phys. Rev. D26, 2326.

36. Kalman, C.S. and Barbari, S., 1983, Phys. Rev. D28, 2321.

37. Kalman, C.S. and Sood, S., 1983, Phys. Rev.

38. Kalman, C.S. and Hall, R.L., 1982, Phys. Rev. D25, 217

39. Lipkin, H.J., 1980, Phys. Lett. 93B, 56

40. Montanet, 1978, Proc. 13th Rencontre de Motoind, Les Arces, 1978, J. Tran Than Van (ed.), Editions Frontiers, II Deux, France, p.285

41. Fukugita, M. and Hansson, T.H., 1979, Phys. Lett. 84B, 493; 1980, INS Symp. on Particle Physics in GeV region, Tokyo, 1979

42. Povh, B., 1980, in Proc. of the Int. Conf. on High Energy Physics Geneva (CERN), p.604

43. Particle Data Group, 1980, Rev. Mod. Phys. 52, No.2, Part II

44. Weinstein, J., University of Toronto internal report, 1980, (unpublished)

45. Weinstein, J., and Misra, S.K., 1982, Phys. Rev. Lett. 48, 659

46. Kalman, C.S. and Misra, S.K., 1982, Phys. Rev. D26, 233

47. Chan Hong-Mo et al., 1978, Phys. Lett. 76B, 634

48. Chan Hong-Mo and Høgaasen, H., 1978, Nucl. Phys. B136, 401

49. Jaffe, R.L., 1977, Phys. Rev. D15, 267

50. Jaffe, R.L., 1977, Phys. Rev. D15, 281

51. Kamae, T., 1982, Nucl. Phys. A374, 25C

52. Bugg, D., 1982, Nucl. Phys. A374, 95C

53. Makarov, M.M., et al., 1983, Phys. Lett. 122B, 343

54. Aner, I. et al., 1983, Phys. Rev. Lett. 51, 1411

55. DeTar, C., 1978, Phys. Rev. D17, 323; 1979, Phys. Rev. D19, 1451

56. Liberman, D.A., 1977, Phys. REv. B16, 1542

57. Ribiero, J.E.F.T., 1980, Z. Phys. C5, 27

58. Barry, G.W., 1977, Phys. Rev. B16, 2886; Warke, C.S. and Shanker, R., 1980, Phys. Rev. C21, 2643; Robson, D., 1978, Nucl. Phys. A308, 381

59. Jaffe, R.L., 1977, Phys. Rev. Lett. 38, 195; 1977, Phys. Rev. Lett. 38, 617

60. Aerts, A.T.M. and Dover, C.B., 1984, Phys. Rev. D29, 433; 1983, Phys. Rev. D28, 450; 1982, Phys. Rev. 49, 1752

61. Høgaasen, H. and Sorba, P., 1978, CERN preprint TH2531

62. Aerts, A.T.M. and Mulders, P.J.G. and de Swart, J.J., 1978, Phys. Rev. D17, 260

63. Oka, M. and Yazaki, K., 1980, Phys. Lett. 93B, 489

64. Cvetič, M. et al., 1980, Phys. Lett. 93B, 489

65. Hall, R.L. and Schwesinger, B., 1979, J. Math. Phys. 20, 2481

66. Hwang, W.Y.P. and Lichtenberg, D.B. and Namgund, W., 1983, Indiana University publication IUHET87.

APPENDIX A

Sample Calculation of Tensor Interaction Matrix Elements

We reproduce here the calculation of the $\langle {}^3S_1|H_{tensor}|{}^3D_1\rangle$ matrix element as an example of tensor term calculations.

We write the Hamiltonian

$$H_{tensor} = A\, H'_{tensor}$$

where, $A = \frac{4\alpha_s}{3m_q^2}$ is a constant

$$H'_{tensor} = \frac{1}{r_{12}^3}\left[\frac{3(\vec{S}_1\cdot\vec{r}_{12})(\vec{S}_2\cdot\vec{r}_{12})}{r_{12}^2} - S_1\cdot S_2\right]$$

$$= \frac{1}{r_{12}^3}\sqrt{\frac{24\pi}{5}}\; Y^{(2)}\cdot V^{(2)}$$

where $Y^{(2)}$ and $V^{(2)}$ are irreducible tensors of rank 2 and are given by,

$$V^{(2)}_{\pm 2} = S_{1\pm 1}S_{2\pm 1}$$

$$V^{(2)}_{\pm 1} = \frac{1}{\sqrt{2}}\left[S_{1\pm 1}S_{2\,0} + S_{1\,0}S_{2\pm 1}\right]$$

$$V^{(2)}_{0} = \frac{1}{\sqrt{6}}\left[3S_{1\,0}S_{2\,0} - \vec{S}_1\cdot\vec{S}_2\right]$$

and,

$$Y^{(2)}_{\pm 2} = \sqrt{\frac{5}{4\pi}}\sqrt{\frac{3}{8}}\,\sin^2\theta e^{\pm 2i\phi}$$

$$Y^{(2)}_{\pm 1} = \mp\sqrt{\frac{5}{4\pi}}\sqrt{\frac{3}{2}}\cos\theta\sin\theta e^{\pm i\phi}$$

$$Y^{(2)}_{\pm 1} = \sqrt{\frac{5}{4\pi}}\sqrt{\frac{1}{4}}\,(3\cos^2\theta - 1)$$

The matrix elements of the scalar product $T^{(k)}.U^{(k)}$ in the coupled representation are given by,

$$\langle \alpha j_1 j_2 jm | T^{(k)}.U^{(k)} | \alpha' j_1' j_2' j' m' \rangle$$

$$= (-1)^{j+j_2+j_1'} \delta_{jj'} \delta_{mm'} \begin{Bmatrix} j_1 & j_2 & j \\ j_2 & j_1 & k \end{Bmatrix}$$

$$\times \sum_{\alpha} \langle \alpha j_1 || T^{(k)} || \alpha'' j_1' \rangle \langle \alpha'' j_2 || U^{(k)} || \alpha' j_2' \rangle$$

where, j_1, j_2, j, m, j_1', j_2', j', m' are angular momentum quantum numbers α, α', include all other quantum numbers defining the state in question.

$\begin{Bmatrix} j_1 & j_2 & j \\ j_2 & j_1 & k \end{Bmatrix}$ is a 6j symbol

$\langle \alpha j_1 || T^{(k)} || \alpha'' j_1' \rangle$,

and $\langle \alpha' j_2 || U^{(k)} || \alpha' j_2' \rangle$ are the reduced matrix elements

From the Wigner-Eckart theorem

$$\langle \alpha j m | T_q^{(k)} | \alpha' j' m' \rangle = (-1)^{j-m} \begin{pmatrix} j & k & j' \\ -m & q & m' \end{pmatrix} \langle \alpha j || T^{(k)} || \alpha' j' \rangle$$

where, $\begin{pmatrix} j & k & j' \\ -m & q & m' \end{pmatrix}$ is a 3j symbol.

Next, we define the tensors

$$T^{(2)} = \sqrt{6}\, V^{(2)}$$

$$U^{(2)} = \sqrt{\frac{4\pi}{5}} \frac{Y^{(2)}}{r_{12}^3}$$

Then in the j=1 sector

$$\langle n j_1 j_2 1 m | T^{(2)}.U^{(2)} | n' j_1' j_2' 1 m' \rangle = (-1)^{1+j_2+j_1'} \delta_{mm'} \begin{Bmatrix} j_1 & j_2 & 1 \\ j_2 & j_1 & 2 \end{Bmatrix}$$

$$\times \langle j_1 || T^{(2)} || j_1' \rangle \langle n j_2 || U^{(2)} || n' j_2' \rangle$$

where n is the principal quantum number.

We then calculate the reduced matrix elements

$$\langle 10 \| T_0^{(2)} \| 10 \rangle = \langle 10 \| \sqrt{6}\, V_0^{(2)} \| 10 \rangle$$

$$= \langle 10 \| 3 S_{1_0} S_{2_0} - \vec{S}_1 . \vec{S}_2 \| 10 \rangle$$

$$= -1$$

$$\therefore \quad -1 = (-1) \begin{bmatrix} 1 & 2 & 1 \\ 0 & 0 & 0 \end{bmatrix} \langle 1 \| T^{(2)} \| 1 \rangle$$

$$= -\sqrt{\frac{2}{15}} \langle 1 \| T^{(2)} \| 1 \rangle$$

$$\therefore \quad \langle 1 \| T^{(2)} \| 1 \rangle = \sqrt{\frac{15}{2}}$$

also

$$\langle 00 | U_0^{(2)} | 20 \rangle = \langle 00 | \sqrt{\frac{4\pi}{5}} \frac{Y_0^{(2)}}{r_{12}^3} | 20 \rangle$$

$(n = 0, n' = 2)$

$$= \langle \Psi_{000} | \sqrt{\frac{4\pi}{5}} \frac{Y_0^{(2)}}{r_{12}^3} | \Psi_{220} \rangle$$

$$= \frac{8\beta^5}{\sqrt{15}\,\pi^{1/2}} \int r_{12}^2 \sqrt{\frac{4\pi}{5}}\, Y_0^{(0)*} \frac{Y_0^{(2)}}{r_{12}^3} Y_0^{(2)} \exp(-\beta^2 r_{12}^2)\, dV$$

where, $dV = r_{12}^2 \sin\theta dr_{12} d\theta d\phi = r_{12}^2 dr_{12} d\Omega$

$$\therefore \quad \langle \Psi_{000} | \sqrt{\frac{4\pi}{5}} \frac{Y_0^{(2)}}{r_{12}^3} | \Psi_{220} \rangle = \frac{16\beta^5}{5\sqrt{3}} \left[\left(\int_0^\infty r_{12} \exp(-\beta^2 r_{12}^2) dr_{12} \right) \right.$$

$$\left. \times \left(\int Y_0^{(0)*} Y_0^{(2)} Y_0^{(2)} d\Omega \right) \right]$$

Using,

$$\int Y^*_{l',m'}(\theta,\phi) Y_{LM}(\theta,\phi) Y_{lm}(\theta,\phi) d\Omega =$$

$$(-1)^{m'} \sqrt{\frac{(2l'+1)(2L+1)(2l+1)}{4\pi}} \begin{bmatrix} l' & L & l \\ -m' & M & m \end{bmatrix} \begin{bmatrix} l' & L & l \\ 0 & 0 & 0 \end{bmatrix}$$

we have,

$$\int Y_0(0)^* Y_0(2) Y_0(2)\, d\Omega = \sqrt{\frac{25}{4\pi}} \begin{pmatrix} 0 & 2 & 2 \\ 0 & 0 & 0 \end{pmatrix} \begin{pmatrix} 0 & 2 & 2 \\ 0 & 0 & 0 \end{pmatrix}$$

$$= \sqrt{\frac{1}{4\pi}}$$

and,

$$\int_0^\infty r_{12} \exp(-\beta^2 r_{12}^2)\, dr_{12} = \frac{1}{2\beta^2}$$

$$\therefore \quad \langle \Psi_{000} | \sqrt{\frac{4\pi}{5}} \frac{Y_0^{(2)}}{r_{12}^3} | \Psi_{220} \rangle = \frac{4\beta^3}{5\sqrt{3\pi}}$$

we also have,

$$\langle 00 | U_0^{(2)} | 20 \rangle = (-1)^0 \begin{pmatrix} 0 & 2 & 2 \\ 0 & 0 & 0 \end{pmatrix} \langle 0 | | U^{(2)} | | 2 \rangle$$

$$\therefore \quad \frac{4\beta^3}{5\sqrt{3\pi}} = \frac{1}{\sqrt{5}} \langle 0 | | U^{(2)} | | 2 \rangle$$

$$\therefore \quad \langle 0 | | U^{(2)} | | 2 \rangle = \frac{4\beta^3}{\sqrt{15\pi}}$$

Next we write the matrix element of the tensor term

$$\langle \Psi_{000} X_1 | H_{tensor} | \Psi_{222} X_1 \rangle = \frac{4}{3} \frac{\alpha_s}{m_q^2} \langle 0110 | T^{(2)} . U^{(2)} | 2110 \rangle 1$$

$$= \frac{4}{3} \frac{\alpha_s}{m_q^2} \left[(-1)^4 \begin{Bmatrix} 2 & 1 & 1 \\ 1 & 0 & 2 \end{Bmatrix} . \sqrt{\frac{15}{2}} . \frac{4\beta^3}{\sqrt{15\pi}} \right]$$

where $\begin{Bmatrix} 2 & 1 & 1 \\ 1 & 0 & 2 \end{Bmatrix} = \frac{1}{\sqrt{15}}$

$$\therefore \quad \langle {}^3S_1 | H_{tensor} | {}^3D_1 \rangle = \frac{4}{3^{5/4}\sqrt{5}} \left(\frac{m_u}{m_q}\right)^{5/4} \delta$$

where

$$\delta = \frac{4\alpha_s \alpha^3}{3\sqrt{2\pi}\, m_u^2} \quad \text{and} \quad \beta = \left(\frac{m_q}{3m_u}\right)^{1/4} \alpha$$

APPENDIX B

Sample Calculation of Spin Orbit Interaction Matrix Elements

We repreduce here the calculation of the $\langle {}^3D_3 | H_{so} | {}^3D_3 \rangle$ matrix element as an example of spin orbit term calculations. The spin orbit Hamiltonian is given by

$$H_{so} = \frac{2}{m_q^2}\left[\frac{\alpha_s}{r_{12}^3} - K\right]\vec{L}.\vec{S}$$

$$= f(r_{12})\,\vec{L}.\vec{S}$$

In the coupled representation

$$\langle lsjm|\vec{L}.\vec{S}|l's'j'm'\rangle = \frac{1}{2}\left[j(j+1)-l(l+1)-s(s+1)\right]\delta_{ll'}.\delta_{ss'}.\delta_{mm'}$$

$\therefore$ in the $j = 1$ sector $(l = 2, s = 1)$ we have

$$\langle \vec{L}.\vec{S}. \rangle = -3$$

The spatial expectation is given by

$$\langle \Psi_{222}|f(r_{12})|\Psi_{222}\rangle = \frac{32\beta^7}{15m_q^2\pi^{1/2}}\int_0^\infty (\alpha_s r_{12}^3 - K r_{12}^4)\exp(-\beta^2 r^2)\,dr_{12}$$

Using the integral

$$\int_0^\infty x^m e^{-ax^n}dx = \frac{\Gamma\left(\frac{m+1}{n}\right)}{n a^{(m+1)/n}}$$

Where, n, m, a are positive constants

we have

$$\langle \Psi_{222}|f(r_{12})|\Psi_{222}\rangle = \frac{32\,\beta^7}{15m_q^2\pi^{1/2}}\left[\frac{\alpha_s\Gamma(2)}{2\beta^4} - \frac{K\Gamma(\frac{7}{2})}{2\beta^7}\right]$$

$$\Gamma(2) = 1 \quad , \quad \Gamma\left(\tfrac{7}{2}\right) = \frac{15\sqrt{\pi}}{8}$$

$$\therefore \quad \langle \Psi_{222} | f(r_{12}) | \Psi_{222} \rangle = \frac{16 a_s \beta^3}{15 m_q^2 \pi^{1/2}} - \frac{2K}{m_q^2}$$

The spin orbit matrix element is therefore

$$\langle \Psi_{222} | H_{so} | \Psi_{222} \rangle = -\frac{16 a_s \beta^3}{5 m_q^2 \pi^{1/2}} + \frac{6K}{m_q^2}$$

$$= -4\sqrt{2}\left[\frac{3^{1/4}}{5}\right]\left(\frac{m_\mu}{m_q}\right)^{5/4} \delta + 2\frac{m_\mu \omega_\mu^2}{m_q^2}$$

THE AMERICAN PHYSICAL SOCIETY
Physical Review D
Volume 28, Number 9

A Test of the Identity of Forces in Mesons and Baryons; Calculating Quarkonium Spectra Using Only Baryon Parameters.

C. S. Kalman
S. Barbari